

# **ADSORPTIVE BUBBLE SEPARATION FOR OIL REMOVAL**

Paweena Kanokkarn

A Dissertation Submitted in Partial Fulfilment of the Requirements  
for the Degree of Doctor of Philosophy  
The Petroleum and Petrochemical College, Chulalongkorn University  
in Academic Partnership with  
The University of Michigan, The University of Oklahoma,  
and Case Western Reserve University  
2017

บทคัดย่อและแฟ้มข้อมูลฉบับเต็มของวิทยานิพนธ์ตั้งแต่ปีการศึกษา 2554 ที่ให้บริการในคลังปัญญาจุฬาฯ (CUIR)  
เป็นแฟ้มข้อมูลของนิสิตเจ้าของวิทยานิพนธ์ที่ส่งผ่านทางบัณฑิตวิทยาลัย

The abstract and full text of theses from the academic year 2011 in Chulalongkorn University Intellectual Repository (CUIR)  
are the thesis authors' files submitted through the Graduate School.

**Thesis Title:** Adsorptive Bubble Separation for Oil Removal  
**By:** Paweena Kanokkarn  
**Program:** Petrochemical Technology  
**Thesis Advisor:** Prof. Sumaeth Chavadej

---

Accepted by The Petroleum and Petrochemical College, Chulalongkorn University, in partial fulfilment of the requirements for the Degree of Doctor of Philosophy.

..... College Dean  
(Prof.Suwabun Chirachanchai)

**Thesis Committee:**

.....  
(Prof. Apanee Luengnaruemitchai)

.....  
(Prof. Sumaeth Chavadej)

.....  
(Prof.Pitt Supaphol)

.....  
(Assoc. Prof. Boonyarach Kitiyanan)

.....  
(Asst. Prof. Wirogana Ruengphrathuengsuka)

## ABSTRACT

5391003063: Petrochemical Technology Program

Paweena Kanokkarn: Adsorptive Bubble Separation for Oil Removal.

Thesis Advisor: Prof. Sumaeth Chavadej 95 pp.

Keywords: Froth flotation/ Dynamic surface tension/ Surfactant adsorption/ Foamability/ Foam stability

This present work emphasized on the current knowledge regarding (i) feasibility of multi-stage froth flotation operation for oil removal, and (ii) comprehension of dynamic surface tensions of surfactant solutions in relation to foam characteristics. A multi-stage froth flotation efficiency depends on the enhancement of interfacial adsorption and the number of bubble caps and tray. The operational parameters including foam height, air flow rate and feed flow rate were controlled to obtain the optimum process performance. Under the optimum conditions—a number of trays of 4, a foam height of 60 cm, an air flow rate of 40 L/min, a feed flow rate of 60 mL/min, a surfactant concentration of 0.3% (w/v), and an NaCl concentration of 1.5% (w/v)—the enrichment ratio and the removal of motor oil could reach as high as 16.3 and 97.9%, respectively. Furthermore, the effects of surfactant structure on the equilibrium and dynamic surface tension were investigated and discussed to correlate with foam properties. For all studied surfactant solutions, the equilibrium experimental data were well fitted with the Langmuir adsorption isotherm, while the dynamic surface tension data were used to calculate diffusivity values of all studied surfactants by using Word-Tordai equation. It was found that a surfactant having longer alkyl group has a lower diffusivity value, whereas a surfactant having larger head group size has a higher diffusivity. The adsorption process of surfactant onto the air/water interface of generated bubbles was controlled by the diffusion.

## บทคัดย่อ

ปริญญากนการ : การแยกน้ำมันโดยกระบวนการดูดซับบนผิวของฟอง (Adsorptive Bubble Separation for Oil Removal) อ. ที่ปรึกษา : ศ. ดร. สุเมธ ชวเดช 95 หน้า

ในงานวิจัยนี้เน้นถึงการนำความรู้ในปัจจุบันมาใช้ในการศึกษา (1) ความเป็นไปได้ของการใช้คอสม์นทำให้ลอยหลายขั้นตอนแบบต่อเนื่องเพื่อแยกน้ำมัน และ (2) ความเข้าใจเกี่ยวกับแรงตึงผิวแบบไดนามิกส์ของสารละลายลดแรงตึงผิวที่สัมพันธ์กับลักษณะเฉพาะตัวของฟอง ประสิทธิภาพของกระบวนการทำให้ลอยแบบหลายขั้นตอนขึ้นอยู่กับ การเพิ่มการดูดซับที่ผิวและจำนวนของถ้วยฟองและถาด ทั้งนี้มีการควบคุมปัจจัยในการดำเนินการ ซึ่งประกอบด้วย ความสูงของฟอง อัตราการไหลของอากาศ อัตราการไหลของสารละลาย รวมถึงความเข้มข้นของสารลดแรงตึงผิวและสารละลายอิเล็กโทรไลต์ (โซเดียมคลอไรด์) เพื่อให้ได้มาซึ่งประสิทธิภาพที่สูงที่สุด ภายใต้สภาวะที่ดีที่สุด (ถาดถ้วยฟองจำนวน 4 ถาด, ความสูงของฟอง 60 เซนติเมตร, อัตราการไหลของอากาศ 40 ลิตรต่อนาที, อัตราการไหลของสารละลาย 60 มิลลิลิตรต่อนาที ความเข้มข้นของสารลดแรงตึงผิว 0.3% โดยน้ำหนักต่อปริมาตร และความเข้มข้นของโซเดียมคลอไรด์ 1.5% โดยน้ำหนักต่อปริมาตร) สามารถได้ค่าอัตราส่วนการกำจัดของน้ำมัน 16.3 และแยกน้ำมันได้ 97.9 เปอร์เซ็นต์ นอกจากนี้ ได้ทำการศึกษาผลของโครงสร้างทางเคมีของสารลดแรงตึงผิวต่อแรงตึงผิวสมดุลและไดนามิกส์ และอภิปรายผลเพื่อนำมาสัมพันธ์กับสมบัติของฟอง ข้อมูลของค่าแรงตึงผิวสมดุลแสดงให้เห็นว่า สารลดแรงตึงผิวที่ศึกษาในงานวิจัยนี้ทุกชนิด มีไอโซเทอมการดูดซับเป็นไปตามโมเดลของแลงเมียร์ (Langmuir isotherm) และในขณะเดียวกัน ข้อมูลของค่าแรงตึงผิวไดนามิกส์ถูกนำมาใช้ในการคำนวณค่าความสามารถในการแพร่ผ่านของสารลดแรงตึงผิวได้ โดยใช้สมการของเวิร์ด-ทอร์ดาย (Word-Tordai) ผลการทดลองแสดงให้เห็นว่าสารลดแรงตึงผิวที่มีหมู่อัลคิลยาวจะมีค่าความสามารถในการแพร่ผ่านที่ต่ำ ในขณะที่สารลดแรงตึงผิวที่ส่วนหัวที่ใหญ่ จะมีค่าความสามารถในการที่สูง และจากผลการทั้งหมด สามารถสรุปได้ว่ากระบวนการแพร่ผ่านเป็นตัวควบคุมการดูดซับที่ผิวฟอง

## ACKNOWLEDGEMENTS

I would like to express my sincere gratitude and acknowledgement to my advisor, Prof. Sumaeth Chavadej for providing me such an opportunity to carry out this interesting topic for my thesis. Throughout my doctoral studies, I have always received great advice and continuous support from him. His expert guidance has helped me in all time of research and writing of this thesis.

I would like to give thanks to Prof. Apanee Luengnaruemitchai, Prof. Pitt Supaphol, Assoc. Prof. Boonyarach Kitiyanan, and Asst. Prof. Wirogana Ruengphrathuengsuka for being my dissertation committees and their useful suggestions on this work. I am grateful for the scholarship and funding of the thesis work provided by the Royal Golden Jubilee Ph.D Program; the Petroleum and Petrochemical College; and the Center of Excellence on Petrochemical and Materials Technology, Thailand.

I would like to thank Prof. Takeo Shiina and Dr. Manasikan Thammawong for taking care of me during visit to Tsukuba, Japan and also giving me for great advice and recommendation.

I would like to extend my sincere thanks to Dr. Orathai Pornsunthorntawee for proofreading of my manuscripts but above this, for her unconditional help and moral support whenever I needed.

Without aids from PPC staffs and my lab seniors, this work cannot be done successfully. I would like to thank all of them. I would like to mention to some friends I have known along the way of my research. Among my friends, I would like to mention my best friends, Ms. Kessara Seneesrisakul and Ms. Achiraya Jiraprasertwong, who are always being with me in ups and downs of life during last 6 years.

Finally, I have no word to express my deepest gratitude goes to my family for unconditional supports and being on my sides throughout my life and my doctoral study.

## TABLE OF CONTENTS

	<b>PAGE</b>
Title Page	i
Abstract (in English)	iii
Abstract (in Thai)	iv
Acknowledgements	v
Table of Contents	vi
List of Tables	x
List of Figures	xii
 <b>CHAPTER</b>	
<b>I INTRODUCTION</b>	<b>1</b>
1.1 State of Problems	1
1.2 Objectives	3
1.3 Scope of Work	3
 <b>II LITERATURE REVIEW</b>	 <b>5</b>
2.1 Surfactants	5
2.2 Foam	6
2.2.1 Foam Formation	7
2.2.2 Structure of Foam	7
2.2.3 Foamability and Foam Stability	8
2.2.3.1 Foambility	8
2.2.3.2 Foam Stability	9
2.3 Surfactant Adsorption at Air/Water Interface	9
2.3.1 Equilibrium Surfactant Adsorption	10
2.3.2 Dynamic Surfactant Adsorption	12
2.3.2.1 Introduction to Dynamic Surface Tension	12
2.3.2.2 Dynamic Adsorption Mechanism	14
2.4 Adsorptive Bubble Separation	18
2.4.1 Froth Flotation	19

<b>CHAPTER</b>	<b>PAGE</b>
2.4.2 Mode of Operation	22
2.4.3 Material Transport in Flotation Column	23
2.4.4 Multistage Froth Flotation	25
<b>III REMOVAL OF MOTOR OIL BY MULTISTAGE FROTH FLOTATION: EFFECT OF OPERATIONAL PARAMETERS</b>	<b>28</b>
3.1 Abstract	28
3.2 Introduction	29
3.3 Experimental	30
3.3.1 Materials and Chemicals	30
3.3.2 CMC and Surface Tension Isotherm Determination	31
3.3.3 Dynamic Surface Tension Measurement	31
3.3.4 Multistage Froth Flotation Experiments	31
3.3.5 Foamability and Foam Stability Measurements	33
3.3.6 Calculation of Process Performance	34
3.4 Results and Discussion	34
3.4.1 Fundamental Properties of Surfactant	34
3.4.2 Dynamic Surface Tension	37
3.4.3 Operating Limits	39
3.4.4 Effects of Foam Height	40
3.4.5 Effect of Air Flow Rate	42
3.4.6 Effect of Feed Flow Rate	44
3.4.7 Effects of Salt Concentration	46
3.4.8 Foam Characteristics	48
3.4.9 Concentration Profiles of Surfactant and Motor Oil	50
3.4.10 Comparisons of Separation Process Performance	51
3.5 Conclusions	53
3.6 Acknowledgements	53
3.7 References	54

<b>CHAPTER</b>	<b>PAGE</b>
<b>IV EQUILIBRIUM AND DYNAMIC SURFACE TENSION OF AQUEOUS SURFACTANT SOLUTIONS IN RELATION TO FOAMING PROPERTIES</b>	<b>53</b>
4.1 Abstract	53
4.2 Introduction	54
4.3 Experimental	55
4.3.1 Materials	55
4.3.2 Surface Tension Measurement	56
4.3.2.1 Equilibrium Surface Tension Measurement	56
4.3.2.2 Dynamic Surface Tension Measurement	56
4.3.3 Foamability and Foam Stability Measurements	56
4.4 Results and Discussion	56
4.4.1 Equilibrium Surface Tension and Adsorption Isotherm Results	56
4.4.2 Dynamic Surface Tension	61
4.4.3 Surfactant Diffusivity Value Results	66
4.4.4 Foam Behaviors	69
4.4.4.1 Foamability Results	69
4.4.4.2 Foam Stability Results	72
4.4.5 Effect of Salt Concentration	73
4.5 Conclusions	74
4.6 Acknowledgements	74
4.7 References	75
<b>V CONCLUSIONS AND RECOMMENDATIONS</b>	<b>80</b>
<b>REFERENCES</b>	<b>82</b>
<b>APPENDIX</b>	<b>91</b>



<b>CHAPTER</b>	<b>PAGE</b>
<b>CURRICULUM VITAE</b>	94

## LIST OF TABLES

<b>TABLE</b>		<b>PAGE</b>
<b>CHAPTER III</b>		
2.1	Classification of the adsorptive bubble separation techniques	19
<b>CHAPTER III</b>		
3.1	Calculated values of CMC, $\gamma_{cmc}$ , $pC_{20}$ , and saturated surface concentrations ( $\Gamma_m$ ) of surfactant with and without NaCl addition	36
3.2	Comparison of the process performance of different froth flotation units	52
<b>CHAPTER IV</b>		
4.1	Calculated values of CMC, $\gamma_{cmc}$ , $pC_{20}$ , saturated surface concentrations ( $\Gamma_m$ ) and Langmuir equilibrium adsorption constant ( $K_L$ ) of all studied surfactants	60
4.2	Dynamic surface tension parameters for all studied surfactant solutions	64
4.3	Apparent diffusion coefficients of all studied surfactants (at concentration of 2.0 mM for MES <sub>x</sub> and 0.2 mM for C <sub>12</sub> EO <sub>n</sub> )	69
4.4	Foam characteristics of all studied surfactants	71
4.5	Saturated surface concentrations ( $\Gamma_m$ ), diffusivity, foamability and foam stability of MES <sub>16</sub> at the concentration of 2.0 mM with different NaCl concentrations	73

<b>TABLE</b>		<b>PAGE</b>
<b>APPENDIX</b>		
A1	Surface tension of surfactant Alfoterra <sup>®</sup> C145–8PO with and without 1.5% (w/v) NaCl addition at 25°C.	91
A2	Surface tension of all studied anionic surfactant solutions at 25 °C	92
A3	Surface tension of all studied non-ionic surfactant solutions at 25 °C	93

## LIST OF FIGURES

FIGURE	PAGE
<b>CHAPTER II</b>	
2.1	Schematic drawing of an amphipathic structure of surfactant molecule. 5
2.2	Schematic drawing of foam formation aspects for different liquid volume fractions. 6
2.3	Model of the monodispersed foam regime along the glass–plate column. 7
2.4	Time windows for various dynamic surface tension techniques. 12
2.5	Generalized dynamic surface tension. 13
2.6	Elementary processes in adsorption of soluble surfactants at air/water interface. 14
2.7	Classification for the adsorptive bubble separation methods. 18
2.8	A rising gas bubble in bubble separation column containing a surface-active agent. 20
2.9	Principle of foam fractionation. 21
2.10	Different effects during formation and stabilization of foam. 21
2.11	Foam separation mode is described by (a) batch and (b) continuous operation. Continuous operations involving counter flow are described by (c) enriching, (d) stripping and (e) combined (stripping and enriching). 22
2.12	Material balances; (a) around well-mixed stage in the foam fractionation of a liquid and (b) around foam phase. 24
2.13	Schematic drawings of (a) bubble caps tray and (b) a multistage foam fractionation column. 27
<b>CHAPTER III</b>	
3.1	Schematic drawing of (a) multistage froth flotation column and (b) foam phase in equilibrium with aqueous phase for froth flotation system. 32

<b>FIGURE</b>	<b>PAGE</b>
3.2 Surface tension isotherms of surfactant with and without NaCl addition at 25°C.	35
3.3 Adsorption density of surfactant with and without 1.5% (w/v) NaCl addition at air/liquid interface at 25°C.	36
3.4 Dynamic surface tension of 0.3% (w/v) surfactant solution with and without 1.5% (w/v) NaCl addition.	38
3.5 Boundaries of operational zone of flotation column [Conditions: Surfactant concentrations of 0.3% and 0.5% (w/v) and motor oil concentration of 500 mg/L].	39
3.6 Effect of foam height on (a) surfactant recovery and motor oil, (b) enrichment ratio, (c) separation factor, (d) residual factor, (e) effluent concentration, and (f) foamate volumetric ratio under two different surfactant concentrations—0.3% and 0.5% (w/v) [Conditions: air flow rate of 40 L/min, feed flow rate of 60 mL/min, and motor oil concentration of 500 mg/L].	41
3.7 Effect of air-flow rate on (a) surfactant recovery and motor oil, (b) enrichment ratio, (c) separation factor, (d) residual factor, (e) effluent concentration, and (f) foamate volumetric ratio under two different surfactant concentrations—0.3% and 0.5% (w/v) [Conditions: foam height of 60 cm, feed flow rate of 60 mL/min, and motor oil concentration of 500 mg/L].	43
3.8 Effect of feed-flow rate on (a) surfactant recovery and motor oil, (b) enrichment ratio, (c) separation factor, (d) residual factor, (e) effluent concentration, and (f) foamate volumetric ratio under two different surfactant concentrations—0.3% and 0.5% (w/v) [Conditions: foam height of 60 cm, air flow rate of 40 L/min, and motor oil concentration of 500 mg/L].	45

<b>FIGURE</b>	<b>PAGE</b>
3.9 Effect of salt concentration on (a) surfactant recovery and motor oil, (b) enrichment ratio, (c) separation factor, (d) residual factor, (e) effluent concentration, and (f) foamate volumetric ratio [Conditions: foam height of 60 cm, air flow rate of 40 L/min, feed flow rate of 60 mL/min, and motor oil concentration of 500 mg/L].	47
3.10 Foam characteristics in terms of foamability and foam stability as a function of NaCl concentration [0.3% (w/v) surfactant and 500 mg/L motor oil].	49
3.11 Concentration profiles of surfactant and motor oil under 0.3% (w/v) surfactant and 1.5% (w/v) NaCl. [Conditions: foam height of 60 cm, air flow rate of 40 L/min, feed flow rate of 60 mL/min, and motor oil concentration of 500 mg/L].	51
 <b>CHAPTER IV</b> 	
4.1 Surface tension of surfactant solution as a function of concentration (a) MES <sub>x</sub> with different alkyl chain length and SDS and (b) C <sub>12</sub> EO <sub>n</sub> with different amounts of EO units.	57
4.2 Adsorption density of surfactant solution as a function of concentration (a) MES <sub>x</sub> with different alkyl chain length and SDS and (b) C <sub>12</sub> EO <sub>n</sub> with different amounts of EO units.	59
4.3 Dynamic surface tension $\gamma(t)$ of surfactant solution (a) MES <sub>16</sub> and (b) C <sub>12</sub> EO <sub>9</sub> at air/water interface for five different concentrations.	62
4.4 Dynamic surface tension of (a) MES <sub>x</sub> with different alkyl chain length at the concentration of 2.0 mM (b) C <sub>12</sub> EO <sub>n</sub> with different amounts of EO units at the concentration of 0.2 mM.	65

<b>FIGURE</b>	<b>PAGE</b>
4.5 The linear behavior of $\gamma(t) - \sqrt{t}$ determined by the short time approximation of (a) $\text{MES}_x$ with different alkyl chain lengths were evaluated at the concentration of 2.0 mM. and (b) $\text{C}_{12}\text{EO}_n$ with different amounts of EO units at the concentration of 0.2 mM.	68

# CHAPTER I

## INTRODUCTION

### 1.1 State of Problems

In order to comply with environment regulations, a proper treatment system for oil contaminated wastewater has to be employed prior to discharging it to the environment. A variety of treatment techniques have been developed and applied for the removal of oil from wastewater, including coagulation/flocculation (Zeng *et al.*, 2007; Shi-Qian Li *et al.*, 2011), biological treatment (Nadarajah *et al.*, 2002; Perez *et al.*, 2007), membrane-separation process (Gryta *et al.*, 2001; Masuelli *et al.*, 2009), and ultrafiltration (Li *et al.*, 2006; Hua *et al.*, 2007; Yan *et al.*, 2009). However, these traditional treatment techniques are not economically feasible for applying to wastewater containing a low concentration of oil. Adsorptive bubble separation, typically a froth flotation technique, is one of the most promising oily wastewater treatment processes due to its several advantages, such as low space and energy requirement; simplicity in design, operation, and scale-up; low operating cost, and no solvent or heat requirement (Wong *et al.*, 2001; Burghoff, 2012). The froth flotation technique has been successfully employed for the removal of various oil types, such as ortho-dichlorobenzene (Pondstabodee *et al.*, 1998; Chavadej *et al.*, 2004), ethylbenzene (Yanatatsaneejit *et al.*, 2005a, b), diesel oil (Watcharasing *et al.*, 2008a, b; Yanatatsaneejit *et al.*, 2008), motor oil (Watcharasing *et al.*, 2009), and cutting oil (Buntornpratoomrat *et al.*, 2013). Based on the mentioned research, it can be concluded that froth flotation is considered one of the most effective treatment processes for concentrating, as well as for separating, both suspended solids and oils, especially at low concentrations.

Fundamentally, the process performance of the froth flotation is governed by two mechanisms of the adsorptive transport and the bulk liquid transport. The former is an upward stream of the adsorbed materials on the foam surface while the latter is an upward stream of lamella liquid with un-adsorbed molecules, known as the entrained liquid. The bulk liquid transport not only contributes to the removal but also causes the reduction of the enrichment ratio and separation factors of any target



material due to the dilution of the entrained liquid. On the other hand, the adsorptive transport is responsible for the increase in the enrichment ratios and separation factors, apart from the removal of both surfactant and target materials (Rujirawanich *et al.*, 2011). It is very meaningful to design a novel flotation column which can enhance adsorptive transport and reduce bulk liquid transport simultaneously. Froth flotation has been mostly applied in single stage systems in either a batch or continuous mode, however, multistage froth flotation has seldom received attention although much higher separation efficiency can be achieved (Boonyasuwat *et al.*, 2005; Rujirawanich *et al.*, 2010, 2011, 2012). In the present work, a continuous multistage froth flotation unit was employed, for the first time, for motor oil removal from water using an extended surfactant (Alfoterra<sup>®</sup> C145–8PO) as a frother. Several factors affecting the separation efficiency including foam height, air flow rate, feed flow rate, and surfactant and salt concentrations were systematically investigated. The separation efficiency was determined based on the following evaluating parameters: removal percentage, enrichment ratios, residual factors, and separation factors of both surfactant and motor oil.

Moreover, a fundamental understanding of surfactant adsorption process at air/water interface and foam properties is essential for successfully froth flotation operation (Stevenson and Li, 2014). Normally, they are governed by the properties of added surfactants including other soluble components present in water especially type, chemical structure and concentration (Tamura *et al.*, 1998; Beneventi *et al.*, 2001, Rosen, 2004; Tan *et al.*, 2005; Wang *et al.*, 2016). Under the flotation process, foam is always formed in a very short time and so the equilibrium adsorption does not reach (Gao *et al.*, 2016; Wang *et al.*, 2016). Therefore, the use of equilibrium surface properties, which has been paid many attentions and researched widely, cannot apply to froth flotation processes. The relation of dynamic surface tension results, lack of supported data, to the foam behaviors and adsorption properties will be, for the first time of its kind, discussed in this work.

Without doubt, the main objective of this work was to employ a numerical approach to dynamic surface tension data for calculating diffusivity and to correlate dynamic surface tension and diffusivity to foaming properties of different surfactant solutions. The influence of surfactant structures—the alkyl chain length of a series of

methyl ester sulfonate (MES<sub>x</sub>) homologues and the head group size of a series of polyoxyethylated dodecyl alcohol (C<sub>12</sub>EO<sub>n</sub>) homologues—on the equilibrium and dynamic surface properties, and adsorption behaviors at air/water interface was also investigated systematically. In addition, the effect of an electrolyte (NaCl) on their surface tension (dynamic and equilibrium) and foaming behaviors was also discussed.

## 1.2 Objectives

The main objectives of this study were to effectively study the separation performance of target materials from their diluted aqueous solution and to elucidate the adsorption mechanism for the froth flotation process. The overall objectives of this work were as follows:

To demonstrate continuous multistage froth flotation with bubble-cap trays for the removal of motor oil from simulated wastewater.

To study the effects of operational parameters—foam height, air flow rate, feed flow rate as well as surfactant and electrolyte concentration—on the separation efficiency of motor oil and surfactant.

To investigate the effect of surfactant molecular structure on the surface properties and foam characteristics.

To correlate both dynamic and equilibrium surface tensions to foam properties.

## 1.3 Scope of Work

In the present study, a continuous multistage froth flotation unit was employed, for the first time, for motor oil removal from water using an extended surfactant (Alfoterra<sup>®</sup> C145–8PO) as a frother. The motor oil concentration of 500 mg/L was fixed and selected in this study because it represented a low oil concentration that is not possible both technically and economically to use a conventional oil-trap chamber for oil separation. Two different surfactant concentrations of 0.3% and 0.5% (w/v) were selected to study the froth flotation performance to represent dry and wet foam, respectively. It was due to the lowest

surfactant concentration of 0.3% (w/v) was found to be capable to produce stable foam to reach a highest foam height of 90 cm. Beyond a surfactant concentration of 0.5% (w/v), the separation efficiency was very low because the system had a very high foamate fraction (high bulk liquid transport). Several factors affecting the separation efficiency including foam height, air flow rate, feed flow rate, and surfactant and electrolyte concentrations were systematically investigated. The separation efficiency was determined based on the following evaluating parameters: removal percentage, enrichment ratios, residual factors, and separation factors of both surfactant and motor oil.

To gain a better understanding of froth flotation operation, surfactant adsorption and foam properties (foamability and foam stability) are crucial to achieve the deep comprehension. They are fundamentally governed by the properties of added surfactants especially type, chemical structure and concentration. In this work, methyl ester sulfonate ( $\text{MES}_x$ ) and polyoxyethylated dodecyl alcohol ( $\text{C}_{12}\text{EO}_n$ ) were selected in this study because they are considered as environmental friendly surfactants, therefore, they were hypothesized to be good for froth flotation application.  $\text{MES}_x$  with different alkyl chain lengths ( $x = 14, 16, \text{ and } 18$ ) and  $\text{C}_{12}\text{EO}_n$  ( $n = 3, 5, 7, \text{ and } 9$ ) with different head group sizes were measured for equilibrium and dynamic surface tension as well as foamability and foam stability to determine the effect of surfactant molecular structure. The relation of dynamic surface tension results of surfactant solutions to the foam behaviors was the first time of its kind, discussed in this work. A numerical approach from dynamic surface tension data was employed for calculating diffusivity and for correlating dynamic surface tension and diffusivity to foaming properties of different surfactant solutions.

## CHAPTER II

### LITERATURE REVIEW

#### 2.1 Surfactants

Surfactant is an abbreviation for Surface Active Agent. It has the unique property of adsorbing onto the surfaces (aqueous and gas or air phase) or interface (a boundary between two immiscible phases) (Holmberg *et al.*, 2003; Rosen, 2004). The characteristic molecular structure of surfactant generally consists of a structural group that has strong attraction with an aqueous solution, called a hydrophilic group (water-loving), and together with another group that has weaker attraction with the aqueous solution, called a hydrophobic group (water-hating). This is known as an amphipathic structure (Holmberg *et al.*, 2003; Tadros, 2005), as shown in Figure 2.1.

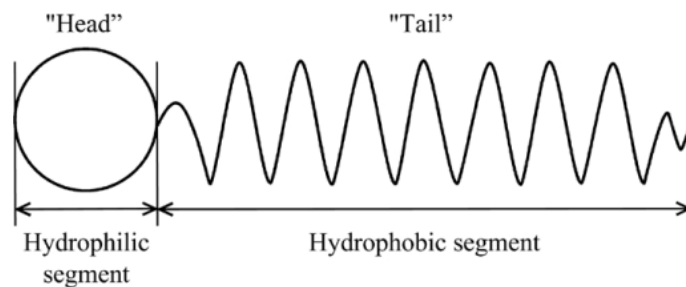


**Figure 2.1** Schematic drawing of an amphipathic structure of surfactant molecule (Szymański, 2008).

Depending on the nature of the hydrophilic group, surfactants can be categorized as follows; (i) Anionic surfactant, the hydrophilic portion of the molecule has negative charge, (ii) Cationic surfactant, hydrophilic portion of the molecule has positive charge, (iii) Zwitterionic surfactant, both positive and negative charges are present in the hydrophilic portion, (iv) Nonionic surfactant, hydrophilic portion of the molecule has no apparent ionic charge (Tadros, 2005; Rosen and Kunjappu, 2012).

According to the dual functionalities—hydrophobic and hydrophilic characteristics—surfactants are widely used in several applications: enhanced oil recovery, detergency and separation process (Schramm *et al.*, 2003). Surfactant-based separation process is one of great interest for industrial separations. It generally requires little energy and provides an energy-efficient alternative to traditional purification method (Scamehorn and Harwell, 1988; Wasan *et al.*, 1988).

## 2.2 Foam

Foam is a multiphase system consisting of a high volume fraction of gas bubbles dispersed in a liquid or solid. For liquid foam, it is produced when air or any other gas is introduced beneath the surface of a liquid, and then quickly separated into two phases; (i) air and/or gas phase that is surrounded by (ii) the liquid and/or medium phase (Rosen and Kunjappu, 2012), as shown in Figure 2.2. Foams are intensive received attention in a variety of applications such as detergency, personal care products, food products, firefighting, enhanced oil recovery, textiles, froth flotation, and foam fractionation (Narsimhan and Wang, 2006; Wang and Narsimhan, 2007).

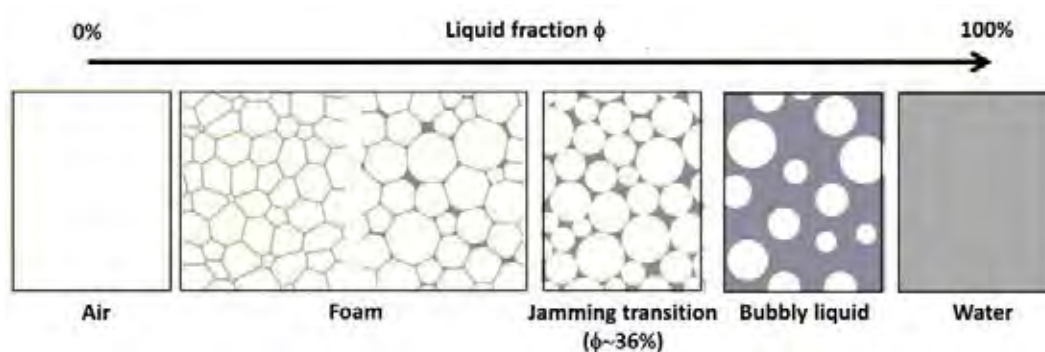


**Figure 2.2** Schematic drawing of foam formation aspects for different liquid volume fractions (Langevin, 2017).

### 2.2.1 Foam Formation

Foam is simultaneously produced when either air or gas is introduced beneath the surface of any liquid, then, the generated gas bubbles rise to form foam on the liquid surface. Fundamentally, all foams are thermodynamically unstable they cannot be generated in the absence of a surfactant due to the fact that the generated gas bubbles can be collapsed immediately once they get out from the surface of liquid (Rosen and Kunjappu, 2012). Two important conditions have to be fulfilled in order to produce the foam (Holmberg *et al.*, 2003). The first one is that a foaming solution has to be sufficiently high surface activity. And the second one is that the foam film has to have a certain surface elasticity to provide sufficiently high foam stability, which will be described in section 2.2.3.2.

### 2.2.2 Foam Structure

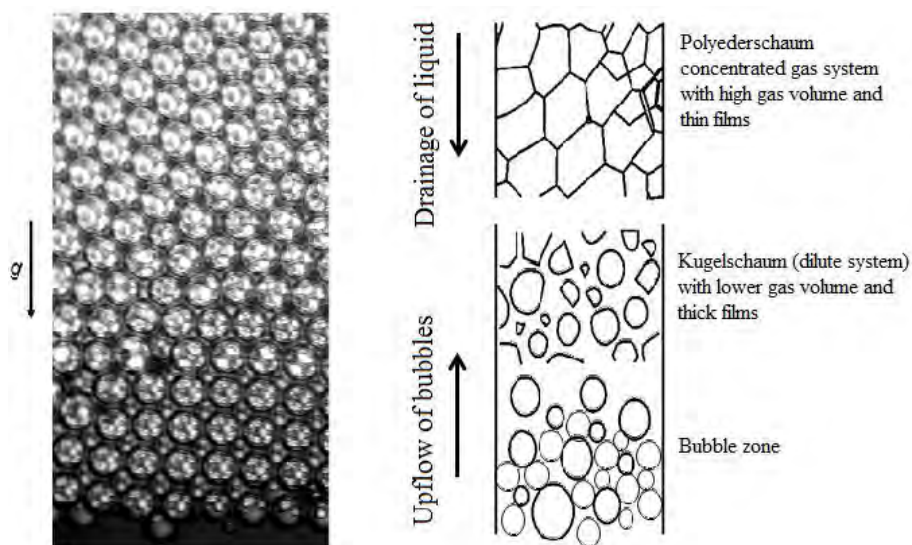


**Figure 2.3** Model of the monodispersed foam regime along the glass-plate column (Tadros, 2005; van der Net *et al.*, 2007).

Foam typically has honeycomb structure. Each gas bubble is enclosed by thin liquid films. The liquid film with two side surfaces is named the *lamellae*, whereas the intersection of three adjacent thin films is designated as *Plateau border*

or *Gibbs triangle* (Narsimhan and Wang, 2006; Wang and Narsimhan, 2007; Rosen and Kunjappu, 2012). It is common observation that foam structure has changed along the foam height in which foam becomes drier from the bottom to the top (Stevenson and Li, 2014). The cause of changing with the height is almost explained by the fact of the liquid film drainage process (Boonyasuwat *et al.*, 2005; Pugh, 2005; Saleh *et al.*, 2006), as shown in Figure 2.3.

Foam can be distinguished to two main types; (i) spherical foam (high water fraction) typically appears near the surface of solution and consists of gas bubbles separated by thick films and (ii) polyhedral foam (low water fraction) commonly appears at the upper part of the generated foam (Tadros, 2005). Foams can be also classified as wet and dry according to liquid content. The former consist of spherical air bubbles surrounded by the liquid phase and has high liquid content while the latter consists polyhedral air cells separated by thin liquid foam films and has low liquid content (Stubenrauch and Khristov, 2005; Stevenson, 2012).

### 2.2.3 Foamability and Foam Stability

Foams are generally described in terms of their foamability and foam stability (Belhajj *et al.*, 2014; Wang *et al.*, 2015, 2016).

#### 2.2.3.1 *Foambility*

The term of foamability is the “ability” of the system to generate foam (Malysa and Lunkenheimer, 2008). It is an overall capacity of surfactant solution to produce foams (Cantat *et al.*, 2013). The addition of surfactant is required to prevent bubble coalescence and alter the interfacial properties, such as the surface tension and surface viscoelasticity, which are crucially important for foamability (Wang *et al.*, 2016). It is well known that the foamability strongly depends many factors including the surfactant having different physico-chemical properties (structure, rate of adsorption, interactions, etc.), the process of foam formation, surfactant concentration, critical micelle concentration (CMC) of the solute, etc. (Rosen and Solash, 1969; Marinova *et al.*, 2009) Generally, the foaming ability (or foamability) of a given solution is quantitatively defined through various parameters including; (i) the maximum height of the foam column,  $h_{\max}$ , (ii) the foam

height after a definite time interval (iii) the physical density of the foam (ratio of volume of foam/ volume of liquid used) (Malysa and Lunkenheimer, 2008).

### 2.2.3.2 Foam Stability

As stated before “all foams are thermodynamically unstable”, they are classified according to the kinetics of their breakdown: (i) unstable (transient) foams, lifetime of seconds and (ii) metastable (permanent) foams, lifetime hours or days (Tadros, 2005; Rosen and Kunjappu, 2012; Pugh, 2016). The foam stability can be explained via several approaches summarized as follow; (i) surface viscosity and elasticity, (ii) Gibbs–Marangoni effect, and (iii) surface forces (disjoining pressure) (Falbe, 1987; Tadros, 2005). Foam stability refers to the ability of the foam to maintain some of its properties constant with time or relevant to the lifetime of foam. There are three different mechanisms governing the foam lifetime: (i) foam drainage caused by gravity, (ii) coarsening caused by the transfer of gas between bubbles induced by the capillary pressure differences, and (iii) bubble coalescence caused by the rupture of liquid films between neighboring bubbles (Marinova *et al.*, 2009; Cantat *et al.*, 2013; Wang *et al.*, 2015). Commonly, the foam stability is determined by various aspects such as (i) the time interval after which the foam column has decayed to half of its maximum height,  $t_{1/2}$ , (ii) the volume and rate of the solution draining out as a function of time, and (iii) the retention time,  $t_r$ , providing the average life time of an unstable foam under steady state conditions (Malysa and Lunkenheimer, 2008)

## 2.3 Surfactant Adsorption at Air/Water Interface

A unique property of surfactants is to have tendency to adsorb at the interfaces of air/water and water/solid. This phenomenon, the surfactant needs to accumulate at the interface, is generally described as adsorption. Commonly, adsorption process has been studied to determine (i) the concentration of surfactant at the interface, (ii) the orientation and packing of the surfactant at the interface, (iii) the rate at which this adsorption occurs, and (iv) the energy changes,  $\Delta G$ ,  $\Delta H$ , and  $\Delta S$  in the system (Rosen and Kunjappu, 2012). Only the determination of surface concentration will be discussed in detail.



### 2.3.1 Equilibrium Surfactant Adsorption

The determination of the amount of surfactant adsorbed per unit area of liquid/gas interface cannot be carried out directly. The amount of surfactant adsorbed at an interface is usually calculated indirectly from surface tension measurements. Basically, the adsorption of surfactant molecules on any air/water interface can be described by Gibbs adsorption isotherm. It relates the surface excess concentration to the bulk concentration of surfactant and surface tension. The Gibbs equation (Tadros, 2005; Rosen and Kunjappu, 2012) can be written as;

$$\Gamma = -\frac{1}{nRT} \frac{d\gamma}{d \ln C} \quad (2.1)$$

where  $\Gamma$  is the surfactant surface excess concentration,  
 $\gamma$  is the surface tension of surfactant solution,  
 $C$  is the bulk surfactant concentration,  
 $R$  is the gas constant,  
 $n$  is the number of solute species whose concentration at the interface changes with change in the value of  $C$ , which is considered to be;  
     1 for a nonionic surfactant system or anionic surfactant with the presence of an excess concentration of electrolyte, and  
     2 for an anionic surfactant system without added electrolyte.  
 $T$  is the absolute temperature.

Apart from the Gibbs adsorption isotherm a number of other equations are also commonly used as summarized below (Chang and Franses, 1995; Eastoe and Dalton, 2000)

#### *Henry isotherm*

The simplest adsorption isotherm is the linear Henry isotherm, the isotherm and surface equation of state can be expressed as shown below;

$$\Gamma = K_H C \quad (2.2)$$

$$\Pi = \gamma_0 - \gamma = nRT\Gamma = nRTK_H C \quad (2.3)$$

where  $K_H$  is the Herry equilibrium adsorption constant, which is an empirical measure of surface activity,

$\Pi$  is the surface pressure,

$\gamma_0$  is the surface tension of pure water.

However, the Henry adsorption isotherm is only valid at very low surface concentrations due to the assumption that there is no interaction between the adsorbed surfactants. Moreover, this isotherm does not provide any the maximum or the level off values.

#### *Langmuir isotherm*

The most commonly used non-linear adsorption isotherm is the Langmuir adsorption isotherm, which based on the assumption of equivalent and independent adsorption sites on the surface. The adsorption rate of surface coverage is proportional to both the surfactant concentration and the number of vacant sites available, whereas the desorption rate is proportional to the number of adsorbed species. At equilibrium, both rates are equal. Therefore, the Langmuir adsorption isotherm and surface equation of state can be expressed as follows;

$$\Gamma = \Gamma_m \frac{K_L C}{1 + K_L C} \quad (2.4)$$

$$\begin{aligned} \Pi = \gamma_0 - \gamma &= nRT\Gamma_m \ln(1 + K_L C) \\ &= -nRT\Gamma_m \ln\left(1 - \frac{\Gamma}{\Gamma_m}\right) \end{aligned} \quad (2.5)$$

where  $K_L$  is the Langmuir equilibrium adsorption constant and

$\Gamma_m$  is the surface excess at saturation

Deviations from the Langmuir isotherm may be attributed to the failure of the assumption of there is no interaction between the adsorbed surfactants.

### Frumkin isotherm

This model has been modified from the Langmuir equation. It considers for solute/solvent interactions at a non-ideal surface.

$$C = \frac{1}{K_F} \cdot \frac{\Gamma}{\Gamma_m - \Gamma} \exp \left[ -A \left( \frac{\Gamma}{\Gamma_m} \right) \right] \quad (2.6)$$

$$\Pi = \gamma_0 - \gamma = -nRT\Gamma_m \ln \left( 1 - \frac{\Gamma}{\Gamma_m} \right) - \frac{1}{2} nRTA\Gamma_m \left( \frac{\Gamma}{\Gamma_m} \right)^2 \quad (2.7)$$

where  $K_F$  is the Frumkin adsorption constant and

$A$  is the constant depended on the non-ideality of the layer. If  $A=0$ , then these equations reduce to the Langmuir isotherm.

## 2.3.2 Dynamic Surfactant Adsorption

### 2.3.2.1. Introduction to Dynamic Surface Tension

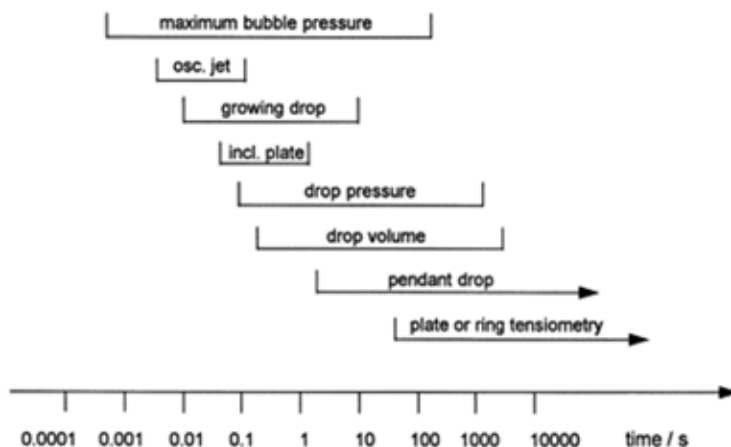


**Figure 2.4** Time windows for various dynamic surface tension techniques (Eastoe and Dalton, 2000).

In many interfacial processes, equilibrium conditions cannot be reached. In such cases, the dynamic surface tension (surface tension as a function of time) is a more important factor in determining the performance of the surfactant

in the process than its equilibrium surface tension (Rosen and Kunjappu, 2012). Figure 2.4 shows the time windows over which dynamic surface tension measurements can be made using the techniques (Dukhin *et al.*, 1995; Eastoe and Dalton, 2000).

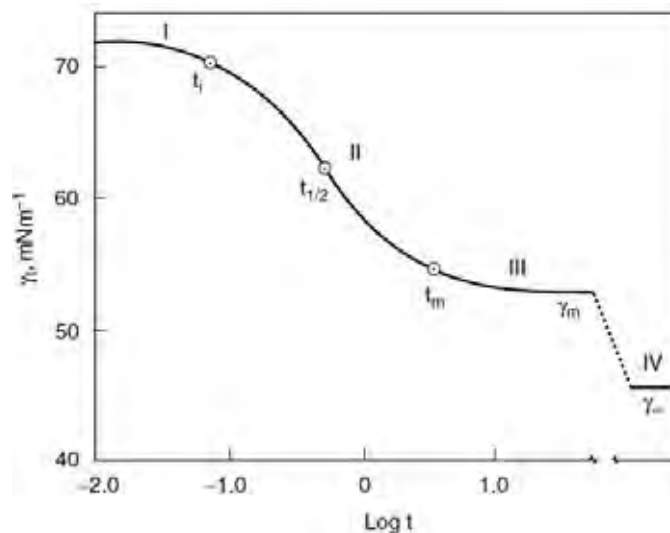


**Figure 2.5** Generalized dynamic surface tension (Rosen and Kunjappu, 2012)

The profile of the dynamic surface tension isotherm (Figure 2.5) can be divided into four regions: (i) the induction region, (ii) the rapid fall region, (iii) the meso-equilibrium region, and (iv) the equilibrium region. The first three regions can be described by the following equation (Hua and Rosen, 1988).

$$\gamma_t = \gamma_m + \frac{(\gamma_o - \gamma_m)}{[1 + (t/t^*)^n]} \quad (2.8)$$

where  $\gamma_t$  is the surface tension at time,  $t$ ,  
 $\gamma_o$  is the solvent (water) surface tension,  
 $\gamma_m$  is the meso-equilibrium surface tension,  
 $t$  is the time,  
 $t^*$  is the time required to attain a half value between  $\gamma_o$  and  $\gamma_m$   
 $n$  is a constant

The  $t^*$  value depends on the diffusion rate of surfactant from the bulk solution to the subsurface. The lower the  $t^*$  value, the lower the hindrance of diffusion, or the faster the diffusion rate of added surfactant. The  $n$  is a constant, depending on the molecular structure of added surfactant. It indicates the difference between the energies of surfactant adsorption and desorption (Hua and Rosen, 1991; Rosen and Kunjappu, 2012).

### 2.3.2.2. Dynamic Adsorption Mechanism

Generally, the adsorption of surfactant molecules on the interface is considered to be governed by two processes; (i) the diffusion of the surfactant molecules from the bulk solution to the sub-surface, and (ii) the transport of the surfactant molecules from the sub-surface onto the interface. There are two main models for surfactant transport and adsorption. Once the surfactant has diffused to the subsurface it will either instantaneously adsorb at the interface in accordance with (i) a diffusion-controlled model or will have to pass through (ii) a potential barrier (mixed kinetic-diffusion controlled model) to adsorb as shown in Figure 2.6 (Chang and Franses, 1995; Li *et al.*, 2010; Junji *et al.*, 2013).

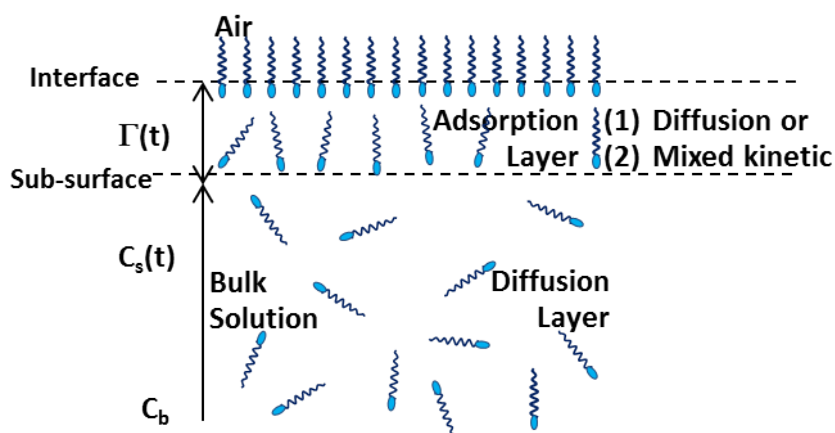


**Figure 2.6** Elementary processes in adsorption of soluble surfactants at air/water interface.

(i) Diffusion controlled adsorption model, there is spontaneous surfactant adsorption onto the air/water interface with a fast rate when the surfactant molecules transport from the bulk liquid phase to the sub-surface by the concentration gradient, known as diffusion. The diffusion-controlled adsorption kinetics was first treated quantitatively by Ward and Tordai (Ward and Tordai, 1946). When the adsorption is controlled by diffusion, then the diffusion equation (Fick's second law) is used to describe the process mechanism:

$$\frac{\partial c(x,t)}{\partial t} = D \frac{\partial^2 c(x,t)}{\partial x^2} \quad (2.9)$$

where  $D$  is the diffusion coefficient of surfactant,  
 $x$  is the distance from the surface, and  
 $C(x, t)$  is the surfactant concentration of surfactant molecules.

Equation (2.9) can be solved by the following initial and boundary conditions (Liu and Messow, 2000; Liu and Zhang, 2006; Li *et al.*, 2010; Junji *et al.*, 2013):

$$\begin{aligned} D \frac{\partial C(0,t)}{\partial x} &= \frac{\partial \Gamma(t)}{\partial t} \\ C(x, 0) &= C_0 \\ \Gamma(0) &= 0 \\ C(\infty, t) &= C_0 \end{aligned}$$

where  $C_0$  is the bulk surfactant concentration,  
 $\Gamma$  is the surface concentration of surfactant and  $\Gamma(0)$  indicates an initially clean air/water surface.

By using the Laplace transforms, the adsorption of surfactant molecules as a function of time can be formulated (Liu and Messow, 2000; Daniel and Berg, 2003; Acharya *et al.*, 2005; Li *et al.*, 2010; Phan *et al.*, 2012; Junji *et al.*, 2013; Casandra *et al.*, 2015; Jiang *et al.*, 2015; Liu *et al.*, 2016):

$$\Gamma(t) = 2c_0\sqrt{\frac{Dt}{\pi}} - 2\sqrt{\frac{D}{\pi}}\int_0^{\sqrt{t}} c_s d(\sqrt{t-\tau}) \quad (2.10)$$

where  $t$  is the time,  
 $\Gamma(t)$  is the surface excess concentration at time  $t$ ,  
 $D$  is the apparent diffusion coefficient,  
 $C_o$  is the bulk surfactant concentration,  
 $C_s$  is the surfactant concentration at the subsurface, and  
 $\tau$  is a dummy time delay variable.

The dynamic surface adsorption,  $\Gamma(t)$ , is not be possible to be directly measured, while dynamic surface tension can be measured accurately by maximum bubble pressure method. Hence, the term of  $\Gamma(t)$ , can be replaced by dynamic surface tension by using the Gibbs adsorption isotherm and the most common non-linear adsorption isotherm, typically Langmuir adsorption isotherm. The combined equation can be simplified to two cases of short and long time adsorption behaviors by using the asymptotic methods (Eastoe *et al.*, 1997; Tamura *et al.*, 1998; Liu and Messow, 2000; Tan *et al.*, 2004; Acharya *et al.*, 2005; Rojas *et al.*, 2010; Junji *et al.*, 2013; Jiang *et al.*, 2015; Chang *et al.*, 2016; Gao *et al.*, 2016; Liu *et al.*, 2016).

$$\text{Short time} \quad \gamma(t)_{t \rightarrow 0} = \gamma_o - 2RTC_o\sqrt{\frac{Dt}{\pi}} \quad (2.11)$$

$$\text{Long time} \quad \gamma(t)_{t \rightarrow \infty} = \gamma_{eq} + \frac{RT\Gamma_{eq}^2}{C_o}\sqrt{\frac{\pi}{4Dt}} \quad (2.12)$$

(ii) Mixed kinetic-diffusion model, this model assumes the surfactant molecules diffuse from the bulk to the subsurface, but the rate-controlling process is transfer of these molecules to the interface. Once the surfactant molecule has diffused to the subsurface, the adsorption does not occur spontaneously. It may have to do any of the following; the potential energy barrier, the correct orientation for adsorption, the strike of an ‘empty site’ in the interface, and the presence of

micelles, and the time-scale for break-up, may hinder adsorption. All of reasons cause the increase in the surface pressure, or attributes to there being less ‘vacant sites’ available for adsorption. This will cause the molecule to back diffuse into the bulk rather than adsorbing, thereby increasing the timescale of the dynamic surface tension decay (Eastoe and Dalton, 2000). This mixed kinetic model is based on the Ward and Tordai, Equation (2.10), and takes the exchange kinetics of surfactant between the interface and the subsurface adjacent into account (Liggieri *et al.*, 1996; Liu *et al.*, 2004). The renormalized diffusion coefficient,  $D^*$ , takes into account this activation barrier, and is related to the physical diffusion coefficient,  $D$ , by an Arrhenius-type relationship and is defined as (Eastoe and Dalton, 2000):

$$D^* = D \exp(-\varepsilon_a/RT) \quad (2.13)$$

where  $D^*$  is the renormalized diffusion coefficient,  
 $D$  is the physical diffusion coefficient,  
 $\varepsilon_a$  is the activation energies of adsorption,  
 $R$  is gas constant, and  
 $T$  is absolute temperature.

Using  $D^*$ , this process can now be considered as a diffusion problem, which can be solved using Fick’s equation with the new boundary condition:

$$\frac{d\Gamma}{dt} = D^* \left( \frac{\delta C}{\delta x} \right)_{x=0} \quad (2.14)$$

When a potential adsorption barrier is taken into account, the Ward and Tordai equation becomes:

$$\Gamma(t) = 2c_0 \sqrt{\frac{D_a t}{\pi}} - 2 \sqrt{\frac{D_a}{\pi}} \int_0^{\sqrt{t}} c_s d(\sqrt{t - \tau}) \quad (2.15)$$



where  $D_a$  is defined as:

$$D_a = \frac{D^{*2}}{D} = D \exp(-2\varepsilon_a/RT) \quad (2.16)$$

## 2.4 Adsorptive Bubble Separation

Adsorptive bubble separation processes are one of effective technology for separation of materials. This process bases on the selective adsorption or attachment of materials on the surfaces of gas bubbles rising through a solution or suspension. The performance of this separation process depends on the proper of chemical reagents used including; (i) frother: which is used to produce a stable froth, and (ii) collector which is used to interact with targeted materials and carries them to adsorb at air/liquid interface of the air bubble (Kawatra, 2011; Stevenson and Lambert, 2012).

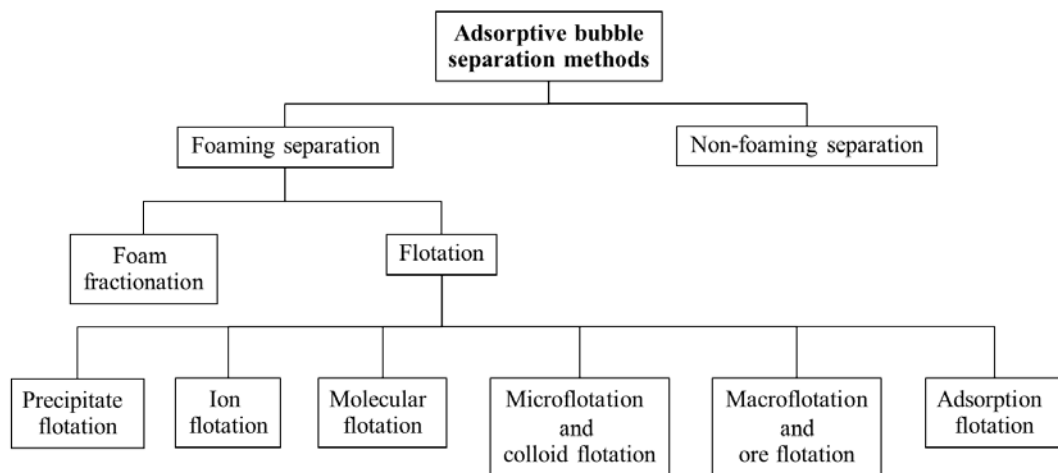


**Figure 2.7** Classification for the adsorptive bubble separation methods (Lemlich, 2012).

Figure 2.7 outlines the most widely accepted classification of the various adsorptive bubble separation processes, which can be divided into two categories; (i) foam separation, which involves the production of foam in the process, and (ii) non-

foaming separation, which involves no production of foam (Wang, 2006). The definitions of those technical terms are briefly summarized in Table 2.1.

**Table 2.1** Classification of the adsorptive bubble separation techniques (Wang, 2006)

I.	Non-foaming adsorptive bubble separations
A.	Solvent sublation
B.	Bubble fractionation
II.	Foam separations
A.	Foam fractionation; a homogeneous aqueous system in which the surface active agent tends to adsorb at the bubble interface generated foam and all targeted materials are mostly transferred in the foam phase.
B.	(Froth) Flotation; a process in which targeted species being separated from the bulk liquid media is insoluble.
1.	Precipitate flotation; the flotation of non-surface active agent (i.e. precipitating agent) by adding surfactant.
2.	Ion flotation; the removal of anions or cations by using an oppositely charged surfactant.
3.	Molecular flotation; very similar to ion flotation, except that the surfactant forms an insoluble complex with a nonsurface-active molecule (i.e., not an ion).
4.	Microflotation and colloid flotation; the removal of microscopic particles such as microorganisms and colloids by attaching to foam.
5.	Macroflotation and ore flotation; the removal of macroscopic particles by attaching to foam.
6.	Adsorption flotation; the removal of dissolved pollutants by adsorbent particles (such as activated carbon) in a bubble reactor, and subsequent the removal of activated carbon as well as other suspended particles by flotation technique.

#### 2.4.1 Froth Flotation

Froth flotation is one of the most broadly used separation, where species with different surface properties is induced to adsorb preferentially at the bubble surface via the interfacial boundary between a dispersed phase (bubble) and

continuous phase (liquid) (Scamehorn and Harwell, 1988; Harwell, 2000). The targeted materials can be effectively separated by means of the physical-chemical bubble attachment mechanism (Wang, 2006; Wills and Napier-Munn, 2015). Figure 2.8 shows a rising gas bubble, which eventually come out from the solution surface to form froth (Wang, 2006). During the process of froth flotation, the targeted material and surface-active substances attached to the generated foam has an upward movement which can then be floated by gas bubbles while the liquid present in foam film or lamellae as well as un-attached materials is drained out by gravitational force (Du *et al.*, 2000; Burghoff, 2012). This process offers many advantages for the treatment of industrial wastewaters as compared to the other treatment processes: low space and energy requirement; simplicity in design, operation and scale-up; low capital and operating costs (Wong *et al.*, 2001). Thus, it is currently in use for many diverse applications, which is particularly useful for processes that are not amenable to conventional gravity concentration.

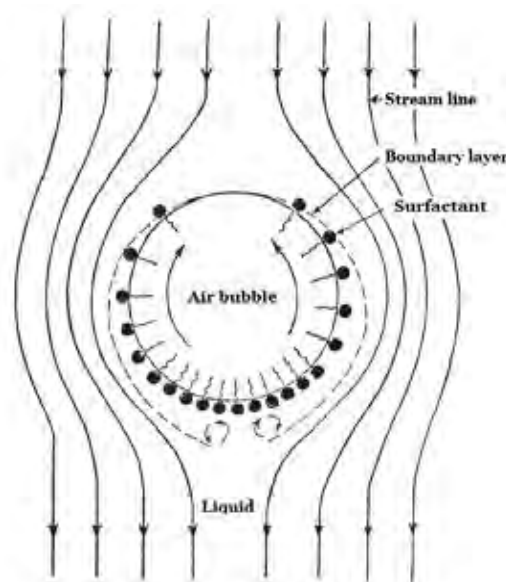


**Figure 2.8** A rising gas bubble in bubble separation column containing a surface-active agent (Wang, 2006).

A basic configuration of froth flotation column can be described in the same manner as foam fractionation, as shown in Figure 2.9. In a froth flotation operation, air is introduced at the bottom of a froth flotation column to generate the rising pneumatic air bubbles. The target material adheres at the surface of the generated bubbles, which have the opportunity to attach to bubbles and commence their journey up the column, and then the air bubbles leave the solution surface to form foam. The generated foam will overflow out of a column or be scrapped off (Harwell, 2000; Boonyasuwat *et al.*, 2003; Stevenson and Lambert, 2012).

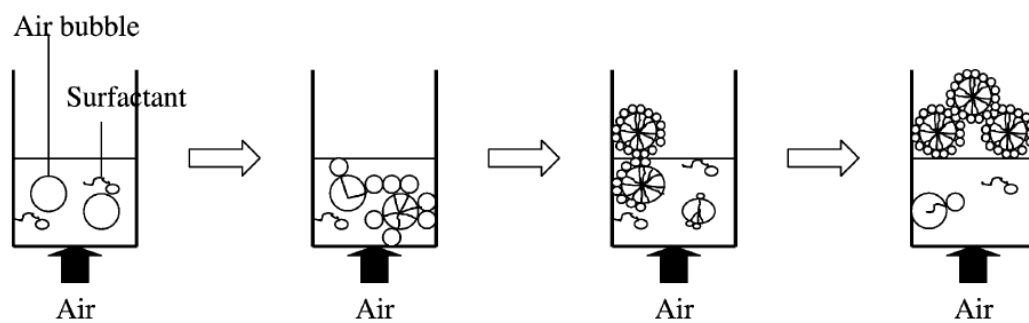


**Figure 2.9** Principle of foam fractionation (Boonyasuwat *et al.*, 2003).

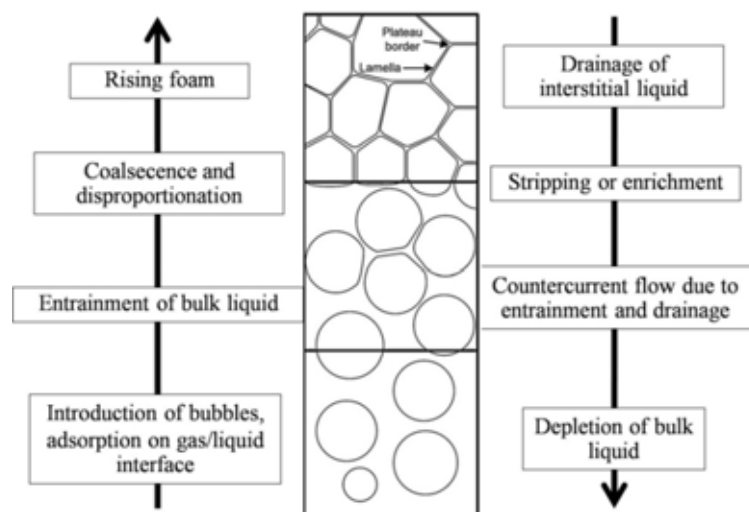


**Figure 2.10** Different effects during formation and stabilization of foam (Burghoff, 2012).

The opposite flow direction of the liquid by gravitational drainage simultaneously occurs with the rise of generated foam. Figure 2.10 illustrates that the upward flow is caused by the entrainment of bulk liquid among introduced gas bubbles; however, this entrained liquid is gravitated back to the feed solution causing a backflow and dryer foams during rising (Burghoff, 2012). Thus, the concentrations of surface active substance and target material increase with increasing foam height. This principle can be used for the separation and concentration of surface active substances as well as target materials.

#### 2.4.2 Mode of Operation

There are two modes of foam separation: (i) simple mode (batch or continuous) and (ii) higher mode (with enriching and/or stripping) as shown in Figure 2.11 (a-e) (Lemlich, 1968; Wang, 2006).

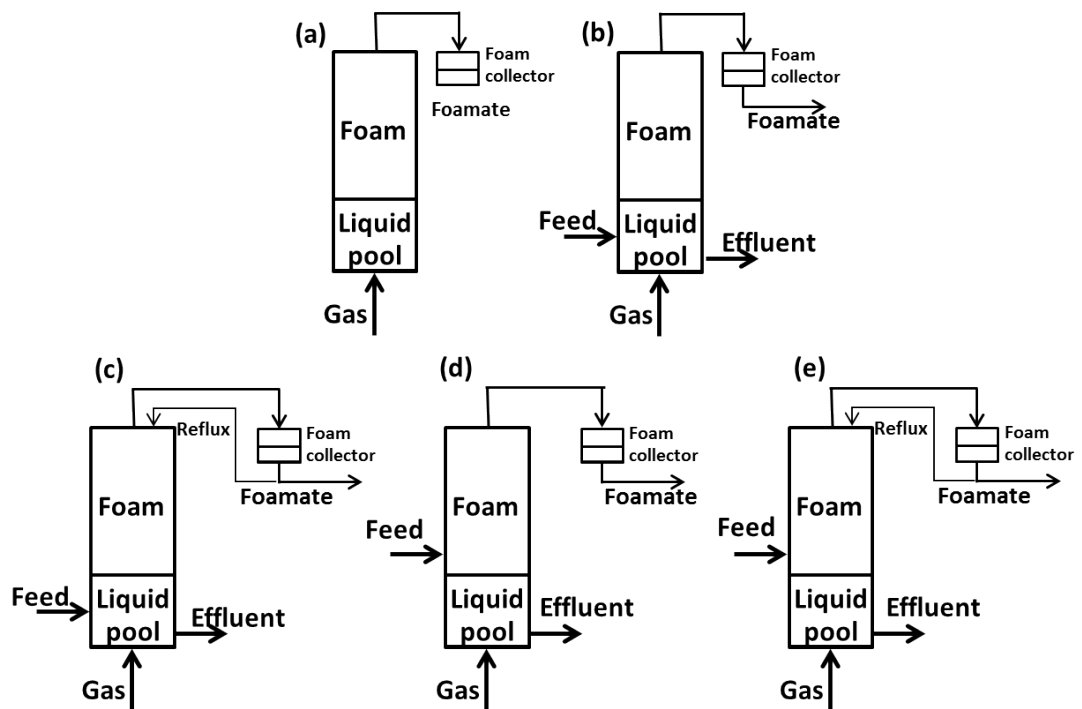


**Figure 2.11** Foam separation mode is described by (a) batch and (b) continuous operation. Continuous operations involving counter flow are described by (c) enriching, (d) stripping and (e) combined (stripping and enriching).

*Simple batch mode* (Figure 2.11a); a certain volume of surfactant solution is added to the foam column to form foam. Foam or product is collected at the top of the column. It can be run with or without reflux. Normally, the batch operation is for a small scale and for high value product.

*Simple continuous mode* (Figure 2.11b); fresh feed is introduced continuously into the liquid pool, while foam and a proportion of the bulk liquid (effluent) are removed from the top and bottom of the foam column, respectively. Collected foam is enriched in surfactant, while the effluent is depleted.

*Enriching mode* (Figure 2.11c); part of the foamate is fed back on the top of the top of the column and flows in counter-current to the rising foam. Since the reflux is richer than the interstitial liquid, the mass transfer resulting from this counter-current may considerably increase the enrichment.

*Stripping mode* (Figure 2.11d); the “stripper” feed enters the column at some distance above the liquid pool in counter-current to the rising foam and tends to replace interstitial liquid.

*Combined mode* (Figure 2.11e); a combination of the enriching and stripping modes.

### 2.4.3 Material Transport in Flotation Column

Basically, a mass balance of surfactant around a well-mixed stage during process can be demonstrated in Figure 2.12a. A feed solution is introduced to a column. Surface-active solutes and targeted materials that are readily attachable to the air bubbles are carried up to the surface of the water by the bubbles. The enriched material at the top (collapsed foam from a foam separation column) and the clarified drain solution at the bottom are withdrawn from the system. The mass balance of a surfactant in the collapsed foam at the top of column under steady state condition is shown in Figure 2.12b. It is the molar flow rate of foamate ( $C_f V_f$ ), which is equal to the sum of the mass transfer by the bulk liquid and the adsorptive transports (Darton *et al.*, 2004).

The overall material balance for the process is as follows:

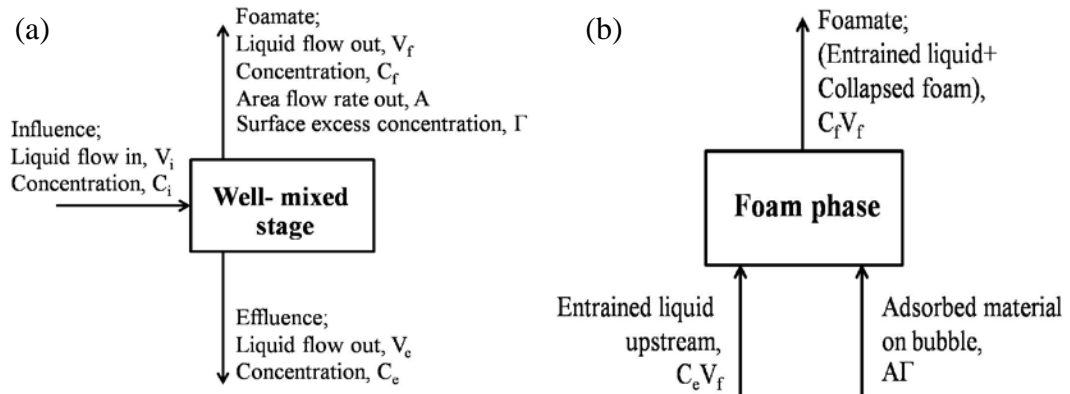


**Figure 2.12** Material balances; (a) around well-mixed stage in the foam fractionation of a liquid and (b) around foam phase (Darton *et al.*, 2004).

Performing overall mass balance;

$$V_i C_i = V_e C_e + V_f C_f \quad (2.17)$$

Performing mass balance in the collapsed foam (foamate);

$$V_f C_f = V_f C_e + A\Gamma \quad (2.18)$$

$$C_f = C_e + A\Gamma \left( \frac{1}{V_f} \right) \quad (2.19)$$

Substitute (2.19) into (2.17);

$$V_i C_i = V_e C_e + V_f C_e + A\Gamma \quad (2.20)$$

$$V_i C_i = (V_e + V_f) C_e + A\Gamma \quad (2.21)$$

For simple mass balance;

$$V_i = V_e + V_f \quad (2.22)$$

Thus 
$$V_i C_i = V_i C_e + A\Gamma \quad (2.23)$$

$$C_i = C_e + A\Gamma \left( \frac{1}{V_i} \right) \quad (2.24)$$

Take (14)-(19), the final equation will be;

$$C_f - C_i = A\Gamma \left( \frac{1}{V_f} - \frac{1}{V_i} \right) \quad (2.25)$$

It is clearly seen that the term of  $(C_f - C_i)$  increases with the increase in surface area provided by the bubble stream and the amount of surface adsorption, and the decrease in entrainment of the liquid in the foamate, implying that the

enrichment ( $C_f/C_i$ ) and recovery act inversely in the flotation applications. Nonetheless, the combination of process parameters and physico-chemical parameters is still necessary to be optimized in order to obtain both high enrichment and high recovery. The separation performance of the flotation column is expressed in term of % surfactant recovery, enrichment ratio, and separation factor, as described below:

$$\% \text{ Surfactant recovery} = \frac{C_f V_f}{C_i V_i} \times 100 \quad (2.26)$$

$$\text{Enrichment ratio} = \frac{C_f}{C_i} \quad (2.27)$$

$$\text{Separation factor} = \frac{C_f}{C_e} \quad (2.28)$$

where  $V_f$  is the volumetric flow rate of the collapsed foam (foamate),  
 $V_i$  is the volumetric flow rate of the feed,  
 $V_e$  is the volumetric flow rate of the effluent,  
 $C_f$  is the surfactant concentration in the collapsed foam,  
 $C_i$  is the surfactant concentration in the feed,  
 $C_e$  is the surfactant concentration in the bulk liquid or in the effluent,  
 $A$  is the flow rate of the interfacial area of the generated foam, and  
 $\Gamma$  is the surface excess concentration.

#### 2.4.4 Multistage Froth Flotation

A conventional method of flotation is already known for almost a century. Various operating parameters had been investigated and concluded that there are the competitive effects on the enrichment and recovery (Wood and Tran, 1966; Lemlich, 1968). Recall that, in flotation column, the two major process performance metrics of the enrichment and the recovery have to be considered. Generally, there is a trade-off between high recovery and high enrichment (Stevenson and Li, 2014); a product stream that is highly concentrated in target



species is often obtained at the expense of low recovery and vice versa. Thus, choices of appropriate operation parameters are made to have the optimal combination of enrichment and recovery for a given system. However, instead of simply making compromises, various process intensification methods have previously been proposed. Most of these methods are based on the fact that enrichment in the flotation process is a combined effect of interfacial adsorption and foam drainage. Therefore, in order to obtain a high enrichment, the process have to generate and maintain a high gas-liquid interface (adsorption enhancement method) while reducing the interstitial liquid (drainage enhancement method) as much as possible (Stevenson and Li, 2014).

Multistage process consists of devices with physically distinct stages, either in the compact form of a single column with internal components that resemble those found in distillation columns (Criswell, 1976; Leonard and Blacyki, 1978; Boonyasuwat *et al.*, 2003, 2005, 2009; Rujirawanich *et al.*, 2011, 2012) or a series of conventional columns connected with pipes and fittings (Morgan and Wiesmann, 2001). Both designs are based on the assumption that adsorption mainly occurs in the liquid pool, and that only one equilibrium stage of adsorption can be achieved in a conventional column. Therefore, a higher surface excess can be achieved by repeated foaming cycles.

Multistage froth flotation with bubble caps is basically analogous to a distillation unit. For an ideal distillation unit, a vapor phase is in equilibrium with an aqueous phase in each tray, whereas, the foam phase is in equilibrium with an aqueous phase in the flotation unit, as illustrated in Figure 2.13a) (Rujirawanich *et al.*, 2012). Taking into account the multistage froth flotation, it can be named as a single stage flotation column connected in series. For its feed position at the top tray (Figure 2.13b), surfactant and/or any target materials molecules found in a lower tray, which come from draining liquid containing residual surfactant passing through downcomer, can be recovered back to the top tray by adsorbing onto the surface of rising foams. Internal bubble coalescence within the rising foam before passing through the bubble caps is also likely to occur due to sudden change in flow cross sectional area, resulting in increasing internal reflux and enhanced enrichment ratio. Thus, the effluent surfactant concentration is very low, while most of surfactant

molecules are carried upward by rising foam to the top tray (Rujirawanich *et al.*, 2011, 2012)

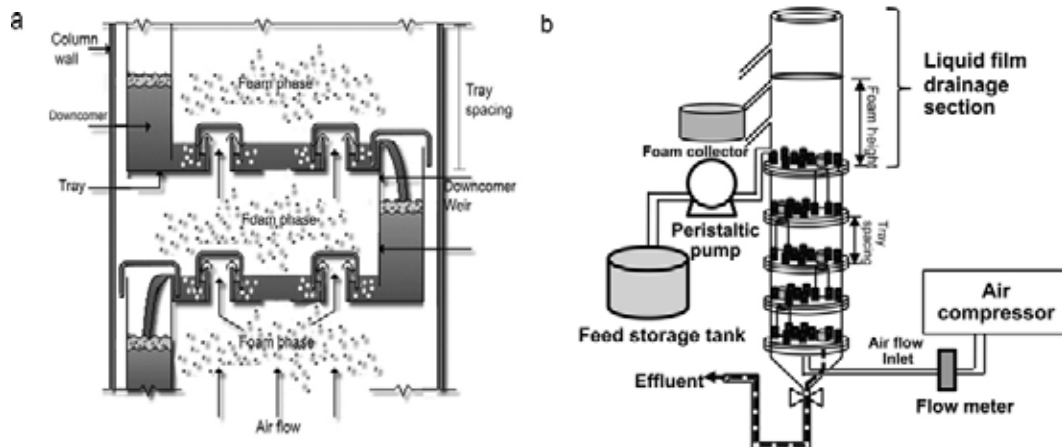


**Figure 2.13** Schematic drawings of (a) bubble caps tray and (b) a multistage foam fractionation column (Rujirawanich *et al.*, 2012).

**CHAPTER III**  
**REMOVAL OF MOTOR OIL BY MULTISTAGE FROTHFLOTATION:**  
**EFFECT OF OPERATIONAL PARAMETERS**

(Published in Separation Science and Technology)

**3.1 Abstract**

A continuous multistage froth flotation column was employed to remove motor oil from water at a low concentration (500 mg/L) using an extended surfactant—branched alcohol propoxylate sulphate sodium salt ( $C_{14-15}-(PO)_8SO_4Na$ )—as a frother. The highest separation efficiency (97% motor oil removal with the enrichment ratio of 16 for motor oil) was obtained at a foam height of 60 cm, an air flow rate of 40 L/min, a feed flow rate of 60 mL/min, a surfactant concentration of 0.3% (w/v), and an NaCl concentration of 1.5% (w/v). The process performance increased with increasing tray number but beyond 4 trays, the system could only offer lower concentrations of motor oil and surfactant in the effluent.

**Keywords:** Multistage froth flotation; Motor oil removal; Extended surfactant

### 3.2 Introduction

Motor oil is a lubricant for the moving parts of internal combustion engines. However, it undergoes thermal as well as mechanical degradation and needs to be periodically replaced, resulting in used motor oil often being found in wastewater. In order to comply with environment regulations, a proper treatment system for motor oil contaminated wastewater has to be employed prior to discharging it to the environment. A variety of treatment techniques have been developed and applied for the removal of oil from wastewater, including coagulation/flocculation [1, 2], biological treatment [3, 4], membrane-separation process [5, 6], and ultrafiltration [7–9]. However, these traditional treatment techniques are not economically feasible for applying to wastewater containing a low concentration of oil. Adsorptive bubble separation, typically a froth flotation technique, is one of the most promising oily wastewater treatment processes due to its several advantages, such as low space and energy requirement; simplicity in design, operation, and scale-up; low operating cost, and no solvent or heat requirement [10, 11]. The froth flotation technique has been successfully employed for the removal of various oil types in our research group, such as ortho-dichlorobenzene [12, 13], ethylbenzene [14, 15], diesel oil [16, 17], motor oil [18] and cutting oil [19]. Based on the above research, it can be concluded that froth flotation is considered one of the most effective treatment processes for concentrating, as well as for separating, both suspended solids and oils, especially at low concentrations.

In a froth flotation operation, air is introduced at the bottom of a froth flotation column to generate rising air bubbles. Both the added surfactant and target material can adsorb preferentially at the air/water interface of the rising air bubbles and then they emerge from the solution surface to form foam (foamate), which flows out from the column or is scraped out from a flotation tank. The process performance of the froth flotation is governed by two mechanisms of the adsorptive transport and the bulk liquid transport. The former is an upward stream of the adsorbed materials on the foam surface while the latter is an upward stream of lamella liquid with unadsorbed molecules, known as the entrained liquid. The bulk liquid transport not only contributes to the removal but also causes the reduction of the enrichment ratio

and separation factors of any target material due to the dilution of the entrained liquid. On the other hand, the adsorptive transport is responsible for the increase in the enrichment ratios and separation factors, apart from the removal of both surfactant and target material [20].

Froth flotation has been mostly applied in single-stage systems in either a batch or continuous mode. Continuous multistage froth flotation has seldom received attention although much higher separation efficiency can be achieved [21, 22]. In the present work, a continuous multistage froth flotation unit was employed, for the first time, for motor oil removal from water using an extended surfactant (Alfoterra<sup>®</sup> C145–8PO) as a frother. Several factors affecting the separation efficiency including foam height, air flow rate, feed flow rate, and surfactant and salt concentrations were systematically investigated. The separation efficiency was determined based on the following evaluating parameters: removal percentage, enrichment ratios, residual factors, and separation factors of both surfactant and motor oil. The process performance was also correlated to surfactant adsorption and dynamic surface tension in order to gain a better understanding of how oil can be removed by generating foam.

### **3.3 Experimental**

#### **3.3.1 Materials and chemicals**

Branched alcohol propoxylate sulphate; sodium salt ( $C_{14-15}(PO)_8SO_4Na$ ) or Alfoterra<sup>®</sup> C145–8PO; an anionic extended surfactant having 14–15 carbon atoms and eight groups of propylene oxide (PO) with sulphate as a hydrophilic group (molecular weight of 783 with of 28.7% in liquid form) was kindly supplied by Sasol North America Inc. (USA). Motor oil (Performa Synthetic grade, SAE 5W–40, API SM/CF, commercially available for gasoline engines in Thailand), model contaminant oil, produced by PTT Public Co., Ltd (Thailand) was used. It consists of 85% v/v of a complex mixture of lubricating oils (petroleum),  $C_{20-50}$  hydrotreated neutral oil–base, and 10–15% (v/v) lubricant additive package. NaCl (analytical grade, 99% purity) was obtained from Labscan Asia Co., Ltd.

(Thailand). All chemicals were used as received without further purification; distilled water was used throughout the experiment.

### 3.3.2 CMC and surface tension isotherm determination

The surface tension of test solutions containing different concentrations of surfactant and NaCl was measured by using a tensiometer (Krüss, K100, Germany) with a Wilhelmy plate at 25 °C. An abrupt change in the slope of the plot between surface tension and log of surfactant concentration was used to identify the critical micelle concentration (CMC). The surface excess concentration or adsorption density of the surfactant ions at the air/water interface ( $\Gamma$ ) in mol/cm<sup>2</sup> was calculated from the following Gibbs adsorption isotherm equation [23]:

$$\Gamma = -\frac{1}{nRT} \frac{d\gamma}{d \ln C} \quad (3.1)$$

where  $\gamma$  is the equilibrium surface tension (mN/m),  $C$  is the bulk surfactant concentration ( $\mu\text{M}$ ),  $n$  can be either 1 or 2—the former for an ionic surfactant with a swarming concentration of added electrolyte or for a nonionic surfactant and the latter for an ionic surfactant in the absence of electrolyte,  $R$  is the gas constant (8.31 J/mol K), and  $T$  is the absolute temperature (K).

### 3.3.3 Dynamic surface tension measurement

Dynamic surface tension was measured using a bubble pressure tensiometer (Krüss, BP2, Germany) at 25 °C. A gas bubble was generated by introducing air zero through a capillary tube. The pressure inside the air bubble generated at the tip of the capillary tube was monitored and recorded with time until the air bubble burst. The final pressure and the diameter of the capillary tube were used to calculate a value of dynamic surface tension at different bubble ages.

### 3.3.4 Multistage froth flotation experiments

Figure 3.1 illustrates the configuration of the multistage froth flotation column and the bubble caps in each tray. The multistage froth flotation column used in this experiment had four stainless steel trays connected in series. Each tray had an inner diameter of 20 cm with a tray spacing of 15 cm. Each tray had 16 bubble caps

with a weir height of 5 cm, a cap diameter of 2.5 cm, and a sample port for taking liquid samples. The top tray was connected to a stainless steel foam column having the same inner diameter (20 cm) with different foam outlet heights of 30, 60, and 90 cm [21,24]. To achieve high process separation performance; (i) the generated foam must pass through the bubble caps (not passing through the downcomer) and (ii) the liquid flows only through the downcomer (not passing through the bubble caps) [22].

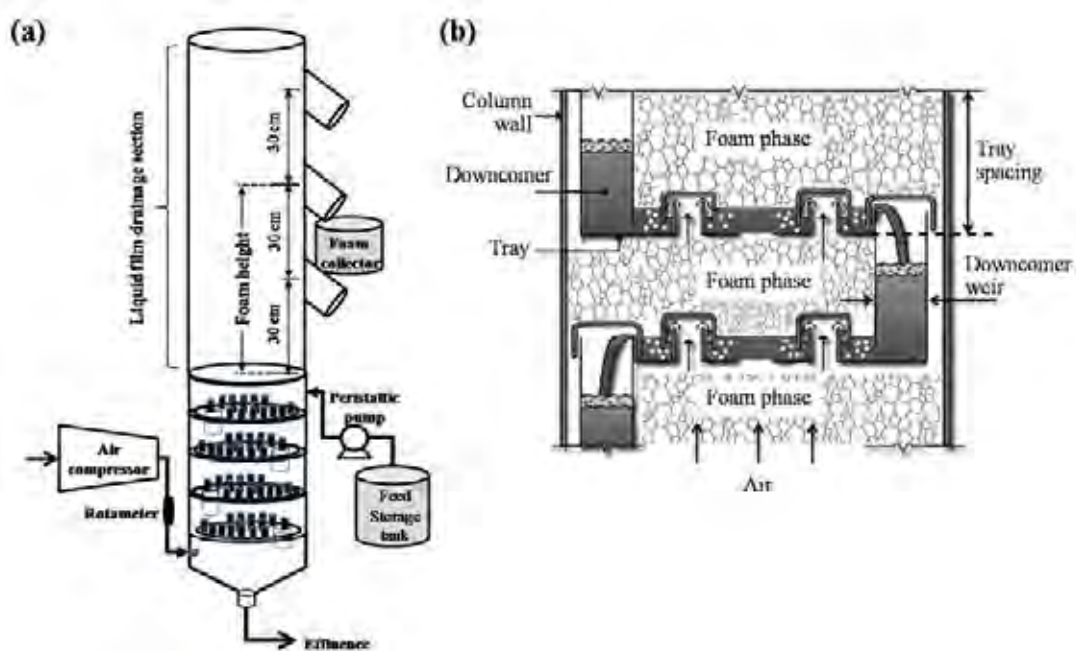


**Figure 3.1** Schematic drawing of (a) multistage froth flotation column and (b) foam phase in equilibrium with aqueous phase for froth flotation system.

A well-mixed solution containing a constant motor oil concentration of 500 mg/L at two different surfactant concentrations, 0.3% and 0.5% (w/v), was fed continuously to the top of the column at different feed flow rates in the range of 40–100 mL/min controlled by a peristaltic pump (Masterflex<sup>®</sup>, L/S<sup>®</sup> Digital Drives). The motor oil concentration of 500 mg/L was selected in this study because it represented a low oil concentration that is not possible both technically and economically to use a conventional oil-trap chamber for oil separation. The water solubility of motor oil was around 10 mg/L in pure water at room temperature while

it increased to 40 mg/L in the 0.3% (w/v) surfactant solution. Hence, the added motor oil in the feed was mostly present in free oil (92%) with a very low portion of 8% solubilized in micelles. The reason why these two surfactant concentrations (0.3% and 0.5%) were used in this study will be explained later. Filtered air was introduced at the bottom of the column and the air flow rate was regulated in the range of 20–80 L/min using a rotameter. The generated foam rose up through the multistage froth flotation column and was collected at the top of the column with different foam heights—30, 60, and 90 cm. The experiments were carried out at room temperature (25–30°C). Each run was operated to reach a steady state, at which both concentrations of surfactant and motor oil in the foamate and effluent samples were invariant with time. The experimental data taken from the steady state condition (at least three replicate) were averaged and these data were then used to determine the process performance. The concentrations of surfactant and the total concentration of both surfactant and motor oil were determined by an UV–visible spectrophotometer (Perkin–Elmer, Lambda 10, USA) at a wavelength of 210 nm and a total organic carbon analyzer (Shimadzu, TOC–VCSH, Japan), respectively. The concentration of motor oil was calculated by subtracting the surfactant concentration in terms of total organic carbon (TOC) from the total TOC concentration. The material balance was used to calculate the error of experimental data. Less than 10% error of surfactant mass balance was acceptable for this experiment [21, 22].

### 3.3.5 Foamability and foam stability measurements

Foamability and foam stability measurements were independently conducted using a glass column, having an internal diameter of 5 cm and a column height of 120 cm. One hundred milliliter of a well-mixed solution, containing a constant motor oil concentration of 500 mg/L and a constant surfactant concentration of 0.3% (w/v) at various NaCl concentrations, was added to the column. Compressed air was introduced at the bottom of the column at a rate of 0.1 L/ min, which was regulated by a mass flow controller (Aalborg, GFC171S), to generate fine air bubbles by passing through a sintered glass disk with pore size diameters in the range of 16–40  $\mu\text{m}$  [18]. The time required to reach a maximum height of 120 cm was used to indicate foamability. The time required for the foam to collapse from 120 cm to 60



cm without introducing air was used to indicate foam stability [21]. The froth characteristic experiments were carried out at room temperature (25–30 °C).

### 3.3.6 Calculation of process performance

The separation efficiency performance of the multistage froth flotation column was determined in terms of the enrichment ratios, removals, residual, and separation factors of surfactant and motor oil [22, 25]. All these evaluating parameters are described below:

$$\begin{aligned} \text{Enrichment ratio} &= \frac{C_f}{C_i} \\ \text{Residual factor} &= \frac{C_e}{C_i} \\ \text{Separation factor} &= \frac{C_f}{C_i} \\ \text{Removal percentage} &= \frac{C_i V_i - C_e V_e}{C_i V_i} \times 100 \\ \text{Foamate volumetric ratio} &= \frac{V_f}{V_i} \end{aligned}$$

where  $C_e$  is the concentration of motor oil or surfactant in the effluent sample,  $C_f$  is the concentration of motor oil or surfactant in the foamate (collapsed foam),  $C_i$  is the initial concentration of motor oil or surfactant in feed solution,  $V_e$  is the volumetric flow rate of effluent,  $V_f$  is the volumetric flow rate of foamate, and  $V_i$  is the volumetric flow rate of inlet (or feed) solution.

## 3.4 Results and Discussion

### 3.4.1 Fundamental properties of surfactant

The use of extended surfactant has been reported to provide potential benefits for treating aqueous systems containing immiscible hydrocarbon oils. This is because the unique molecular structure of extended surfactant provides a smoother transition between hydrophilic and hydrophobic regions of the interface between aqueous and hydrocarbon phases to create a more suitable environment for solubilization of both water and oil [17, 26]. The presence of propoxylate (PO) group

in the alkyl chain length of surfactant can lower the critical microemulsion concentration ( $C_{\mu C}$ ) and increase oil solubilization, resulting in an increase in oil removal in a single stage froth flotation system [27, 28]. In our previous studies, it was revealed that the maximum oil removal well corresponded to the minimum interfacial tension (IFT) of the system [13–17, 29]. Later, both process parameters of foamability (how easy to form foam) and foam stability (how long the generated foam to exist) are very crucial to the oil separation efficiency. Hence, the extended surfactant (Alfoterra<sup>®</sup> C145–8PO), as anionic surfactant, was chosen for this study, which can provide high oil solubilization with a high water solubility, low IFT, and high foamability and foam stability. It was hypothesized to be a good frother to remove motor oil from water.

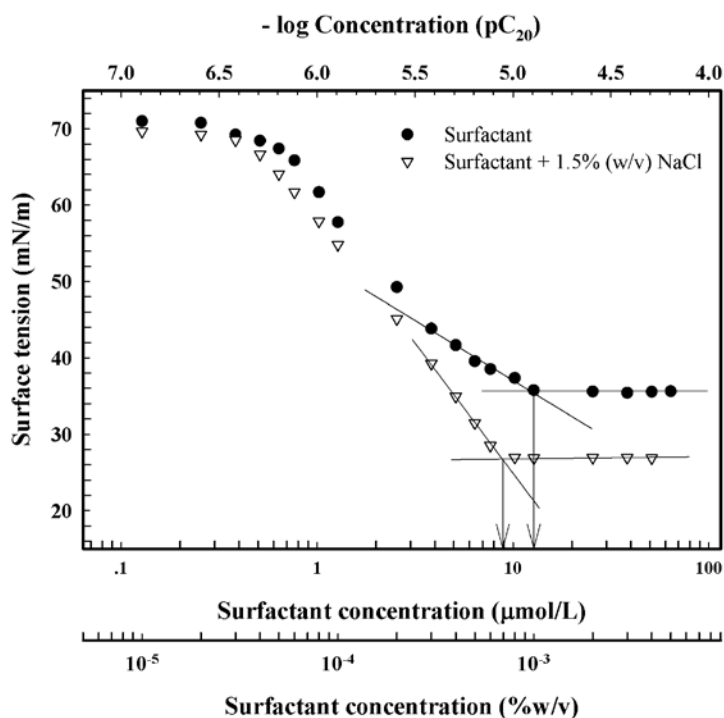


**Figure 3.2** Surface tension isotherms of surfactant with and without NaCl addition at 25°C.

The plots of surface tension versus log of the initial surfactant concentration with and without 1.5% (w/v) NaCl for determining the CMC and the

calculated values of surfactant adsorption density are shown in Figure 3.2 and 3.3, respectively. The reason for investigating only the addition of 1.5% (w/v) NaCl will be described later.

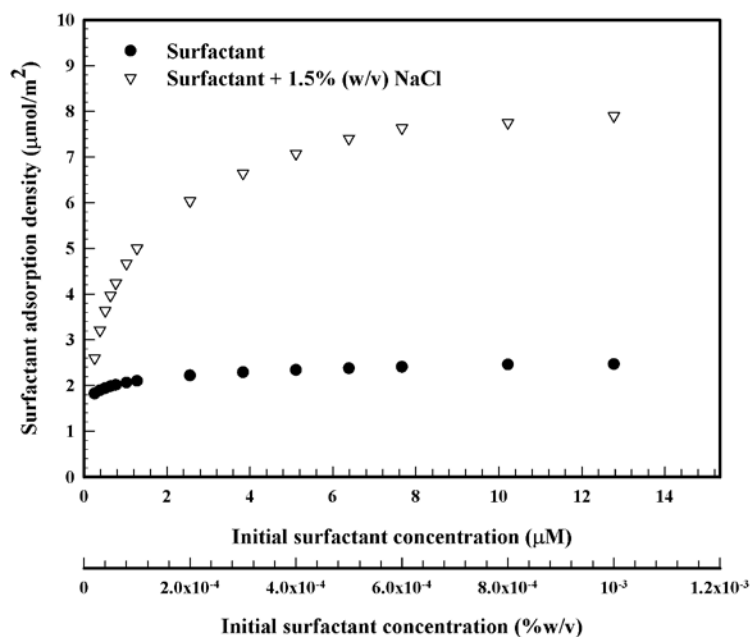


**Figure 3.3** Adsorption density of surfactant with and without 1.5% (w/v) NaCl addition at air–liquid interface at 25°C.

**Table 3.1** Calculated values of CMC,  $\gamma_{\text{CMC}}$ ,  $pC_{20}$ , and saturated surface concentrations ( $\Gamma_m$ ) of surfactant with and without NaCl addition

Solution	CMC ( $\mu\text{M}$ )	$\gamma_{\text{CMC}}$ (mN/m)	$pC_{20}$	$\Gamma_m$ ( $\mu\text{mol}/\text{m}^2$ )
Surfactant	12.75	35.5	5.38	2.39
Surfactant + 1.5% (w/v) NaCl	8.87	27	5.74	7.83

Table 3.1 summarizes the CMC, the surface tension at CMC ( $\gamma_{\text{CMC}}$ ), the negative logarithm of surfactant concentration in the bulk phase required to reduce the surface tension by 20 mN/m ( $pC_{20}$ ), and the effectiveness of adsorption

( $\Gamma_m$ ) of the surfactant with and without NaCl. The surface tension isotherm shifted toward lower surfactant concentration and the surface tension above the CMC decreased greatly with the addition of 1.5% (w/v) NaCl. The values of CMC of the 0.3% (w/v) surfactant solution and the 0.3% (w/v) surfactant solution with 1.5% (w/v) NaCl were 12.75 and 8.75  $\mu\text{M}$  or 9.98 and 6.96 mg/L, respectively. Hence, the added surfactant was in the form of micelles. A larger value of  $pC_{20}$  indicates higher surfactant adsorption efficiency at the air/water interface and a higher ability for the reduction of surface tension [23]. The  $pC_{20}$  value of the surfactant with 1.5% (w/v) NaCl was observed to be higher than that without NaCl, suggesting that the addition of NaCl can enhance the surfactant adsorption density. The effectiveness of surfactant adsorption onto the air/water interface is an important factor affecting several properties of the surfactant, including foaming, which directly governs the process performance of froth flotation. By using the Gibbs close-pack monolayer equation [23, 25, 30], the surfactant adsorption density was reviewed to be greatly enhanced (approximately four times) by adding NaCl (see Figure 3.3). The increase in surfactant adsorption at the air/water interface by adding NaCl results from the counterion effect ( $\text{Na}^+$ ) to reduce the repulsion force between the negatively charged head group of the surfactant [31]. The higher the surfactant adsorption onto the air/water interface, the higher the foamability and foam stability.

In this study, the lowest surfactant concentration of 0.3% (w/v) was found to be capable to produce stable foam to reach a highest foam height of 90 cm. Beyond a surfactant concentration of 0.5% (w/v), the separation efficiency was very low because the system had a very high foamate fraction (high bulk liquid transport). Thus, only two surfactant concentrations, 0.3% and 0.5% (w/v), to represent dry and wet foam, respectively, were selected to study the froth flotation performance.

### 3.4.2 Dynamic surface tension

Froth flotation is a process fundamentally governed by foam formation (foamability) and foam stability, which are related to the surfactant adsorption density at the air bubble interface between a dispersed gas phase and a bulk liquid phase [24].

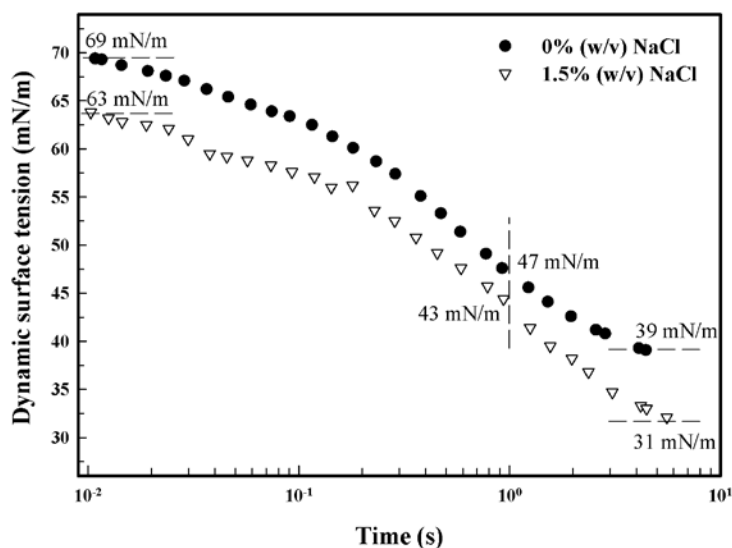


**Figure 3.4** Dynamic surface tension of 0.3% (w/v) surfactant solution with and without 1.5% (w/v) NaCl addition.

A sufficient air flow rate is basically needed to generate air bubbles through the retaining solution in each tray to produce foam rising up through the bubble caps of an upper tray. The superficial velocity of air was used to correlate how fast air bubbles pass through the solution in each tray. Dynamic surface tension can be used to indicate how fast an added surfactant adsorbs on the interface of generated air bubbles, which can directly affect the process performance of the froth flotation [32]. Figure 3.4 shows the dynamic surface tension profiles of the 0.3% (w/v) surfactant solution with and without added NaCl. The presence of NaCl lowered the dynamic surface tension, indicating that the addition of NaCl can shorten the time for surfactant adsorption on the air/water interface [18]. Under the studied conditions, the superficial air velocity was in the range of 1.06–4.24 cm/s and so the required time for air bubbles to pass through the solution in each tray was greater than 1 s. Based on the minimum contact time of rising air bubbles of 1 s, the surface tension reduction is about 72% for the pure surfactant solution or 62% for the surfactant solution with 1.5% (w/v) NaCl, suggesting that both foamability and foam stability in each tray could reach at least more than 50% of their maximum values.

The results suggest that an increase in the liquid depth in each tray can improve the process performance of the studied multistage froth flotation unit.

### 3.4.3 Operating limits

The principles of the multistage froth flotation system with bubble caps are quite similar to those of a distillation unit. Vapour–liquid phase equilibrium is applied for the distillation unit while foam–liquid phase equilibrium is applied for the froth flotation unit. The efficiency of the multistage froth flotation depends on column configuration, operational conditions, and the types and concentrations of surfactants and electrolytes [22, 25, 33]. Hence, the multistage froth flotation has to be appropriately operated to achieve the expected functions. Foam rises only through the bubble caps (not passing through the downcomer) and the liquid flows down only through the downcomer (not passing through the bubble caps) for all trays [25].

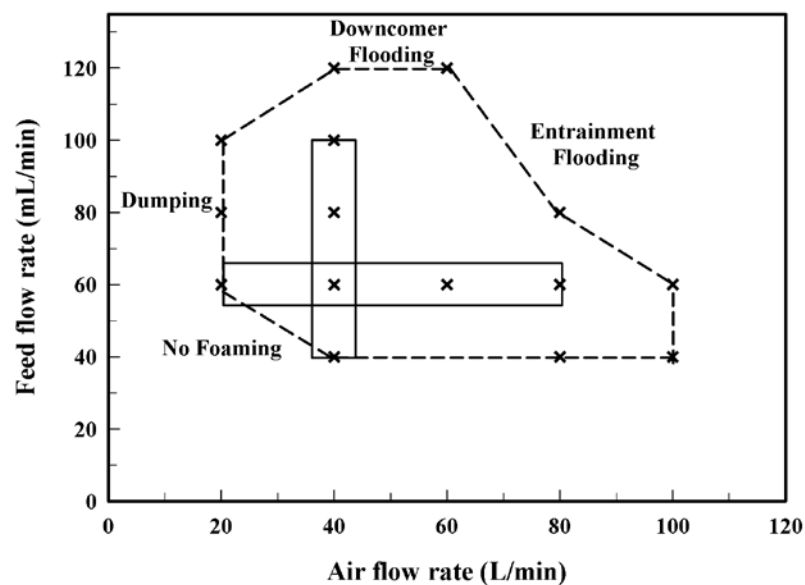


**Figure 3.5** Boundaries of operational zone of flotation column [Conditions: Surfactant concentrations of 0.3% and 0.5% (w/v) and motor oil concentration of 500 mg/L].

Figure 3.5 shows the operational region (dash line) of the studied multistage froth flotation column operated at a feed solution having 0.3% or 0.5% (w/v) surfactant concentration and 500 mg/L motor oil. As shown in Figure 3.5, there are three unstable regions: (i) no foaming region, (ii) dumping region, and (iii) flooding region [34]. The first region occurred when the system was operated at both very low air and feed flow rates. The generated foam could not reach the foam outlet, causing no separation of both surfactant and motor oil. The second region only took place at a very low air flow rate. Since the pressure of the air was not high enough to hold up the liquid in each tray, a substantial portion of liquid could flow down through bubble caps and finally dump through to the base of the column; therefore, performance separation significantly could decrease [25]. The last region was the flooding, which can be classified into two sub-regions: (i) downcomer flooding and (ii) entrainment flooding. The downcomer flooding occurred when the liquid level in each tray was higher than the overflow weir of the downcomer when the system was operated under a very high air flow rate with a moderate feed flow rate. At a very high throughput of feed with a moderate air flow rate, a significant quantity of liquid could pass through the upper tray through the downcomer, resulting in entrainment flooding [34]. To conduct all experiments, both air and liquid flow rates selected were located in the operational zone. The air flow rate was investigated in the range of 20–80 L/min, while the feed flow rate varied in the range of 40–100 mL/min.

#### 3.4.4 Effects of foam height

Figure 3.6 shows the effect of the foam height on the process performance of the multistage froth flotation unit operated at an air flow rate of 40 L/min, a feed flow rate of 60 mL/min, and two different surfactant concentrations of 0.3% and 0.5% (w/v). For any surfactant concentration in the feed solution, both motor oil removal and surfactant recovery decrease with the increase in foam height, whereas the enrichment ratios, separation factors, residual factors, and effluent concentrations of both motor oil and surfactant increase, as shown in Figure 3.6a–e, respectively.

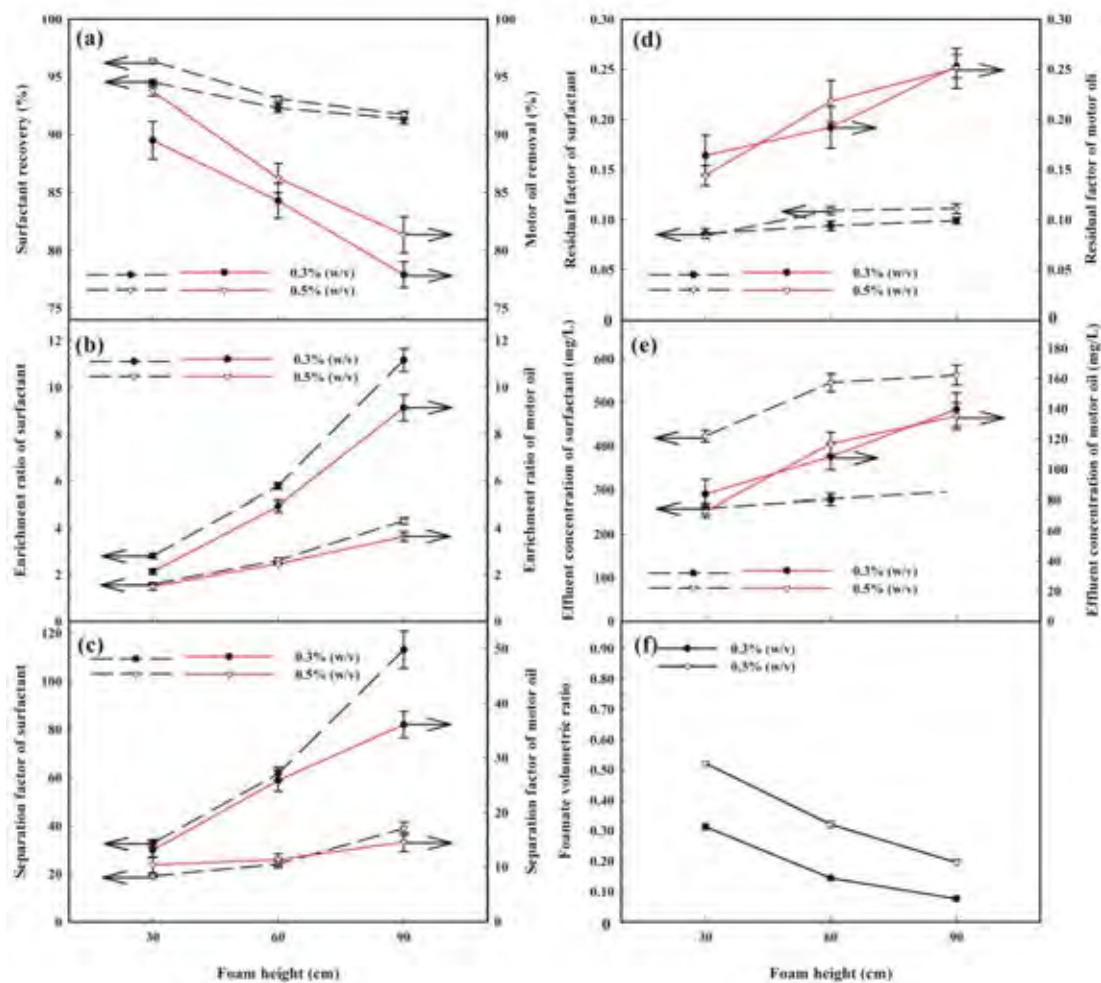


**Figure 3.6** Effect of foam height on (a) surfactant recovery and motor oil, (b) enrichment ratio, (c) separation factor, (d) residual factor, (e) effluent concentration, and (f) foamate volumetric ratio under two different surfactant concentrations—0.3% and 0.5% (w/v) [Conditions: air flow rate of 40 L/min, feed flow rate of 60 mL/min, and motor oil concentration of 500 mg/L].

The present results are in good agreement with several previous studies [17, 20, 21, 24, 35, 36]. The results can be explained by the fact that an increase in foam height basically increases the residence time of generated foam, allowing more liquid to drain out from the foam lamellae, resulting in drier foam, as evidenced experimentally by the reduction of the foamate volumetric ratio, as shown in Figure 3.6f. Hence, an increase in foam height simply reduces the bulk liquid



transport, causing increases in the enrichment ratios and separation factors of both surfactant and motor oil, except the motor oil removal and surfactant recovery, which rely on both adsorptive and bulk liquid transports. However, surfactant recovery was found to be moderately decreased with increasing foam height as compared with the drastic decrease in motor oil removal. It is due to most of the surfactant molecules adsorbing at the air/water interface of generated foam, leading to a small fraction of surfactant in the liquid drainage [22, 23].

It is very interesting to point out that by visual observation, the structures of generated foam changed along the foam height. The generated foam at the bottom of the foam column, known as fresh foam, had a spherical shape with thick liquid films while the foam, especially at the highest foam height, looked polyhedral with thinner liquid films.[33,37] This observation confirms that the drainage of excess liquid from the foam lamellae increased as foam height increased.

In a comparison of the two surfactant concentrations, the low surfactant concentration of 0.3% (w/v), which was found to be the lowest surfactant concentration capable of producing stable foam to reach the highest foam height of 90 cm, provided better separation efficiency than the high surfactant concentration of 0.5% (w/v). From the foamate volumetric ratio results (Figure 3.6f), it can be concluded that a lower surfactant concentration can reduce the bulk liquid transport. The results are in good agreement with previous studies.[20,24,35]

The present results suggest that an optimum foam height has to trade off between the bulk liquid transport and the adsorptive transport in order to achieve both high removal and high enrichment ratio of motor oil. Hence, a foam height of 60 cm was selected for further investigation of the effects of other operational parameters.

#### 3.4.5 Effect of air flow rate

Figure 3.7 shows the effects of the air flow rate on the separation performance of the studied multistage froth flotation unit by varying the air flow rate stepwise from 20 to 80 L/min at a foam height of 60 cm, a feed flow rate of 60 mL/min and two different feed surfactant concentrations, 0.3 and 0.5% (w/v), with 500 mg/L motor oil.

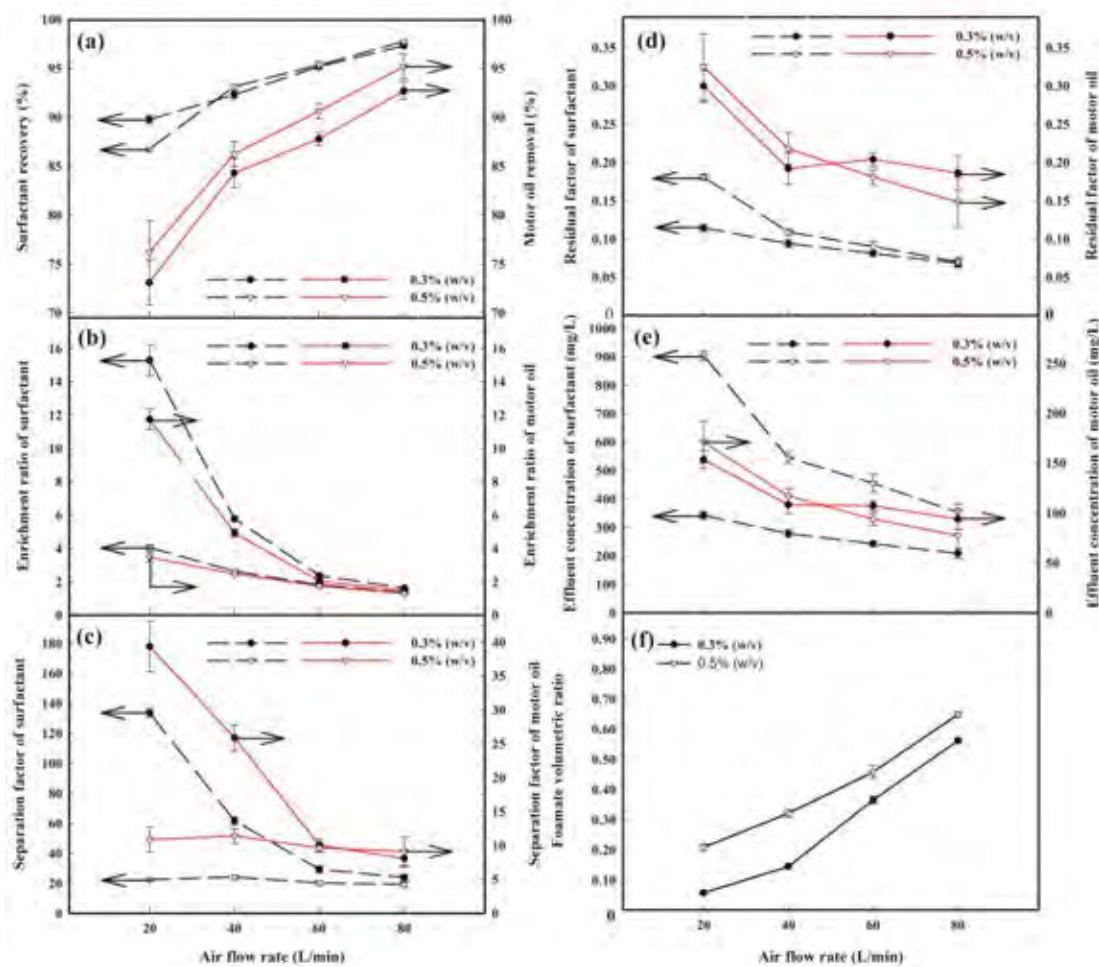


**Figure 3.7** Effect of air-flow rate on (a) surfactant recovery and motor oil, (b) enrichment ratio, (c) separation factor, (d) residual factor, (e) effluent concentration, and (f) foamate volumetric ratio under two different surfactant concentrations—0.3% and 0.5% (w/v) [Conditions: foam height of 60 cm, feed flow rate of 60 mL/min, and motor oil concentration of 500 mg/L].

As the air flow rate increased, both motor oil removal and surfactant recovery increased for both surfactant concentrations (Figure 3.7a). Conversely, the enrichment ratios, separation factors, residual factors, and effluent concentrations of both motor oil and surfactant decreased markedly with increasing air flow rate, as shown in Figure 3.7b–e, respectively. These observations are in good agreement with those of other studies [19, 21, 24, 38–40]. The results of the increase in foamate

volumetric ratio with increasing air flow rate (see Figure 3.7f), suggest that the bulk liquid transport increases with the increase in air flow rate. It can be explained by the fact that an increase in air flow rate (increasing superficial velocity from 1.06 to 4.24 cm/s) increases both foam production rate and foam rising velocity, leading to a lowering of the residence time of generated foam. The higher the air flow rate, the higher the amount of water entrained by the bubbles (wetter foam) or the higher the bulk liquid transport [35]. It can be used to explain why the motor oil removal and surfactant recovery increased while the enrichment ratios and separation factors decreased with the increase in the air-flow rate [14, 25].

An increase in surfactant concentration from 0.3% to 0.5% (w/v) caused significant reduction of the enrichment ratios and separation factors but had an insignificant effect on both motor oil removal and surfactant recovery; this is consistent with some previous works [10, 24, 39, 41]. An increase in surfactant concentration basically increases both foam production rate and water content in produced foam as indicated experimentally by the increase in foamate volumetric ratio, causing a large increase in the bulk liquid transport with a small increase in the adsorptive transport. The results presented earlier suggest that a multistage froth flotation column has to be operated at a proper air flow rate (not too low and not too high) to trade off between the two removal mechanisms of adsorptive transport and bulk liquid transport in order to achieve both high removal and enrichment ratio of oil. Hence, the optimum air flow rate of 40 L/min was chosen for further investigation of other effects in order to maximize the process performance of the studied multistage froth flotation unit.

#### 3.4.6 Effect of feed flow rate

An increase in the feed flow rate results in the decreases in motor oil removal, surfactant recovery, enrichment ratios and separation factors of both surfactant and motor oil, as shown in Figure 3.8a–c, respectively. In contrast, Figure 3.8d and e show the residual factors and effluent concentrations of both surfactant and motor oil increase substantially with the increase in feed flow rate, especially at high feed flow rates (beyond 80 mL/min).

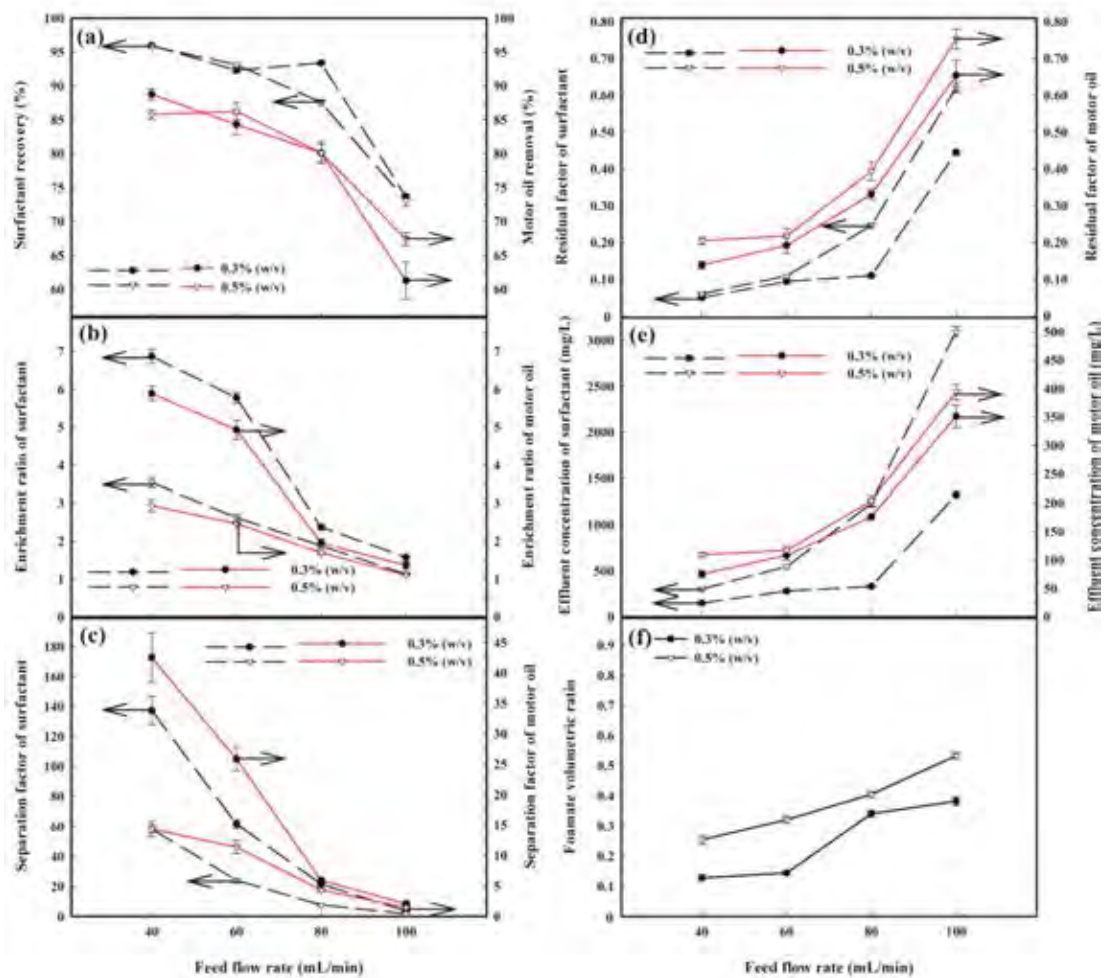


**Figure 3.8** Effect of feed-flow rate on (a) surfactant recovery and motor oil, (b) enrichment ratio, (c) separation factor, (d) residual factor, (e) effluent concentration, and (f) foamate volumetric ratio under two different surfactant concentrations—0.3% and 0.5% (w/v) [Conditions: foam height of 60 cm, air flow rate of 40 L/min, and motor oil concentration of 500 mg/L].

The results can be explained by the fact that an increased feed flow rate expands the quantity of surfactant to promote a foam production rate, leading to higher bulk liquid transport as confirmed experimentally in Figure 3.8f (an escalation in foamate volumetric ratio with increasing feed flow rate). However, at a very high feed flow rate, the separation performance in terms of motor oil removal, surfactant recovery, enrichment ratios, and separation factors of both surfactant and motor oil

decreased sharply with the increase in feed flow rate. At a very high feed flow rate (greater than 80 mL/min), an increase in feed flow rate directly increased the quantities of both surfactant and motor oil in the system, leading to lowering the separation efficiency. The results are consistent with previous studies [20, 22].

In a comparison between the two surfactant concentrations in the feed solution, the motor oil removal and surfactant recovery did not depend on the surfactant concentration but the enrichment ratios and separation factors of both motor oil and surfactant decreased significantly with increasing surfactant concentration from 0.3% to 0.5% (w/v). As can be seen in Figure 3.8f, the foamate volumetric ratio escalates with increasing surfactant concentration from 0.3% to 0.5% (w/v), indicating that the increasing surfactant concentration from 0.3% to 0.5% (w/v) simply increased the bulk liquid transport, leading to lowering both enrichment and separation factors but it did not affect the motor oil removal and surfactant recovery [41, 42].

#### 3.4.7 Effects of salt concentration

The presence of salt is one of the key factors affecting the froth flotation performance when an ionic surfactant is used as a frother. Most of real wastewaters contain a significant concentration of salts and so studies of salt effects are directly beneficial to the application of froth flotation to wastewater treatment. Several studies reported that the addition of salt in an anionic surfactant system could enhance oil removal efficiency [16–18]. Hence, the effect of NaCl concentration on the froth flotation performance was observed in this study under the base operational conditions (a foam height of 60 cm, an air flow rate of 40 L/min, a feed flow rate of 60 mL/min, and a surfactant concentration of 0.3% wt/v with 500 mg/L motor oil).

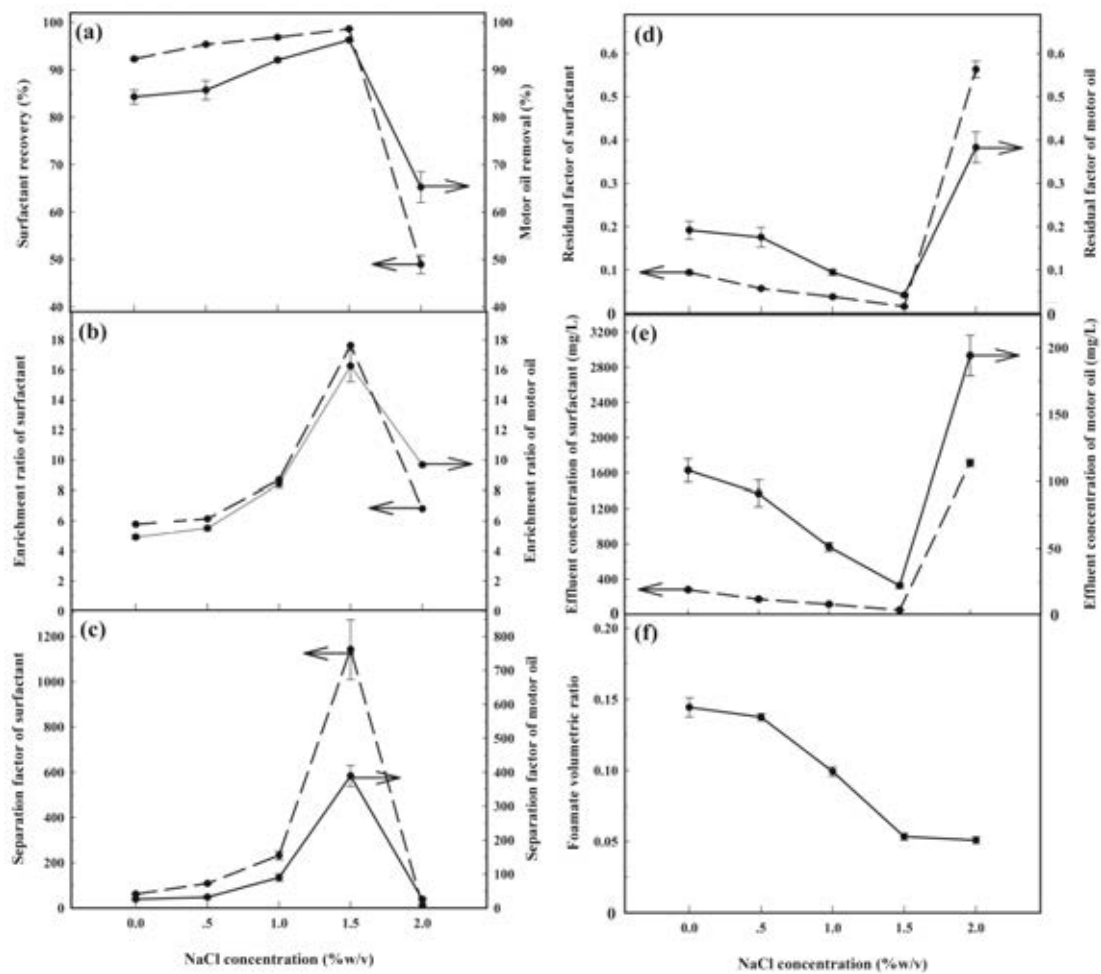


**Figure 3.9** Effect of salt concentration on (a) surfactant recovery and motor oil, (b) enrichment ratio, (c) separation factor, (d) residual factor, (e) effluent concentration, and (f) foamate volumetric ratio [Conditions: foam height of 60 cm, air flow rate of 40 L/min, feed flow rate of 60 mL/min, and motor oil concentration of 500 mg/L].

Figure 3.9 shows the effect of added NaCl on the separation process performance of the studied multistage froth flotation column. As shown in Figure 3.9a–c, both motor oil removal and surfactant recovery slightly rise and the enrichment ratios and separation factors remarkably increase with the increase in NaCl concentration up to 1.5% (w/v) and they reached maximum levels at a NaCl concentration of 1.5% (w/v). However, with a further rise in the NaCl concentration from 1.5% (the optimum NaCl concentration) to 2.0% (w/v), they decreased

drastically. In contrast, both residual factors and effluent concentrations of surfactant and motor oil showed opposite trends (see Figure 3.9d and e). The foamate volumetric ratio was found to significantly decrease with the increase in NaCl concentration up to 1.5% (w/v). Beyond the optimum NaCl concentration of 1.5% (w/v), the foamate volumetric ratio slightly decreased with further increase in NaCl concentration (see Figure 3.9f). An addition of NaCl in any ionic surfactant system can affect both foamability and foam stability, leading to significant effects on the separation process performance of the studied multistage froth flotation unit. The foam characteristics as a function of NaCl concentration will be discussed later.

From the results, the best process performance for motor oil removal as well as surfactant recovery by the studied multistage froth flotation system can be achieved at a foam height of 60 cm, an air flow rate of 40 L/min, a feed flow rate of 60 mL/min, and a NaCl concentration of 1.5% (w/v).

#### 3.4.8 Foam characteristics

For a better understanding of the separation mechanisms of the multistage froth flotation column, foam characteristic experiments were carried out to determine both foamability and foam stability of the generated foam in order to correlate to the separation process performance. The longer the time to reach the maximum foam height (120 cm), the lower the ability to produce foam (foamability), whereas the longer the time required for the generated foam to collapse from 120 to 60 cm, the higher the foam stability. The effects of NaCl concentration on foamability and foam stability are shown in Figure 3.10.

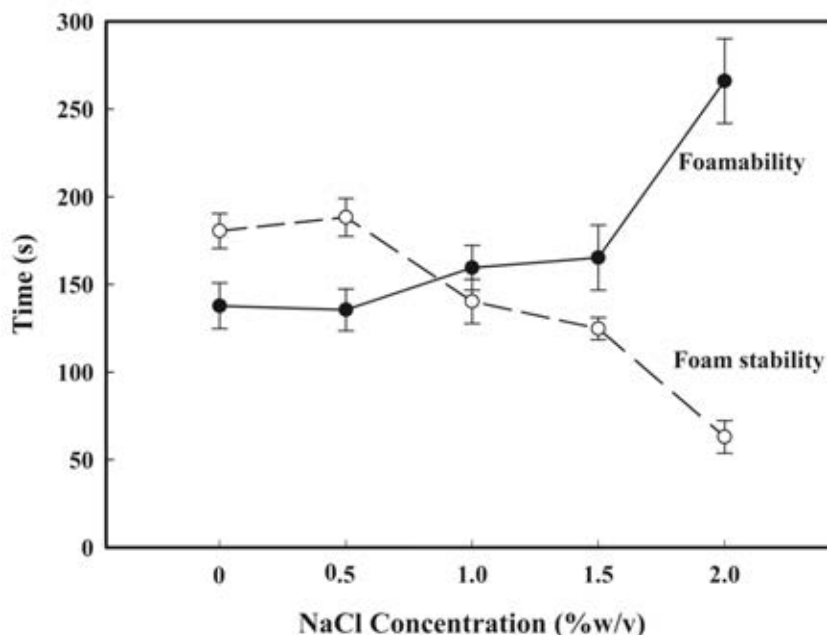


**Figure 3.10** Foam characteristics in terms of foamability and foam stability as a function of NaCl concentration [0.3% (w/v) surfactant and 500 mg/L motor oil].

An increase in NaCl concentration up to 0.5% (w/v) slightly increased foamability but beyond the optimum salinity of 0.5% (w/v), both foamability and foam stability decreased remarkably with further increase in NaCl concentration. An addition of NaCl can provide the co-adsorption of counterions of  $\text{Na}^+$  ions to reduce the repulsion force between negatively charged head groups of the surfactant, resulting in increasing surfactant adsorption on the foam lamella surfaces. As a result, both foamability and foam stability increased when NaCl was added up to 0.5% (w/v). However, when NaCl was further added beyond the optimum NaCl concentration of 0.5% (w/v), both foamability and foam stability decreased remarkably with further increase in NaCl concentration. When too much NaCl is added, it simply reduces the repulsion forces between the two surfaces of foam lamellae by adding  $\text{Na}^+$  ions to neutralize the negatively charged head group of surfactant adsorbing on the foam lamellae surfaces, causing a reduction of both foamability and foam stability. This explanation can be used for the effects of added NaCl on the separation process performance of the continuous multistage froth flotation system, as described earlier. Interestingly, the optimum NaCl concentration,



as shown in Figures 3.9 and 3.10, was much different. The great difference in the optimum NaCl concentrations in these two experiments resulted from the different operational conditions. The multistage froth flotation column was operated in a continuous mode while the foam characteristic experiment was operated in a batch mode.

#### 3.4.9 Concentration profiles of surfactant and motor oil

Figure 3.11 shows the concentration profiles of surfactant and motor oil in the solution in each tray, as compared to those in the feed solution and effluent under the optimum operational conditions. The lowest concentrations of both surfactant and motor oil were observed at the bottom tray while the highest concentration could be found at the topmost tray. In each tray, surfactant and motor oil adsorbing on the air bubble surface and then were carried together with the rising air bubbles and emerged from the solution to form foam. After that, the rising foam was collapsed when passing through the caps on the upper tray of the column, causing the enrichments of both surfactant and motor oil in the solution of the upper tray. As a result, the transport direction of both surfactant and motor oil is upward. From the results, it can be concluded that the higher the tray number, the higher the removal efficiencies of both surfactant and motor oil. However, in a comparison of the concentrations of both surfactant and motor oil in the solution in each tray to those in a lower tray, they decreased greatly for the first two top trays (tray 4 and tray 3). The removal efficiency by the last tray (tray 1) was relatively low. Hence, an increase in tray number greater than 4 is not recommended for a design and operation of a multistage froth flotation column.

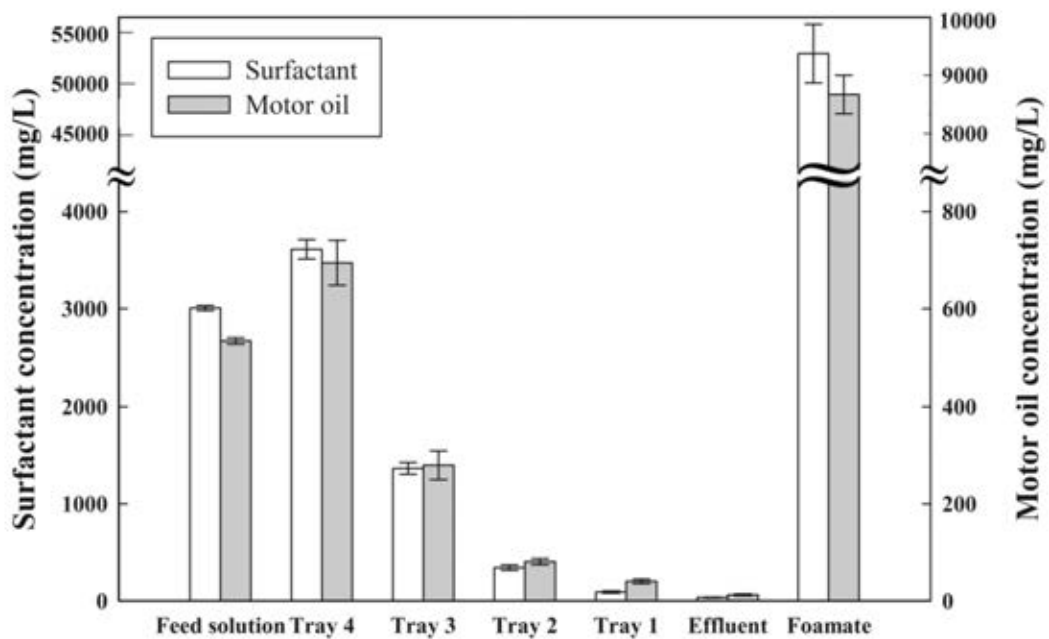


**Figure 3.11** Concentration profiles of surfactant and motor oil under 0.3% (w/v) surfactant and 1.5% (w/v) NaCl. [Conditions: foam height of 60 cm, air flow rate of 40 L/min, feed flow rate of 60 mL/min, and motor oil concentration of 500 mg/L].

#### 3.4.10 Comparisons of separation process performance

Table 3.2 shows a comparison of the separation performance of the studied multistage with previous batch and single-stage froth flotation units. It can be clearly observed that the main problem of batch and continuous mode of all single-stage froth flotation could provide almost complete removal of any studied oil (>99%) with a very low enrichment ratio of oil (~2), while this studied multistage froth flotation column gave more or less high oil removal with extremely high enrichment ratios of both motor oil and surfactant (16.3 and 17.6, respectively).

Table 3.2 Comparison of the process performance of different froth flotation units

Type of oil	Surfactant	NaCl (% w/v)	Oil concentration	Process	HRT (min)	% Removal		Enrichment ratio		Ref
						Oil	Surfactant	Oil	Surfactant	
ODCB	SDS (3.5% w/v)	1.25	Oil/water = 1/100	Batch, Single stage	-	~ 40	~20	-	-	12
	CPC (3.5% w/v)	1.75				~55	~35	-	-	
	DADS (3.5% w/v)	7				~50	~25	-	-	
ODCB	Total surf conc. (5% w/v) (SDS/NP(EO)10 = 4/1)	-	Oil/water = 1/100	Batch, Single stage	-	Almost 100%	100 % for NP(EO)10 80 % for SDS	-	-	13
Ethylbenzene	AMA (0.3% w/v)	3	Oil/water = 1/1	Batch, Single stage	-	Almost 100%	~80	1.75	-	14, 15
Diesel Oil	Alfoterra 145-4PO (0.1% w/v)	3	Oil/water = 1/1	Batch, Single stage	-	91.54	98.3	1.53	-	16
Diesel Oil	Alfoterra 145-4PO (0.1% w/v) and SDS (0.5% w/v)	4	Oil/water = 1/19	Continuous, Single stage	60	~75	~96	~2	~1.8	17
Motor oil	Alfoterra 145-5PO (0.5% w/v)	5	Oil 500 mg/L	Continuous, Single stage	30	~60	~50	~1.7	~2	18
Cutting oil	SDS (0.1% w/v)	6	Oil 500 mg/L	Continuous, Single stage with packing volume of 50%	60	98.1	84.9	2.3	7.8	19
Motor oil	Alfoterra 145-8PO (0.3% w/v)	1.5	Oil 500 mg/L	Continuous, Multi stage	94*	97.9	98.9	16.3	17.6	This study

Note : ODCB is ortho-dichlorobenzene, SDS is sodium dodecyl sulfate, DADS is mono and di-hexadecyl diphenyloxide disulfonate sodium salt, NP(EO)10 is nonylphenol AMA is di-1, 3-dimethylbutyl sulfosuccinate and Alfoterra 145-4PO / Alfoterra 145-5PO / Alfoterra 145-8PO is Branched alcohol propoxylate sulfate sodium salt with 14 to 15 carbons in the alkyl chain, and an average of 4, 5 and 8 propylene oxides, respectively.

\*Hydraulic retention time (HRT) calculated from the liquid volume in the column divided by the feed flow rate.

Similar to a distillation column, both motor oil and surfactant can be enriched in the upward direction for a multistage froth flotation column. Both high enrichment ratios of motor oil and surfactant can lead to a possibility of both economic recovery of the motor oil and surfactant.

### **3.5 Conclusions**

In the present work, a continuous multistage froth flotation system was found to be a promising technique for motor oil removal. When it was operated under the optimum operational conditions, the highest motor oil removal performance (97.9%) could be achieved with the highest values of enrichment ratios of 16.3 and 17.6 for motor oil and surfactant, respectively, which are much higher than those of previous batch and continuous single-stage systems. To optimize the process performance of a continuous multistage froth flotation system in terms of high removal and high enrichment ratio of oil, it has to be operated to obtain high adsorptive transport with low bulk liquid transport. An addition of NaCl, at a proper concentration, can enhance the separation performance of a continuous multistage froth flotation column when an ionic surfactant is used as a frother. The higher the stage number, the higher the separation process performance. However, it has a maximum stage number for operating a multistage froth flotation column because at a very low surfactant concentration in any tray, the generated foam cannot reach an upper tray.

### **3.6 Acknowledgements**

The Sustainable Petroleum and Petrochemicals Research Unit under the Center of Excellence on the Petrochemical and Materials Technology, Chulalongkorn University, is acknowledged for providing research facilities. The author would like to thank Sasol North America Inc. (USA) for providing the extended surfactant used in this research. Thailand Research Fund (TRF) is greatly acknowledged for providing a RGJ Ph.D. grant (PHD/0242/2552) to the first author and a TRF Senior Research Scholar grant (RTA 5780008) to the corresponding

author. The Sustainable Petroleum and Petrochemicals Research Unit under the Center of Excellence on the Petrochemical and Materials Technology, Chulalongkorn University, is also acknowledged for providing partial financial support.

### 3.7 References

- [1] Zeng, Y.; Yang, C.; Zhang, J.; Pu, W. (2007) Feasibility investigation of oily wastewater treatment by combination of zinc and PAM in coagulation/flocculation. *Journal of Hazardous Materials*, 147: 991–996.
- [2] Shi-Qian, L.; Pei-Jiang, Z.; Ling, D.; Kai, F. (2011) Treatment of oily wastewater using composite flocculant of polysilicate ferro–aluminum sulfate–rectorite. *Journal of Water Resource and Protection*, 3: 253–261.
- [3] Nadarajah, N.; Singh, A.; Ward, O.P. (2002) De-emulsification of petroleum oil emulsion by a mixed bacterial culture. *Process Biochemistry*, 37: 1135–1141.
- [4] Perez, M.; Rodriguez-Cano, R.; Romero, L.I.; Sales, D. (2007) Performance of anaerobic thermophilic fluidized bed in the treatment of cutting-oil wastewater. *Bioresource Technology*, 8: 3456–3463.
- [5] Gryta, M.; Karakulski, K.; Morawski, A.W. (2001) Purification of oily wastewater by hybrid UF/MD. *Water Research*, 35: 3665–3669.
- [6] Masuelli, M.; Marchese, J.; Ochoa, N.A. (2009) SPC/ PVDF membranes for emulsified oily wastewater treatment. *Journal of Membrane Science*, 326: 688–693.
- [7] Li, Y.S.; Yan, L.; Xiang, C.B.; Hong, L.J. (2006) Treatment of oily wastewater by organic–inorganic composite tubular ultrafiltration (UF) membranes. *Desalination and Water Treatment*, 196: 76–83.
- [8] Hua, F.L.; Tsang, Y.F.; Wang, Y.J.; Chan, S.Y.; Chua, H.; Sin, S.N. (2007) Performance study of ceramic microfiltration membrane for oily wastewater treatment. *Chemical Engineering Journal*, 128: 169–175.
- [9] Yan, L.; Hong, S.; Li, M.L.; Li, Y.S. (2009) Application of the Al<sub>2</sub>O<sub>3</sub>–PVDF nanocomposite tubular ultrafiltration (UF) membrane for oily wastewater

- treatment and its antifouling research. *Separation and Purification Technology*, 66: 347–352.
- [10] Wong, C.; Hossain, M.; Davies, C. (2001) Performance of a continuous foam separation column as a function of process variables. *Bioprocess and Biosystems Engineering*, 24: 73–81.
- [11] Burghoff, B. (2012) Foam fractionation applications. *Journal of Biotechnology* 161: 126–137.
- [12] Pondstabodee, S.; Scamehorn, J.F.; Chavadej, S.; Harwell, J.H. (1998) Cleanup of oily wastewater by froth flotation: Effect of microemulsion formation. *Separation Science and Technology*, 33: 591–609.
- [13] Chavadej, S.; Ratanarojanatam, P.; Phoochinda, W.; Yanatatsaneejit, U.; Scamehorn, J.F. (2004) Clean-up of oily wastewater by froth flotation: Effect of microemulsion formation II: Use of anionic/nonionic surfactant mixtures. *Separation Science and Technology*, 39: 3079–3096.
- [14] Yanatatsaneejit, U.; Chavadej, S.; Rangsunvigit, P.; Scamehorn, J.F. (2005) Ethylbenzene removal by froth flotation under conditions of middle-phase microemulsion formation II: Effects of air flow rate, oil-to-water ratio, and equilibration time. *Separation Science and Technology*, 40: 1609–1620.
- [15] Yanatatsaneejit, U.; Witthayapanyanon, A.; Rangsunvigit, P.; Acosta, E.J.; Sabatini, D.A.; Scamehorn, J.F.; Chavadej, S. (2005) Ethylbenzene removal by froth flotation under conditions of middle-phase microemulsion formation I: Interfacial tension, foamability, and foam stability. *Separation Science and Technology*, 40: 1537–1553.
- [16] Watcharasing, S.; Angkathunyakul, P.; Chavadej, S. (2008) Diesel oil removal from water by froth flotation under low interfacial tension and colloidal gas aphyron conditions. *Separation and Purification Technology*, 62: 118–127.
- [17] Yanatatsaneejit, U.; Chavadej, S.; Scamehorn, J.F. (2008) Diesel oil removal by froth flotation under low interfacial tension conditions I: Foam characteristics, and equilibration time. *Separation Science and Technology*, 43: 1520–1534.
- [18] Watcharasing, S.; Kongkowitz, W.; Chavadej, S. (2009) Motor oil removal from water by continuous froth flotation using extended surfactant: Effects of air

- bubble parameters and surfactant concentration. *Separation and Purification Technology*, 70: 179–189.
- [19] Bunturongpratoomrat, A.; Pornsunthorntawe, O.; Nitivattananon, S.; Chavadej, J.; Chavadej, S. (2013) Cutting oil removal by continuous froth flotation with packing media under low interfacial tension conditions. *Separation and Purification Technology*, 107: 118–128.
- [20] Rujirawanich, V.; Chavadej, S.; O'Haver, J.H.; Rujiravanit, R. (2011) Removal of trace  $\text{Cd}^{2+}$  using continuous multistage ion foam fractionation: Part II — the effects of operational parameters. *Separation Science and Technology*, 46: 1673–1683.
- [21] Boonyasuwat, S.; Chavadej, S.; Malakul, P.; Scamehorn, J.F. (2005) Surfactant Recovery from water using a multistage foam fractionator: Part I effects of air flow rate, foam height, feed flow rate and number of stages. *Separation Science and Technology*, 40: 1835–1853.
- [22] Rujirawanich, V.; Chuyingsakultip, N.; Triroj, M.; Malakul, P.; Chavadej, S. (2012) Recovery of surfactant from an aqueous solution using continuous multistage foam fractionation: Influence of design parameters. *Chemical Engineering and Processing: Process Intensification*, 52: 41–46.
- [23] Rosen, M.J. (2004) *Surfactants and Interfacial Phenomena*. John Wiley & Sons, Inc., p. 34–104.
- [24] Boonyasuwat, S.; Chavadej, S.; Malakul, P.; Scamehorn, J.F. (2003) Anionic and cationic surfactant recovery from water using a multistage foam fractionator. *Chemical Engineering Journal*, 93: 241–252.
- [25] Rujirawanich, V.; Chavadej, S.; O'Haver, J.H.; Rujiravanit, R. (2010) Removal of trace  $\text{Cd}^{2+}$  using continuous multistage ion foam fractionation: Part I — The effect of feed SDS/Cd molar ratio. *Journal of Hazardous Materials*, 182: 812–819.
- [26] Tamura, T.; Kaneko, Y.; Ohyama, M. (1995) Dynamic surface tension and foaming properties of aqueous polyoxyethylene n-dodecyl ether solutions. *Journal of Colloid and Interface Science*, 173: 493–499.

- [27] Childs, J.D.; Acosta, E.; Scamehorn, J.F.; Sabatini, D.A. (2000) Dynamic surface tension and adsorption mechanisms of surfactants at the air–water interface. *Advances in Colloid and Interface Science*, 85: 103–144.
- [28] Childs, J.D.; Acosta, E.; Scamehorn, J.F.; Sabatini, D.A. (2004) Surfactant-enhanced treatment of oil-based drill cuttings. *Journal of Energy Resources Technology*, 127 153–162.
- [29] Witthayapanyanon, A.; Phan, T.; Heitmann, T.; Harwell, J.; Sabatini, D. (2010) Interfacial properties of extended surfactant based microemulsions and related macroemulsions. *Journal of Surfactants and Detergents*, 13: 127–134.
- [30] Witthayapanyanon, A.; Acosta, E.J.; Harwell, J.H.; Sabatini, D.A. (2006) Formulation of ultralow interfacial tension systems using extended surfactants. *Journal of Surfactants and Detergents*, 9: 331–339.
- [31] Wang, L.; Yoon, R.H. (2004) Hydrophobic forces in the foam films stabilized by sodium dodecyl sulfate: Effect of electrolyte. *Langmuir*, 20: 11457–11464.
- [32] Comley, B.A.; Harris, P.J.; Bradshaw, D.J.; Harris, M.C. (2002) Frother characterisation using dynamic surface tension measurements. *International Journal of Mineral Processing*, 64: 81–100.
- [33] Chuang, K.T.; Nandakumar, K. (2000) Tray columns: Design. *Encyclopedia of Separation Science*, 1135–1140.
- [34] Bennett, D.L.; Douglas, L. (2000) Optimize distillation columns. *Chemical Engineering Progress*, 96(5): 19–34.
- [35] Tadakamalla, K.; Marathe, K.V. (2011) Hydrodynamic study and optimization strategy for the surfactant recovery from aqueous solutions. *Desalination and Water Treatment*, 266: 98–107.
- [36] Tharapiwattananon, N.; Scamehorn, J.F.; Osuwan, S.; Harwell, J.H.; Haller, K.J. (1996) Surfactant recovery from water using foam fractionation. *Separation Science and Technology*, 31: 1233–1258.
- [37] Pugh, R.J. (2005) Experimental techniques for studying the structure of foams and froths. *Advances in Colloid and Interface Science*, 114–115:239–251.
- [38] Chungchamroenkit, P.; Chavadej, S.; Scamehorn, J.F.; Yanatatsaneejit, U.; Kitiyanan, B. (2009) Separation of carbon black from silica by froth



- flotation part 1: Effect of operational parameters. *Separation Science and Technology*, 44: 203–226.
- [39] Zhang, J.; Jing, Y.; Wu, Z.; Li, Q. (2009) Removal of trace  $\text{Cu}^{2+}$  from aqueous solution by foam fractionation. *Desalination and Water Treatment*, 249: 503–506.
- [40] Yang, Q.W.; Wu, Z.L.; Zhao, Y.L.; Wang, Y.; Li, R. (2011) Enhancing foam drainage using foam fractionation column with spiral internal for separation of sodium dodecyl sulfate. *Journal of Hazardous Materials*, 192: 1900–1904.
- [41] Gerken, B.M.; Nicolai, A.; Linke, D.; Zorn, H.; Berger, R.G.; Parlar, H. (2006) Effective enrichment and recovery of laccase C using continuous foam fractionation. *Separation Science and Technology*, 49: 291–294.
- [42] Qu, Y.H.; Zeng, G.M.; Huang, J.H.; Xu, K.; Fang, Y.Y.; Li, X.; Liu, H.L. (2008) Recovery of surfactant SDS and  $\text{Cd}^{2+}$  from permeate in MEUF using a continuous foam fractionator. *Journal of Hazardous Materials*, 155: 32–38.
- [43] Persson, C.M.; Jonsson, A.P.; Bergström, M.; Eriksson, J. C. (2003) Testing the Gouy–Chapman theory by means of surface tension measurements for SDS–NaCl– $\text{H}_2\text{O}$  mixtures. *Journal of Colloid and Interface Science*, 267: 151–154.

**CHAPTER IV**  
**EQUILIBRIUM AND DYNAMIC SURFACE TENSION IN RELATION**  
**TO DIFFUSIVITY AND FOAMING PROPERTIES: EFFECT OF**  
**SURFACTANT TYPE AND STRUCTURE**

(Published in Colloids and Surfaces A: Physicochemical and Engineering  
Aspects)

**4.1 Abstract**

The main objectives of this study were to investigate the effects of molecular structure of surfactant on surface properties and foam characteristics and to correlate surface tension to foam properties. Two series of methyl ester sulfonate with different alkyl chain lengths ( $\text{MES}_x$ ,  $x = 14, 16, \text{ and } 18$ ) and polyoxyethylated dodecyl alcohol with different head group sizes ( $\text{C}_{12}\text{EO}_n$ ,  $n = 3, 5, 7, \text{ and } 9$ ) were measured for equilibrium and dynamic surface tension as well as foamability and foam stability. The equilibrium experimental data were well fitted with the Langmuir adsorption isotherm. The dynamic surface tension data were used to calculate diffusivity values of all studied surfactants by using Word–Tordai equation. The longer the alkyl group of  $\text{MES}_x$ , the lower the diffusivity value. The larger the EO head group size, the higher the diffusivity. For both studied surfactant groups, the higher the maximum rate of surface tension reduction, the higher the diffusivity and foaming properties in terms of foamability and foam stability.

**Keywords:** Dynamic surface tension, Surfactant adsorption, Diffusivity coefficient, Foamability, Foam stability

## 4.2 Introduction

The scarcity of clean fresh water has become a serious issue in relation to urbanization in the last few decades because of the limitations of water resources and increasing pollution. Purification and the treatment of polluted water have become more and more common. Among wastewater technologies available, froth flotation is of great interest for removing oils [1–4], metals [5–7], and solid particles [8–10] from wastewaters at low concentrations because of its simplicity in operation and design and low operational cost [11, 12]. To successfully operate froth flotation, both high foamability and high foam stability with dry foam (low water content in generated foam) are crucial to achieve high separation efficiency (high removal with high enrichment ratio) [13]. Therefore, an important point is that the understanding of foam behaviors, which are fundamentally governed by the properties of added surfactants including other soluble components present in water especially type, chemical structure and concentration [14–18]. Under the flotation process, foam is always formed in a very short time and so the equilibrium adsorption does not reach [18, 19]. Therefore, the use of equilibrium surface properties cannot apply to froth flotation processes. The relation of dynamic surface tension results of surfactant solutions to the foam behaviors will be, for the first time of its kind, discussed in this work. The main objective of this work was to employ a numerical approach to dynamic surface tension data for calculating diffusivity and to correlate dynamic surface tension and diffusivity to foaming properties of different surfactant solutions. The influence of surfactant structures—the alkyl chain length of a series of methyl ester sulfonate ( $\text{MES}_x$ ) homologues and the head group size of a series of polyoxyethylated dodecyl alcohol ( $\text{C}_{12}\text{EO}_n$ ) homologues—on the equilibrium and dynamic surface properties, and adsorption behaviors at air/water interface was also investigated systematically. In addition, the effect of an electrolyte ( $\text{NaCl}$ ) on their surface tension (dynamic and equilibrium) and foaming behaviors was also discussed. Both  $\text{MES}_x$  and  $\text{C}_{12}\text{EO}_n$  were selected in this study because they are considered as environmental friendly surfactants and they were hypothesized to be good for froth flotation application.

## 4.3 Experimental

### 4.3.1 Materials

Methyl ester sulfonate anionic surfactant homologues with different alkyl chain lengths ( $\text{MES}_x$ ,  $x = 14, 16$  and  $18$ ) were kindly supplied by the Lion Corporation. In this,  $x$  stands for average alkyl units having a molecular weight of 372, 400 and 428, respectively with of  $\geq 99\%$  purity in powder form. Sodium dodecyl sulfonate (SDS) having  $\geq 99\%$  purity and a molecular weight of 288.4 in powder form was purchased from Sigma-Aldrich. Commercial polyoxyethylated dodecyl alcohol nonionic surfactant homologues with different head group sizes (a narrow distribution of EO units,  $\text{C}_{12}\text{EO}_n$ ,  $n = 3, 5, 7,$  and  $9$ ) were kindly supplied by the Thai Ethoxylate Co., Ltd. In this,  $n$  stands for the average number of EO units having molecular weights of 332, 420, 508, and 596, respectively with of  $\geq 99\%$  purity in liquid form. Sodium chloride ( $\text{NaCl}$ , analytical grade, having 99% purity) was obtained from Labscan Asia Co., Ltd. (Thailand). All chemicals were used as received without further purification and distilled water was used throughout all experiments. A certain amount of each surfactant was dissolved in distilled water to obtain a desired concentration. All surfactant solutions were freshly prepared before used.

### 4.3.2 Surface tension measurement

#### 4.3.2.1 *Equilibrium surface tension measurement*

Surface tension measurement of various surfactant solutions was carried out by a tensiometer (Krüss, Germany, K100) with a Wilhelmy plate at  $25.0 \pm 0.1$  °C. The plate was cleaned with ethanol and distilled water and flamed before each measurement. Each sample was measured for equilibrium surface tension after at least 10 min to ensure the saturation of surfactant adsorption on the air/water interface.

#### 4.3.2.2 *Dynamic surface tension measurement*

The measurement of dynamic surface tension of all surfactant solutions was performed using a bubble pressure tensiometer (Krüss, Germany, BP2)

at  $25.0 \pm 0.1$  °C. It involved the measurement of the maximum bubble pressure to blow out a gas bubble through a capillary tube (having a diameter of 0.234 mm), which was submerged in a sample liquid. The measurements of dynamic surface tension were conducted with different surface ages in the range of 5–20,000 ms.

#### 4.3.3 Foamability and foam stability measurements

Foamability and foam stability measurements were conducted using a glass column having an internal diameter of 5 cm and a column height of 120 cm. A quantity of 200 mL of any aqueous surfactant solutions was added to the column. Compressed air was introduced at the bottom of the column at a constant rate of 0.3 L/min regulated by a mass flow controller (Cole-Parmer, 32457–42) to generate fine air bubbles by passing through a sintered glass disk with pore size diameters in the range of 16–40  $\mu\text{m}$  [2, 3]. The time required to reach a maximum height of 120 cm was used to indicate foamability. The time required for the foam height to collapse from 120 to 60 cm without introducing air was used to indicate foam stability [20]. The foam characteristic experiments were carried out at room temperature (25–30 °C).

### 4.4 Results and Discussion

#### 4.4.1 Equilibrium surface tension and adsorption isotherm results

Figure 4.1 a and b illustrates the equilibrium surface tension isotherms of two series of  $\text{MES}_x$  with different alkyl chain lengths (14, 16 and 18) and  $\text{C}_{12}\text{EO}_n$  with different amounts of EO units (3, 5, 7, and 9) to indicate the effects of the chain length of the hydrophobic portion and the size of the hydrophilic portion, respectively, as compared with that of well-known anionic surfactant, SDS. The surface tension isotherm shifted towards lower surfactant concentrations with increasing either alkyl chain length or the size of the hydrophilic head group but the effect of the increase in alkyl chain length was much more pronounced than that of the increase in the size of the hydrophilic head group.

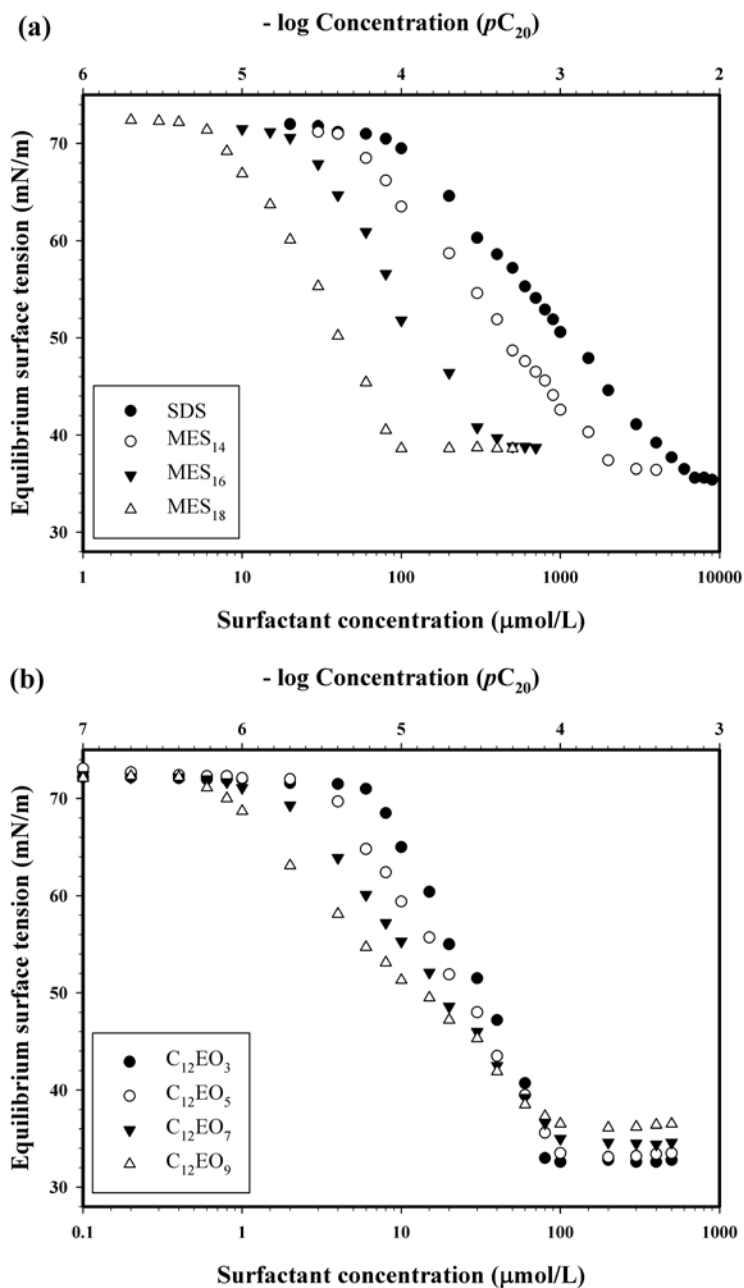


**Figure 4.1** Surface tension of surfactant solution as a function of concentration (a) MES<sub>x</sub> with different alkyl chain length and SDS and (b) C<sub>12</sub>EO<sub>n</sub> with different amounts of EO units.

The Gibbs adsorption isotherm equation (Eq. (4.1)) [15, 19, 21, 22] was used to calculate the equilibrium surfactant adsorption densities (saturation

surface excess concentrations) for the two series of studied surfactants at the air/water interface.

$$\Gamma = -\frac{1}{nRT} \cdot \left( \frac{d\gamma}{d \ln C} \right) \quad (4.1)$$

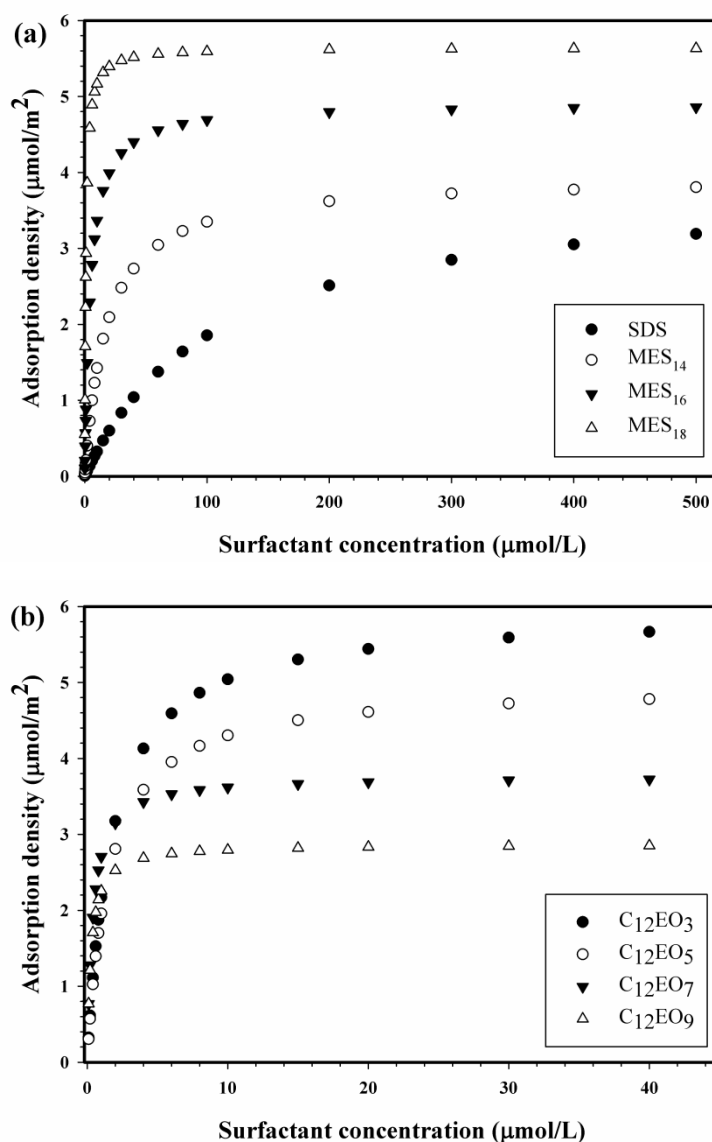
where  $\gamma$  is the surface tension of surfactant solution (mN/m),  $C$  is the bulk concentration of surfactant ( $\mu\text{M}$ ),  $R$  is the gas constant value (8.314 J/mol K),  $T$  is the temperature of a solution (K),  $\Gamma$  is the excess surface concentration ( $\mu\text{mol}/\text{m}^2$ ), and  $n$  is the number of solute species whose concentration at the interface changes with change in the value of  $C$ , which is considered to be 1 for a nonionic surfactant system or anionic surfactant with the presence of an excess concentration of electrolyte and 2 for an anionic surfactant system without added electrolyte.

Figure 4.2 a and b shows the effects of alkyl chain length of  $\text{MES}_x$  and the size of the hydrophilic head group of  $\text{C}_{12}\text{EO}_n$  on the equilibrium surfactant adsorption density at the air/water interface, respectively, as a function of initial surfactant concentration. The results revealed that the adsorption density of any studied surfactant increased with increasing surfactant concentration and reached a maximum value. The region of constant surfactant adsorption density is known as the Gibbs–close pack monolayer [23]. It also showed that the surfactant with a longer alkyl chain length had a higher adsorption density but the surfactant with a larger hydrophilic head group size had a lower adsorption density. The explanation of the effect of the surfactant structure on the adsorption density will be described later.

The surfactant adsorption density isotherms, as shown in Figure 4.2, were found to fit well to the Langmuir adsorption isotherm (Eq. (4.2)), with two important parameters of the excess surface concentration at saturation or the maximum surfactant adsorption density ( $\Gamma_m$ ) and the Langmuir equilibrium adsorption constant ( $K_L$ ) [24, 25].

$$\Gamma = \frac{\Gamma_m K_L C}{1 + K_L C} \quad (4.2)$$

where  $\Gamma_m$  is the maximum (saturated) excess surface concentration ( $\mu\text{mol}/\text{m}^2$ ), and  $K_L$  is the Langmuir equilibrium adsorption constant (L/mol).



**Figure 4.2** Adsorption density of surfactant solution as a function of concentration (a)  $\text{MES}_x$  with different alkyl chain length and SDS and (b)  $\text{C}_{12}\text{EO}_n$  with different amounts of EO units.



**Table 4.1** Calculated values of CMC,  $\gamma_{\text{cmc}}$ ,  $pC_{20}$ , saturated surface concentrations ( $\Gamma_m$ ) and Langmuir equilibrium adsorption constant ( $K_L$ ) of all studied surfactants

Surfactant	CMC (mol/L)	$\gamma_{\text{cmc}}$ (mN/m)	$pC_{20}$	$\Gamma_{\text{max}}$ ( $\mu\text{mol/m}^2$ )	$K_L$ (L/mol)
SDS	$7.25 \times 10^{-3}$	36.3	3.08	3.89	$9.11 \times 10^3$
MES <sub>14</sub>	$2.16 \times 10^{-3}$	36.7	3.4	3.94	$5.66 \times 10^4$
MES <sub>16</sub>	$3.26 \times 10^{-4}$	38.6	3.93	4.90	$2.19 \times 10^5$
MES <sub>18</sub>	$1.00 \times 10^{-4}$	38.5	4.47	5.64	$1.08 \times 10^6$
C <sub>12</sub> EO <sub>3</sub>	$8.00 \times 10^{-5}$	32.4	4.53	5.91	$5.80 \times 10^5$
C <sub>12</sub> EO <sub>5</sub>	$9.00 \times 10^{-5}$	33.4	4.7	4.96	$6.51 \times 10^5$
C <sub>12</sub> EO <sub>7</sub>	$1.00 \times 10^{-4}$	34.9	4.81	3.76	$2.57 \times 10^6$
C <sub>12</sub> EO <sub>9</sub>	$1.00 \times 10^{-4}$	36.1	4.97	2.87	$3.67 \times 10^6$

As shown in Table 4.1, for the homologous series of MES<sub>x</sub>, an increase in the alkyl chain length (increasing hydrophobic tail group) increases the steric effect, causing an increase in the aggregation number and the enhancement of micelle formation, leading to a decrease in CMC. For the homologous series of C<sub>12</sub>EO<sub>n</sub>, an increase in the number of EO units (increasing hydrophilic head group size) results in a decrease in surfactant adsorption density, causing the reduction of surface activity and an increase in CMC. The present results of CMC,  $\gamma_{\text{cmc}}$  and  $pC_{20}$  are in excellent agreement with other surfactants, for example SDS, investigated previously [14, 16, 26–28]. The  $\gamma_{\text{cmc}}$  value slightly increased with an increase in alkyl chain length of MES<sub>x</sub> series or the number of EO units of C<sub>12</sub>EO<sub>n</sub> series because the longer the alkyl chain length (larger hydrophobic tail group) and the higher the number of EO units (larger hydrophilic head group), the larger the volume of the hydrophobic and hydrophilic portions, respectively, leading to a looser arrangement at the interface of air/water [28]. A higher  $pC_{20}$  value was obtained from a longer alkyl chain length or a larger number of EO units, suggesting that both changes in hydrophobic and hydrophilic portions can affect surfactant adsorption efficiency [15,

28]. A higher value of  $pC_{20}$  generally indicates higher surfactant adsorption efficiency at the air/water interface and a greater ability for the reduction of surface tension, implying that lower energy is needed to bring the surfactant molecules to the air/water interface [15]. For the homologous series of anionic surfactants, the  $\Gamma_m$  value increased with an increase in alkyl chain length since this simply increases the steric effect, causing a closer pack of surfactant molecules [29]. It is directly analogous to the corresponding reduction in CMC as explained previously [16, 30–32]. For the homologous series of nonionic surfactants, the  $\Gamma_m$  value decreased with the increasing amount of EO units. It can be explained in that the higher the amount of the EO unit, the larger the head group size of surfactant to lower the surfactant adsorption [26, 28, 32–34]. The value of free energy ( $\Delta G^\circ$ ) for surfactant adsorption onto the air/water interface directly relates to both  $pC_{20}$  and  $K_L$  [15, 35–38]. A large  $K_L$  caused  $\Delta G^\circ$  to become more negative, resulting in higher surfactant adsorption efficiency. The  $K_L$  value increased with increasing alkyl chain length or the number of EO units, which corresponded well with the results of  $pC_{20}$ . From the results, it can be concluded that the structures of both hydrophobic and hydrophilic portions significantly affect surfactant adsorption at the air/water interface.

#### 4.4.2 Dynamic surface tension results

Dynamic surface tension measurements were performed using a maximum bubble–pressure technique to investigate the kinetic adsorption at the air/water interface of all studied surfactants. The dynamic surface tension values of two series of studied surfactants (MES<sub>16</sub> and C<sub>12</sub>EO<sub>9</sub>) as a function of bubble age at different concentrations are shown in Figure 4.3a and b, respectively.

For any given surfactant concentration, an increase in air bubble age provided a higher reduction of surface tension. It was observed that as the surfactant concentration increased, the dynamic surface tension reduction was faster and greater.

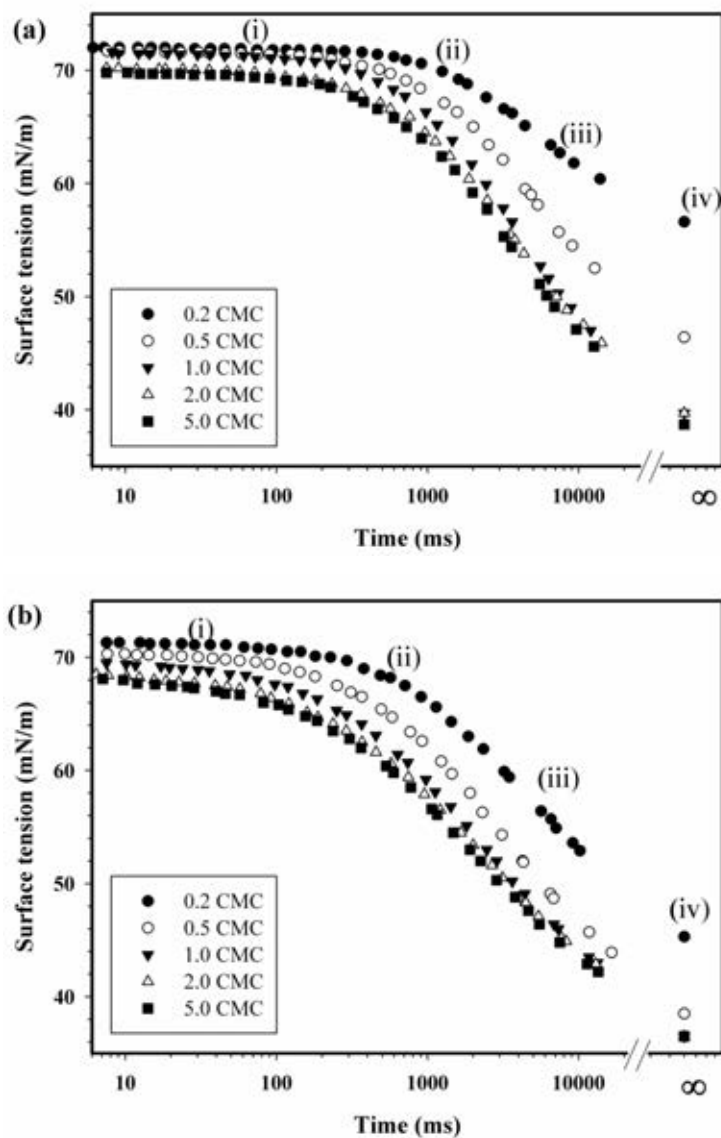


**Figure 4.3** Dynamic surface tension  $\gamma(t)$  of surfactant solution (a)  $\text{MES}_{16}$  and (b)  $\text{C}_{12}\text{EO}_9$  at air/water interface for five different concentrations.

The profile of the dynamic surface tension isotherm can be divided into four regions: (i) the induction region, (ii) the rapid fall region, (iii) the meso-equilibrium region, and (iv) the equilibrium region. The first three regions can be described by the following equation [15, 16, 39–41]:

$$\gamma_t = \gamma_m + \frac{(\gamma_o - \gamma_m)}{[1 + (t/t^*)^n]} \quad (4.3)$$

where  $\gamma_t$  is the dynamic surface tension at time  $t$ ,  $\gamma_o$  is the surface tension of pure solvent (water),  $\gamma_m$  is the meso-equilibrium surface tension of surfactant solution,  $t^*$  is the time required to attain a half value between  $\gamma_o$  and  $\gamma_m$ , and  $n$  is a constant. The values of  $t^*$  and  $n$  are determined by fitting the above equation with the measured values of dynamic surface tension at different times. The  $t^*$  value depends on the diffusion rate of surfactant from the bulk solution to the subsurface. The lower the  $t^*$  value, the lower the hindrance of diffusion, or the faster the diffusion rate of added surfactant. The  $n$  is a constant, depending on the molecular structure of added surfactant. It indicates the difference between the energies of surfactant adsorption and desorption [15, 42]. The higher the  $n$  value, the higher the potential barrier of surfactant adsorption or the greater the difficulty for a surfactant to adsorb at the air/water interface [43].

As shown in Table 4.2, both values of  $t^*$  and  $n$  decrease with an increase in surfactant concentration of both groups of studied surfactants according to an increase in the driving force from the increase in concentration gradient [15]. For any given surfactant concentration, an increase in the alkyl chain length of  $MES_x$  series resulted in the increase in the  $t^*$  value, indicating a decrease in the diffusion rate whereas an increase in the head group size (higher EO units) of  $C_{12}EO_n$  series causes a reduction of the  $t^*$  value (an increase in diffusion rate). The results can be explained by the fact that an increase in the hydrophobic portion (alkyl chain length) of the  $MES_x$  series caused a larger structure size to delay the transport of surfactant molecules from the bulk liquid to the subsurface or to decrease the surfactant diffusivity [27]. The decrease in the size of the head group (lower EO units) of the  $C_{12}EO_n$  series can slow down the transport of surfactant molecules from the bulk liquid to the subsurface or cause a decrease in the surfactant diffusivity [28].

**Table 4.2** Dynamic surface tension parameters for all studied surfactant solutions

Surfactant	Concentration (times of CMC)	n	t* (ms)	$\left(\frac{\partial \gamma_t}{\partial t}\right)_{max}$
<b>MES<sub>14</sub></b>	0.2	1.20	5,200	1.16
	0.5	1.13	4,515	1.84
	1	1.09	3,772	2.50
	2	1.06	3,472	2.72
	5	1.00	3,355	2.65
<b>MES<sub>16</sub></b>	0.2	1.24	5,370	0.89
	0.5	1.16	4,739	1.57
	1	1.13	4,012	2.27
	2	1.06	3,796	2.32
	5	1.03	3,680	2.33
<b>MES<sub>18</sub></b>	0.2	1.28	5,446	0.70
	0.5	1.24	5,286	1.56
	1	1.18	4,815	2.05
	2	1.14	4,333	2.20
	5	1.08	4,184	2.16
<b>C<sub>12</sub>EO<sub>3</sub></b>	0.2	1.20	6,273	1.28
	0.5	1.08	6,094	1.48
	1	0.97	5,868	1.47
	2	0.95	5,866	1.44
	5	0.90	5,710	1.40
<b>C<sub>12</sub>EO<sub>5</sub></b>	0.2	1.11	4,893	1.36
	0.5	0.98	4,578	1.53
	1	0.97	4,431	2.11
	2	0.92	4,101	2.16
	5	0.85	3,991	2.05
<b>C<sub>12</sub>EO<sub>7</sub></b>	0.2	1.05	4,846	1.59
	0.5	0.98	4,409	1.97
	1	0.96	3,923	2.27
	2	0.89	3,579	2.32
	5	0.81	3,344	2.26
<b>C<sub>12</sub>EO<sub>9</sub></b>	0.2	0.95	4,089	1.56
	0.5	0.93	3,042	2.56
	1	0.84	2,432	3.05
	2	0.81	2,276	3.14
	5	0.73	2,090	3.10

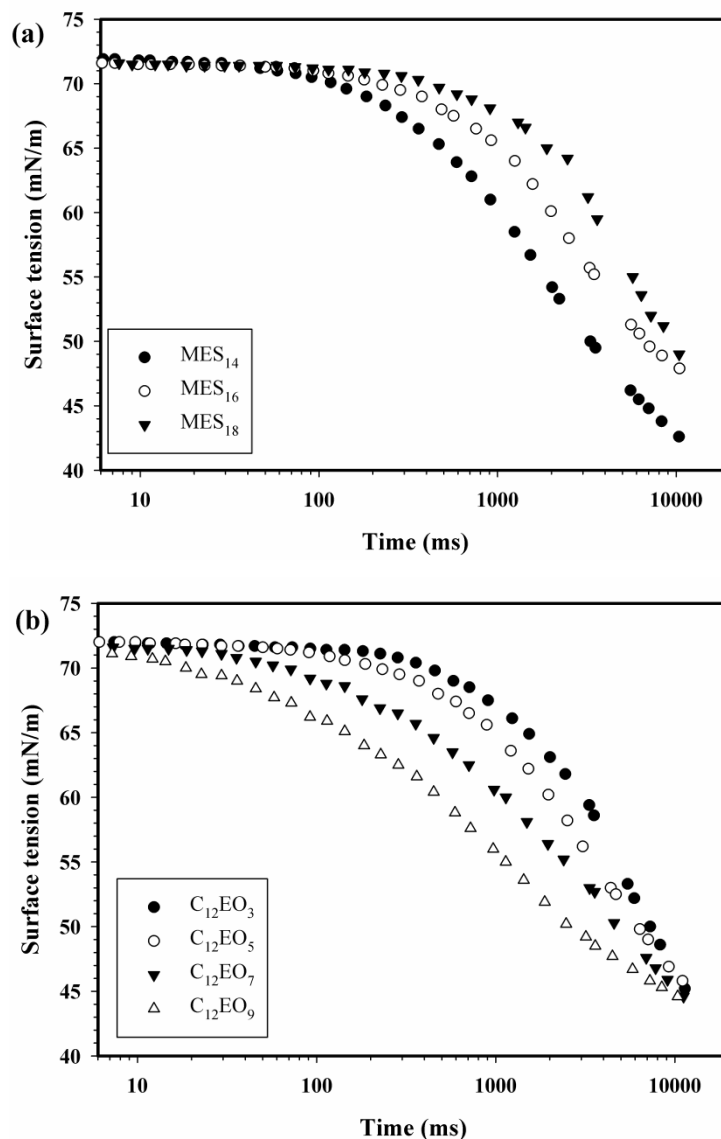


**Figure 4.4** Dynamic surface tension of (a) MES<sub>x</sub> with different alkyl chain length at the concentration of 2.0 mM/L (b) C<sub>12</sub>EO<sub>n</sub> with different amounts of EO units at the concentration of 0.2 mM/L.

Figure 4.4 a and b illustrates the dynamic surface tension as a function of time for MES<sub>x</sub> with different alkyl chain lengths and C<sub>12</sub>EO<sub>n</sub> with different amounts of EO units, respectively at very high surfactant concentrations (several times their CMC values). The use of high surfactant concentrations in these experiments was to minimize the lateral surfactant diffusion from the thick surface to

the thin surface of a generated air bubble, known as the Gibbs–Marangoni effect [15, 23, 25], causing the dominance of the vertical surfactant diffusion from the bulk liquid to the new surface of a generated air bubble. From Figure 4.4, the time required to reach the equilibrium surface tension increased with increasing alkyl chain length for the  $\text{MES}_x$  series, while it decreased with an increasing number of EO units for the  $\text{C}_{12}\text{EO}_n$  series. The same explanation used for the  $t^*$  results can be used to point out the effects of both alkyl chain length and size of the hydrophilic head group on the dynamic surface tension

#### 4.4.3 Surfactant diffusivity value results

The surfactant adsorption process consists of two sequential steps of the diffusion of surfactant molecules from the bulk aqueous phase to the subsurface due to the concentration gradient, and the adsorption of surfactant molecules from the subsurface to the air/water interface [16, 44, 45]. Generally, the diffusion rate is much slower than that of the adsorption rate, thus, the whole process can be reasonably assumed that it is basically controlled by diffusion [44, 45]. By using Fick's law to describe the diffusion of surfactant molecules from the bulk liquid to the subsurface and Langmuir adsorption isotherm to describe the surfactant adsorption onto the air/water interface of generated foam, dynamic surfactant adsorption as a function of time can be derived, as shown in Eq. (4.4) [21, 25, 27, 28, 34, 44–50]:

$$\Gamma(t) = 2C_o\sqrt{\frac{Dt}{\pi}} - 2\sqrt{\frac{D}{\pi}} \int_0^{\sqrt{t}} C_s d(\sqrt{t-\tau}) \quad (4.4)$$

where  $\Gamma(t)$  is the surface excess concentration at time  $t$ ,  $D$  is the apparent diffusion coefficient,  $C_o$  is the bulk surfactant concentration, and  $C_s$  is the surfactant concentration at the subsurface and  $\tau$  is a dummy time delay variable. The term of  $\Gamma(t)$  in Eq. (4.4) is then replaced by the dynamic surface tension from Eq. (4.1) and finally the combined equation is simplified for two cases of short time and long time,

as shown in Eqs. (4.5) and (4.6), respectively [16, 19, 21, 22, 27, 28, 32, 40, 44, 45, 47, 48]:

$$\text{Short time} \quad \gamma(t)_{t \rightarrow 0} = \gamma_o - 2nRT C_o \sqrt{\frac{Dt}{\pi}} \quad (4.5)$$

$$\text{Long time} \quad \gamma(t)_{t \rightarrow \infty} = \gamma_{eq} + \frac{nRT\Gamma_{eq}^2}{C_o} \sqrt{\frac{\pi}{4Dt}} \quad (4.6)$$

where  $R = 8.314 \text{ J/molK}$ ,  $T$  is the absolute temperature (K),  $C_o$  is the bulk surfactant concentration (mol/L),  $\gamma_o$  is the surface tension of pure water (mN/m),  $\gamma(t)$  is the dynamic surface tension at time  $t$  (mN/m),  $\gamma_{eq}$  is the equilibrium surface tension at infinite time (mN/m),  $\Gamma_{eq}$  is the equilibrium surface excess concentration (mol/m<sup>2</sup>) obtained from the equilibrium surface tension measurement which is equal to  $\Gamma_m$  and  $n$  is considered to be 1 for a nonionic surfactant system or anionic surfactant with the presence of an excess concentration of electrolyte and 2 for an anionic surfactant system without added electrolyte.

For any constant bulk surfactant concentration, the plots of  $\gamma$  versus  $\sqrt{t}$  based on Eq. (4.5) and  $\gamma$  versus  $1/\sqrt{t}$  based on Eq. (4.6) should be linear if the adsorption is diffusion-controlled, allowing the evaluation of  $D$  value from the slope of each plot. It is worthwhile to point out again that both equations are valid at high surfactant concentrations (many times their CMC values) in order to minimize the lateral surfactant diffusion. As shown in Figure 4.5, only the  $\gamma-\sqrt{t}$  plot was found to exhibit linear behavior ( $R^2 > 0.99$ ) for two series of surfactants, suggesting that the adsorption is really controlled by diffusion in the short time range (0.1–3 s). However, there is a deviation from linear behavior once it was plot based on Eq. (4.6). This is because the surfactant backward diffusion becomes significant at a long time [25,27,28,34]. The diffusion coefficients of all studied surfactants in water could be estimated by simply fitting the initial slope equal to at short time (<3 s).



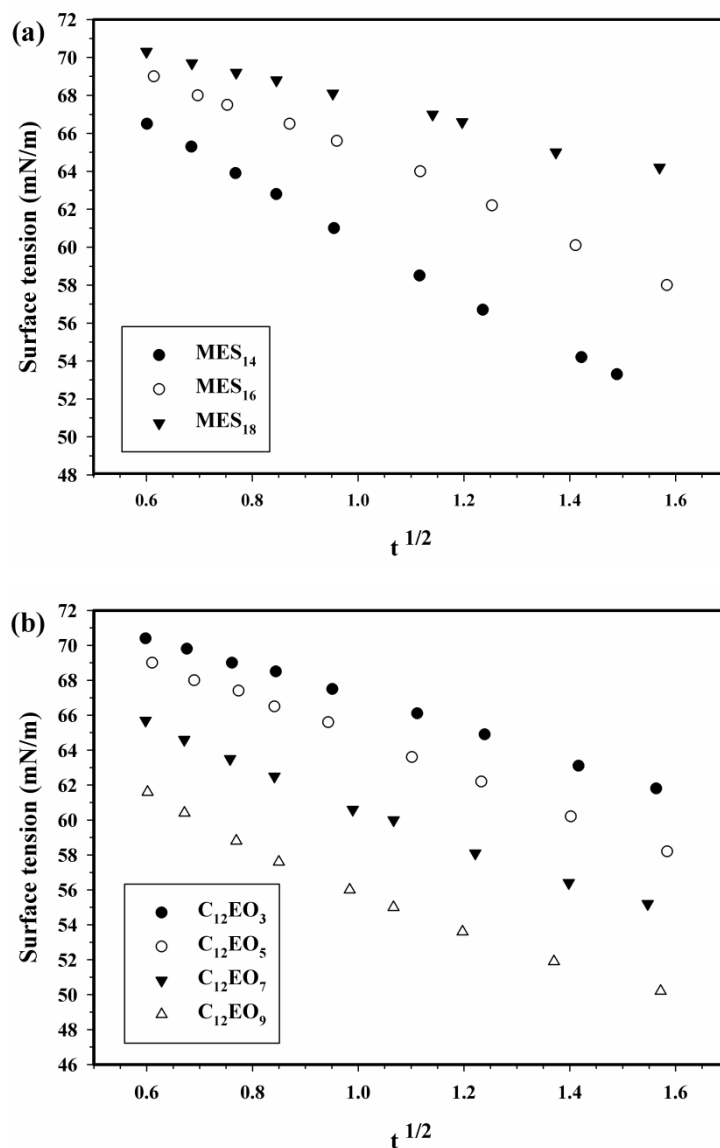


**Figure 4.5** The linear behavior of  $\gamma(t) - \sqrt{t}$  determined by the short time approximation of (a) MES<sub>x</sub> with different alkyl chain lengths were evaluated at the concentration of 2.0 mM/L and (b) C<sub>12</sub>EO<sub>n</sub> with different amounts of EO units at the concentration of 0.2 mM/L.

The calculated diffusion coefficient values of all studied surfactants are listed in **Table 3**. The D value decreased with an increase in alkyl chain length but increased with an increasing amount of EO units. The results suggest that the adsorption rate at the air/water interface strongly depends on the molecular structure

of the surfactant. The increase in alkyl chain length causes the reduction of mobility, leading to the lowering of the diffusion coefficient. On the other hand, the increase in EO units caused a larger hydrophilic head group increases the mobility of surfactant in water, leading to an increase in diffusion coefficient [51]. Moreover, the calculated D value of SDS and C<sub>12</sub>EO<sub>n</sub> series were found to be of the same order of magnitude of other measurements [51, 52], implying that a dynamic surface tension measurement can be pronounced to be a simple technique for the diffusion coefficient determination.

**Table 4.3** Apparent diffusion coefficients of all studied surfactants (at concentration of 2.0 mM for MES<sub>x</sub> and 0.2 mM for C<sub>12</sub>EO<sub>n</sub>)

Surfactant	D (m <sup>2</sup> /s)
SDS	$3.65 \times 10^{-10}$
MES <sub>14</sub>	$7.21 \times 10^{-12}$
MES <sub>16</sub>	$4.03 \times 10^{-12}$
MES <sub>18</sub>	$1.40 \times 10^{-12}$
C <sub>12</sub> EO <sub>3</sub>	$2.50 \times 10^{-10}$
C <sub>12</sub> EO <sub>5</sub>	$3.92 \times 10^{-10}$
C <sub>12</sub> EO <sub>7</sub>	$4.30 \times 10^{-10}$
C <sub>12</sub> EO <sub>9</sub>	$5.06 \times 10^{-10}$

#### 4.4.4 Foam behaviors results

##### 4.4.4.1 Foamability results

Foamability is a parameter to indicate how easy or difficult foam can be produced. It is measured by the time required to reach any specific foam height. The shorter the time to reach a specific foam height, the higher the ability to produce foam (higher foamability). An empirical correlation between dynamic surface tension (as shown in Eq. (4.3)) and foamability has been proved in this present work. To find the time for the maximum change in surface tension, Eq. (4.3) is differentiated to obtain the following equation [16, 41, 53]:

$$-\frac{d\gamma}{dt} = \frac{(\gamma_o - \gamma_m) \left[ n \left( \frac{t}{t^*} \right)^{n-1} \right]}{t^* \left[ 1 + \left( \frac{t}{t^*} \right)^n \right]^2} \quad (4.7)$$

The maximum change of dynamic surface tension is at  $t = t^*$  and Eq. (7) becomes:

$$\left( \frac{\partial \gamma_t}{\partial t} \right)_{max} = \frac{n(\gamma_o - \gamma_m)}{4t^*} \quad (4.8)$$

For all studied surfactants, the calculated values of  $\left( \frac{\partial \gamma_t}{\partial t} \right)_{max}$  (Table 4.2) and foamability (Table 4.4) were found to have good correlation. Both values of  $\left( \frac{\partial \gamma_t}{\partial t} \right)_{max}$  and foamability increased with an increase in surfactant concentration. Interestingly, both  $\left( \frac{\partial \gamma_t}{\partial t} \right)_{max}$  value and foamability tended to slightly decrease with increasing surfactant concentration beyond the CMC for most studied surfactants. These results suggest that the term  $\left( \frac{\partial \gamma_t}{\partial t} \right)_{max}$  can be used to indicate foaming properties because it reflects the maximum rate of dynamic surface tension reduction [16, 53]. The dependence of foamability on the surfactant molecular structure was also investigated. The results show that for the MES<sub>x</sub> series, both values of  $\left( \frac{\partial \gamma_t}{\partial t} \right)_{max}$  and foamability decreased with increasing alkyl chain length from 14 to 16. However, MES<sub>18</sub> showed a very low foamability compared to the others in the homologous because of the very low water solubility of MES<sub>18</sub> [48]. For the C<sub>12</sub>EO<sub>n</sub> series, an increase in EO units (or head group size) increased both value of  $\left( \frac{\partial \gamma_t}{\partial t} \right)_{max}$  and foamability.

**Table 4.4** Foam characteristics of all studied surfactants

Surfactant	Concentration (times of CMC)	Foamability(s)	Foam Stability(s)
MES <sub>14</sub>	0.2	1,036	35.9
	0.5	791	50.4
	1	676	109
	2	641	111
	5	615	121
MES <sub>16</sub>	0.2	1,624	48.0
	0.5	1,208	55.5
	1	998	161
	2	994	180
	5	987	191
MES <sub>18</sub>	0.2	2,258	20.3
	0.5	1,743	4701
	1	1,383	72.0
	2	1,337	84.2
	5	1,351	78.7
C <sub>12</sub> EO <sub>3</sub>	0.2	2,890	<10
	0.5	2,539	<10
	1	2,289	25.4
	2	2,254	30.1
	5	2,233	34.4
C <sub>12</sub> EO <sub>5</sub>	0.2	2,711	<10
	0.5	2,364	<10
	1	2,081	39.0
	2	1,983	35.8
	5	1,972	37.7
C <sub>12</sub> EO <sub>7</sub>	0.2	2,478	14.2
	0.5	0.98	4,409
	1	0.96	3,923
	2	0.89	3,579
	5	0.81	3,344
C <sub>12</sub> EO <sub>9</sub>	0.2	0.95	4,089
	0.5	0.93	3,042
	1	0.84	2,432
	2	0.81	2,276
	5	0.73	2,090

#### 4.4.4.2 Foam stability results

As shown in **Table 4.4**, for any given studied surfactant, the foam stability increased greatly with increasing surfactant at a concentration lower than its CMC. The high increment of the foam stability was found with increasing surfactant concentration around its CMC because the Gibbs–Marangoni effect was maximized [16]. The increase in foam stability obviously became insignificant with increasing surfactant concentration beyond its CMC because the Gibbs–Marangoni effect became lower. At a certain surfactant concentration, foam stability increased with an increase in either the alkyl chain length, except  $\text{MES}_{18}$ , or the number of EO units for  $\text{MES}_x$  and  $\text{C}_{12}\text{EO}_n$ , respectively. Fundamentally, two main factors are responsible for foam destruction. One is the drainage of liquid in the lamellae by gravitational force and another one is the elasticity of the lamellae [15, 43, 54]. The two factors are directly correlated to the strength of surfactant close packed monolayer [43] and dilatational rheology of the adsorbed foaming agent film [55]. With increasing alkyl chain length of  $\text{MES}_x$  series, the foam stability increased suggesting that an increase in surface excess concentration can lower liquid drainage and increase film elasticity. The higher the surfactant adsorption density ( $\Gamma$ ), the higher the foam stability [56]. Surprisingly, with an increase in the number of EO units of  $\text{C}_{12}\text{EO}_n$  series, even though the surfactant adsorption density ( $\Gamma$ ) decreased, foam stability still increased. It can be explained by means of the fact that a large hydrophilic head group (high numbers of EO units) can increase the mobility and diffusivity of surfactant [28, 34, 51]. The diffusivity of surfactant increases, therefore, the dilational surface elasticity increases accordingly, which can exceed the local depletion of surfactant in the interface. In a comparison between the two groups of studied surfactants,  $\text{MES}_x$  provided much higher foam stability than that of  $\text{C}_{12}\text{EO}_n$ . The negatively charged adsorbed  $\text{MES}_x$  on the two surfaces of the foam lamellae and the compactness of adsorbed surfactant at the air/water interface are responsible for high foam stability, as compared to that of  $\text{C}_{12}\text{EO}_n$  [15].

#### 4.4.5 Effect of salt concentration

**Table 4.5** clearly shows that  $\Gamma_m$  increases significantly with an increasing NaCl concentration up to 1.5 wt%, leading to maximum foamability and foam stability. It is because the counterion effect ( $\text{Na}^+$ ) reduces the repulsion force between the negatively charged head group of the surfactant, causing an increase in surfactant adsorption density of both surfaces of foam lamellae. As a result, the increasing repulsion force between two surfaces of foam lamellae from the increasing in surfactant adsorption density leads to both increases in foamability and foam stability. However, in further increases in the NaCl concentration beyond 1.5 wt%, both foamability and foam stability drastically decreased. It is because too much NaCl caused the reduction of the repulsion forces between the two surfaces of foam lamellae, resulting from the neutralization effect by the  $\text{Na}^+$  counterion to the negatively charged head group of surfactant adsorbing on the foam lamellae surfaces, causing both reduction of foamability and foam stability. Moreover, the addition of NaCl showed a significantly negative effect on the surfactant diffusivity. It can be explained by the fact that the co-adsorption of  $\text{Na}^+$  counterion is responsible for the obstruction of new MES molecules to diffuse and adsorb at the air/water interface.

**Table 4.5** Saturated surface concentrations ( $\Gamma_m$ ), diffusivity, foamability and foam stability of  $\text{MES}_{16}$  at the concentration of 2.0 mM with different NaCl concentrations.

NaCl concentration (wt%)	$\Gamma_m$ ( $\mu\text{mol}/\text{m}^2$ )	Diffusivity ( $\text{m}^2/\text{s}) \times 10^{-12}$	Foamability (min)	Foam stability (min)
0	4.01	3.73	11.3 $\pm$ 0.8	2.2 $\pm$ 0.2
0.5	4.56	3.51	10.1 $\pm$ 0.5	2.6 $\pm$ 0.1
1.0	5.15	3.38	8.6 $\pm$ 0.7	3.0 $\pm$ 0.2
1.5	6.04	3.12	7.8 $\pm$ 0.7	3.9 $\pm$ 0.2
2.0	6.87	2.89	15.6 $\pm$ 1.0	1.6 $\pm$ 0.3

## 4.5 Conclusion

A systematic investigation of the equilibrium and dynamic surface tension as well as foam properties of two series of  $\text{MES}_x$  with different alkyl chain lengths (14, 16 and 18)  $\text{C}_{12}\text{EO}_n$  with different amounts of EO units (3, 5, 7, and 9) was carried out. The equilibrium surface tension results of all studied surfactants were well fitted with the Langmuir adsorption model. The adsorption process was controlled by the diffusion step of surfactant, which was verified by the linear relation between  $\gamma(t)$  and  $\sqrt{t}$ . The term of  $\left(\frac{\partial\gamma_t}{\partial t}\right)_{max}$  obtained from the dynamic surface tension data can be used to indicate foaming properties in terms of foamability. The anionic surfactant with a moderate alkyl chain length—  $\text{MES}_{14}$  or  $\text{MES}_{16}$  —showed higher foamability and foam stability, which is considered to be a promising surfactant for flotation process. In addition, an addition of NaCl provided both a positive and negative effect on the foam properties for the MES anionic surfactant.

## 4.6 Acknowledgements

Thailand Research Fund (TRF) is greatly acknowledged for providing a RGJ Ph.D. grant (PHD/0242/2552) to the first author and a TRF Senior Research Scholar grant (RTA 5780008) to the corresponding author. The sustainable Petroleum and Petrochemicals Research Unit under the Center of Excellence on the Petrochemical and Materials Technology, Chulalongkorn University is acknowledged for providing research facilities and partial financial support. Prof. Masahiko Abe, Tokyo University of Science and Lion Coparation are also acknowledged for providing the MES surfactants used in this work.

## 4.7 References

- [1] B. Ramaswamy, D. Kar, S. De, A study on recovery of oil from sludge containing oil using froth flotation, *J. Environ. Manage.* 85 (2007) 150–154.
- [2] S. Watcharasing, W. Kongkowitz, S. Chavadej, Motor oil removal from water by continuous froth flotation using extended surfactant: effects of air bubble parameters and surfactant concentration, *Sep. Purif. Technol.* 70 (2009) 179–189.
- [3] A. Bunturongpratoomrat, O. Pornsunthorntawe, S. Nitivattananon, J. Chavadej, S. Chavadej, Cutting oil removal by continuous froth flotation with packing media under low interfacial tension conditions, *Sep. Purif. Technol.* 107 (2013) 118–128.
- [4] P. Kanokkarn, T. Shiina, T. Suttikul, S. Chavadej, Removal of motor oil by continuous multistage froth flotation: effect of operational parameters, *Sep. Sci. Technol.* (2016) 1847–1861.
- [5] G. Dermont, M. Bergeron, M. Richer-Lafèche, G. Mercier, Remediation of metal-contaminated urban soil using flotation technique, *Sci. Total Environ.* 408 (2010) 1199–1211.
- [6] I. Ogunniyi, M.K.G. Vermaak, Investigation of froth flotation for beneficiation of printed circuit board comminution fines, *Miner. Eng.* 22 (2009) 378–385.
- [7] A. Vidyadhar, A. Das, Enrichment implication of froth flotation kinetics in the separation and recovery of metal values from printed circuit boards, *Sep. Purif. Technol.* 118 (2013) 305–312.
- [8] F. Maoming, T. Daniel, R. Honaker, L. Zhenfu, Nanobubble generation and its applications in froth flotation (part II): fundamental study and theoretical analysis, *Min. Sci. Technol. (China)* 20 (2010) 159–177.
- [9] P. Chungchamroenkit, S. Chavadej, J.F. Scamehorn, U. Yanatatsaneejit, B. Kitiyanan, Separation of carbon black from silica by froth flotation part 1: Effect of operational parameters, *Sep. Sci. Technol.* 44 (2009) 203–226.
- [10] O. Pornsunthorntawe, S. Chuaybumrung, B. Kitiyanan, S. Chavadej, Purification of single-walled carbon nanotubes (SWNTs) by acid leaching,



- NaOH dissolution, and froth flotation, *Sep. Sci. Technol.* 46 (2011) 2056–2065.
- [11] C. Wong, M.M. Hossain, C. Davies, Performance of a continuous foam separation column as a function of process variables, *Bioprocess Biosyst. Eng.* 24 (2001) 73–81.
- [12] B. Burghoff, Foam fractionation applications, *J. Biotechnol.* 161 (2012) 126–137.
- [13] R. Lemlich, *Adsorptive Bubble Separation Techniques*, Elsevier, 2012.
- [14] D. Beneventi, B. Carre, A. Gandini, Role of surfactant structure on surface and foaming properties, *Coll. Surf. A* 189 (2001) 65–73.
- [15] M.J. Rosen, *Surfactants and Interfacial Phenomena*, Wiley, 2004.
- [16] T. Tamura, Y. Takeuchi, Y. Kaneko, Influence of surfactant structure on the drainage of nonionic surfactant foam films, *J. Colloid Interface Sci.* 206 (1998) 112–121.
- [17] S.N. Tan, D. Fornasiero, R. Sedev, J. Ralston, The role of surfactant structure on foam behaviour, *Coll. Surf. A* 263 (2005) 233–238.
- [18] J. Wang, A.V. Nguyen, S. Farrokhpay, A critical review of the growth, drainage and collapse of foams, *Adv. Colloid Interface Sci.* 228 (2016) 55–70.
- [19] X. Gao, Y. Wang, X. Zhao, W. Wei, H. Chang, Equilibrium and dynamic surface tension properties of Gemini quaternary ammonium salt surfactants with ester groups, *Coll. Surf. A* 509 (2016) 130–139.
- [20] S. Boonyasuwat, S. Chavadej, P. Malakul, J.F. Scamehorn, Surfactant recovery from water using a multistage foam fractionator: part I effects of air flow rate, foam height, feed flow rate and number of stages, *Sep. Sci. Technol.* 40 (2005) 1835–1853.
- [21] D.P. Acharya, J.M. Gutiérrez, K. Aramaki, K.-i. Aratani, H. Kunieda, Interfacial properties and foam stability effect of novel gemini-type surfactants in aqueous solutions, *J. Colloid Interface Sci.* 291 (2005) 236–243.
- [22] H. Chang, Y. Wang, Y. Cui, G. Li, B. Zhang, X. Zhao, W. Wei, Equilibrium and dynamic surface tension properties of Gemini quaternary ammonium salt surfactants with hydroxyl, *Coll. Surf. A* 500 (2016) 230–238.

- [23] L.L. Schramm, *Surfactants: Fundamentals and Applications in the Petroleum Industry*, Cambridge University Press, 2000.
- [24] S.I. Karakashev, R. Tsekov, E.D. Manev, A.V. Nguyen, Elasticity of foam bubbles measured by profile analysis tensiometry, *Coll. Surf. A* 369 (2010) 136–140.
- [25] C.M. Phan, T.N. Le, S.-i. Yusa, A new and consistent model for dynamic adsorption of CTAB at air/water interface, *Coll. Surf. A* 406 (2012) 24–30.
- [26] B.W. Barry, D.I.D. Eini, Surface properties and micelle formation of long-chain polyoxyethylene nonionic surfactants, *J. Colloid Interface Sci.* 54 (1976) 339–347.
- [27] Y. Jiang, T. Geng, Q. Li, G. Li, H. Ju, Equilibrium and dynamic surface tension properties of salt-free cationic surfactants with different hydrocarbon chain lengths, *J. Mol. Liq.* 204 (2015) 126–131.
- [28] X. Liu, Y. Zhao, Q. Li, T. Jiao, J. Niu, Surface and interfacial tension of nonylphenol polyethylene oxides sulfonate, *J. Mol. Liq.* 216 (2016) 185–191.
- [29] K. Karraker, C. Radke, Disjoining pressures, zeta potentials and surface tensions of aqueous non-ionic surfactant/electrolyte solutions: theory and comparison to experiment, *Adv. Colloid Interface Sci.* 96 (2002) 231–264.
- [30] X. Qu, L. Wang, S.I. Karakashev, A.V. Nguyen, Anomalous thickness variation of the foam films stabilized by weak non-ionic surfactants, *J. Colloid Interface Sci.* 337 (2009) 538–547.
- [31] R. Atkin, V.S.J. Craig, E.J. Wanless, S. Biggs, The influence of chain length and electrolyte on the adsorption kinetics of cationic surfactants at the silica-aqueous solution interface, *J. Colloid Interface Sci.* 266 (2003) 236–244.
- [32] J. Eastoe, J.S. Dalton, P.G.A. Rogueda, E.R. Crooks, A.R. Pitt, E.A. Simister, Dynamic surface tensions of nonionic surfactant solutions, *J. Colloid Interface Sci.* 188 (1997) 423–430.
- [33] I. Varga, R. Mészáros, C. Stubenrauch, T. Gilányi, Adsorption of sugar surfactants at the air/water interface, *J. Colloid Interface Sci.* 379 (2012) 78–83.

- [34] A. Casandra, S. Ismadji, B.A. Noskov, L. Liggieri, S.-Y. Lin, A study on the method of short-time approximation-Criteria for applicability, *Int. J. Heat Mass Transf.* 90 (2015) 752–760.
- [35] A. Makievski, D. Grigoriev, Adsorption of alkyl dimethyl phosphine oxides at the solution/air interface, *Coll. Surf. A* 143 (1998) 233–242.
- [36] Y. Liu, Is the free energy change of adsorption correctly calculated?, *J. Chem. Eng. Data* 54 (2009) 1981–1985.
- [37] A. Zdziennicka, B. Jańczuk, Behavior of cationic surfactants and short chain alcohols in mixed surface layers at water-air and polymer-water interfaces with regard to polymer wettability. I. Adsorption at water-air interface, *J. Colloid Interface Sci.* 349 (2010) 374–383.
- [38] T. Gilányi, I. Varga, C. Stubenrauch, R. Mészáros, Adsorption of alkyl trimethylammonium bromides at the air/water interface, *J. Colloid Interface Sci.* 317 (2008) 395–401.
- [39] J. Eastoe, J.S. Dalton, Dynamic surface tension and adsorption mechanisms of surfactants at the air-water interface, *Adv. Colloid Interface Sci.* 85 (2000) 103–144.
- [40] M.J. Rosen, T. Gao, Dynamic surface tension of aqueous surfactant solutions: 5. Mixtures of different charge type surfactants, *J. Colloid Interface Sci.* 173 (1995) 42–48.
- [41] T. Tamura, Y. Kaneko, M. Ohyama, Dynamic surface tension and foaming properties of aqueous polyoxyethylene n-dodecyl ether solutions, *J. Colloid Interface Sci.* 173 (1995) 493–499.
- [42] X.Y. Hua, M.J. Rosen, Dynamic surface tension of aqueous surfactant solutions: 3. Some effects of molecular structure and environment, *J. Colloid Interface Sci.* 141 (1991) 180–190.
- [43] X.-C. Wang, L. Zhang, Q.-T. Gong, L. Zhang, L. Luo, Z.-Q. Li, S. Zhao, J.-Y. Yu, Study on foaming properties and dynamic surface tension of sodium branched-alkyl benzene sulfonates, *J. Dispers. Sci. Technol.* 30 (2009) 137–143.
- [44] J. Liu, U. Messow, Diffusion-controlled adsorption kinetics at the air/solution interface, *Colloid. Polym. Sci.* 278 (2000) 124–129.

- [45] L. Junji, X. Yun, S. Hongxiu, Diffusion-controlled adsorption kinetics of surfactant at air/solution interface, *Chin. J. Chem. Eng.* 21 (2013) 953–958.
- [46] R.C. Daniel, J.C. Berg, A simplified method for predicting the dynamic surface tension of concentrated surfactant solutions, *J. Colloid Interface Sci.* 260 (2003) 244–249.
- [47] Y.V. Rojas, C.M. Phan, X. Lou, Dynamic surface tension studies on poly (N vinylcaprolactam/ N-vinylpyrrolidone/N, N-dimethylaminoethyl methacrylate) at the air-liquid interface, *Coll. Surf. A* 355 (2010) 99–103.
- [48] S.N. Tan, D. Fornasiero, R. Sedev, J. Ralston, The interfacial conformation of polypropylene glycols and foam behaviour, *Coll. Surf. A* 250 (2004) 307–315.
- [49] M. Eftekhardakhah, P. Reynders, G. Øye, Dynamic adsorption of water soluble crude oil components at air bubbles, *Chem. Eng. Sci.* 101 (2013) 359–365.
- [50] X. Li, R. Shaw, G.M. Evans, P. Stevenson, A simple numerical solution to the Ward-Tordai equation for the adsorption of non-ionic surfactants, *Comp. Chem. Eng.* 34 (2010) 146–153.
- [51] R. Wang, *Effect of Non-Ionic Surfactants and Nano-Particles on the Stability of Foams*, 2010.
- [52] A.J.M. Valente, H.D. Burrows, M.G. Miguel, V.M.M. Lobo, Diffusion coefficients of sodium dodecyl sulfate in water swollen cross-linked polyacrylamide membranes, *Eur. Polym. J.* 38 (2002) 2187–2196.
- [53] M.J. Rosen, X.Y. Hua, Z.H. Zhu, Dynamic surface tension of aqueous surfactant solutions: IV relationship to foaming, In: K.L. Mittal, D.O. Shah (Eds.), *Surfactants in Solution*, vol. 11, Springer US, Boston, MA, 1991, pp. 315–327.
- [54] V. Carrier, A. Colin, Coalescence in draining foams, *Langmuir* 19 (2003) 4535–4538.
- [55] L. Trujillo-Cayado, P. Ramírez, L. Pérez-Mosqueda, M. Alfaro, J. Muñoz, Surface and foaming properties of polyoxyethylene glycerol ester surfactants, *Coll. Surf. A* 458 (2014) 195–202.
- [56] D. Nguyen, Fundamental surfactant properties of foamers for increasing gas production, *Pet. Sci. Technol.* 27 (2009) 733–745.

## CHAPTER V

### CONCLUSIONS AND RECOMMENDATIONS

#### 5.1 Conclusions

A continuous multistage froth flotation system was found to be a promising technique for motor oil removal. When it was operated under the optimum operational conditions, the highest motor oil removal performance could be achieved with the highest values of enrichment ratios, which are much higher than those of previous batch and continuous single-stage systems. To optimize the process performance of a continuous multistage froth flotation system in terms of high removal and high enrichment ratio of oil, it has to be operated to obtain high adsorptive transport with low bulk liquid transport. An addition of NaCl, at a proper concentration, can enhance the separation performance of a continuous multistage froth flotation column when an ionic surfactant is used as a frother.

A systematic investigation of the equilibrium and dynamic surface tension as well as foam properties of two series of  $MES_x$  with different alkyl chain lengths (14, 16 and 18)  $C_{12}EO_n$  with different amounts of EO units (3, 5, 7, and 9) was carried out. The equilibrium surface tension results of all studied surfactants were well fitted with the Langmuir adsorption model. The adsorption process was controlled by the diffusion step of surfactant, which was verified by the linear relation between  $\gamma(t)$  and  $\sqrt{t}$ . The term of  $\left(\frac{\partial\gamma}{\partial t}\right)_{max}$  obtained from the dynamic surface tension data can be used to indicate foaming properties in terms of foamability. The anionic surfactant with a moderate alkyl chain length— $MES_{14}$  or  $MES_{16}$ —showed higher foamability and foam stability, which is considered to be a promising surfactant for flotation process. An addition of NaCl provided both a positive and negative effect on the foam properties for the MES anionic surfactant.

## 5.2 Recommendations

The recommendations for future work are as follows:

1. To effectively and respectively separate, for example, phenolic compounds, pyridine compounds, organic acid from fermentation process, mixed heavy metals etc. by adsorptive bubble separation technique. Under the hypothesis that all of materials can be adsorbed on the bubble surfaces and have significant differences of surface excess under a certain condition.

2. To use mixed surfactant system as frother, which hypothesized that mixed system would provide synergism effect of formation and preservation of small bubbles, retarding the rising bubble velocity and stabilizing the froth.

3. To deeply study the adsorption process of molecular species to air/water interface both in equilibrium and dynamic conditions.

4. To intensive study the hydrodynamics of air bubble swarm in aqueous solution and correlate to the hydrodynamics of pneumatic foam drainage.

5. To evaluate the process performance of flotation column by comparing between surface excess concentration determined by using the basis of material balance and by using Gibbs adsorption isotherm equation.

6. To compare the flotation efficiency between plate and packed column.

7. To study the effect of tray type (bubble cap, sieve, and valve) of the separation efficiency of multistage froth flotation.

## REFERENCES

- Acharya, D. P., Gutiérrez, J. M., Aramaki, K., Aratani, K., and Kunieda, H. (2005) Interfacial properties and foam stability effect of novel gemini-type surfactants in aqueous solutions. Journal of Colloid and Interface Science, 291(1), 236-243.
- Belhajj, A., AlQuraishi, A., and Al-Mahdy, O. (2014, April) Foamability and foam stability of several surfactants solutions: The role of screening and flooding. Paper presented at Society of Petroleum Engineers Saudi Arabia Section Technical Symposium and Exhibition, Al-Khobar, Saudi Arabia.
- Beneventi, D., Carre, B., and Gandini, A. (2001) Role of surfactant structure on surface and foaming properties. Colloids and Surfaces A: Physicochemical and Engineering Aspects, 189(1–3), 65-73.
- Boonyasuwat, S., Chavadej, S., Malakul, P., and Scamehorn, J. F. (2003) Anionic and cationic surfactant recovery from water using a multistage foam fractionator. Chemical Engineering Journal, 93(3), 241-252.
- Boonyasuwat, S., Chavadej, S., Malakul, P., and Scamehorn, J. F. (2005) Surfactant recovery from water using a multistage foam fractionator: Part I Effects of air flow rate, foam height, feed flow rate and number of stages. Separation Science and Technology, 40(9), 1835-1853.
- Boonyasuwat, S., Chavadej, S., Malakul, P., and Scamehorn, J. F. (2009) Surfactant recovery from water using a multistage foam fractionator: Effect of surfactant type. Separation Science and Technology, 44(7), 1544-1561.
- Bunturngpratoomrat, A., Pornsunthorntawe, O., Nitivattananon, S., Chavadej, J., and Chavadej, S. (2013) Cutting oil removal by continuous froth flotation with packing media under low interfacial tension conditions. Separation and Purification Technology, 107(0), 118-128.
- Burghoff, B. (2012) Foam fractionation applications. Journal of Biotechnology, 161(2), 126-137.
- Cantat, I., Cohen-Addad, S., Elias, F., Graner, F., Höhler, R., Pitois, O., Rouyer, F., and Saint-Jalmes, A. (2013) Foams: Structure and Dynamics. OUP Oxford.

- Casandra, A., Ismadji, S., Noskov, B. A., Liggieri, L., and Lin, S.-Y. (2015) A study on the method of short-time approximation–Criteria for applicability. International Journal of Heat and Mass Transfer, 90, 752-760.
- Chang, C.-H. and Franses, E. I. (1995) Adsorption dynamics of surfactants at the air/water interface: A critical review of mathematical models, data, and mechanisms. Colloids and Surfaces A: Physicochemical and Engineering Aspects, 100, 1-45.
- Chang, H., Wang, Y., Cui, Y., Li, G., Zhang, B., Zhao, X., and Wei, W. (2016) Equilibrium and dynamic surface tension properties of Gemini quaternary ammonium salt surfactants with hydroxyl. Colloids and Surfaces A: Physicochemical and Engineering Aspects, 500, 230-238.
- Chavadej, S., Ratanarajanatam, P., Phoochinda, W., Yanatatsaneejit, U., and Scamehorn, J. F. (2004) Clean-up of oily wastewater by froth flotation: Effect of microemulsion formation II: Use of anionic/nonionic surfactant mixtures. Separation Science and Technology, 39(13), 3079-3096.
- Criswell, L. G. (1976) U.S. Patent 3 969 336.
- Daniel, R. C. and Berg, J. C. (2003) A simplified method for predicting the dynamic surface tension of concentrated surfactant solutions. Journal of Colloid and Interface Science, 260(1), 244-249.
- Darton, R. C., Supino, S., and Sweeting, K. J. (2004) Development of a multistaged foam fractionation column. Chemical Engineering and Processing: Process Intensification, 43(3), 477-482.
- Du, L., Loha, V., and Tanner, R.D. (2000) Modeling a protein foam fractionation process. Applied Biochemistry and Biotechnology, 84(1), 1087-1099.
- Dukhin, S. S., Kretzschmar, G., and Miller, R. (1995) Dynamics of Adsorption at Liquid Interfaces: Theory, Experiment, Application. Elsevier.
- Eastoe, J. and Dalton, J. (2000) Dynamic surface tension and adsorption mechanisms of surfactants at the air–water interface. Advances in Colloid and Interface Science, 85(2), 103-144.
- Eastoe, J., Dalton, J. S., Rogueda, P. G. A., Crooks, E. R., Pitt, A. R., and Simister, E. A. (1997) Dynamic surface tensions of nonionic surfactant solutions. Journal of Colloid and Interface Science, 188(2), 423-430.



- Falbe, J. (1987) Surfactants in Consumer Products: Theory, Technology and Application. Berlin, Heidelberg: Springer Berlin Heidelberg.
- Gao, X., Wang, Y., Zhao, X., Wei, W., and Chang, H. (2016) Equilibrium and dynamic surface tension properties of Gemini quaternary ammonium salt surfactants with ester groups. Colloids and Surfaces A: Physicochemical and Engineering Aspects, 509, 130-139.
- Gryta, M., Karakulski, K., and Morawski, A. W. (2001) Purification of oily wastewater by hybrid UF/MD. Water Research, 35(15), 3665-3669.
- Holmberg, K., Jönsson, B., Kronberg, B., and Lindman, B. (2003) Foaming of surfactant solutions. Surfactants and polymers in aqueous solution (pp. 437-450). Hoboken, NJ : John Wiley&Sons, Ltd.
- Holmberg, K., Jönsson, B., Kronberg, B., and Lindman, B. (2003) Introduction to surfactants. Surfactants and polymers in aqueous solution (pp. 1-37). Hoboken, NJ : John Wiley&Sons, Ltd.
- Hua, X. Y. and Rosen, M. J. (1988) Dynamic surface tension of aqueous surfactant solutions: I. Basic parameters. Journal of Colloid and Interface Science, 124(2), 652-659.
- Hua, X. Y. and Rosen, M. J. (1991) Dynamic surface tension of aqueous surfactant solutions: 3. Some effects of molecular structure and environment. Journal of Colloid and Interface Science, 141(1), 180-190.
- Jiang, Y., Geng, T., Li, Q., Li, G., and Ju, H. (2015) Equilibrium and dynamic surface tension properties of salt-free cationic surfactants with different hydrocarbon chain lengths. Journal of Molecular Liquids, 204, 126-131.
- Junji, L., Yun, X., and Hongxiu, S. (2013) Diffusion-controlled adsorption kinetics of surfactant at air/solution interface. Chinese Journal of Chemical Engineering, 21(9), 953-958.
- Kawatra, S. K. (2011) Fundamental principles of froth flotation. In: P. Darling (Ed), SME Mining engineering handbook (Society for mining, metallurgy, and exploration) (pp. 1517-1531). Englewood.
- Langevin, D. (2017) Aqueous foams and foam films stabilised by surfactants. Gravity-free studies. Comptes Rendus Mécanique, 345(1), 47-55.

- Lemlich, R. (1968) Adsorptive bubble separation methods—foam fractionation and allied techniques. Industrial & Engineering Chemistry, 60(10), 16-29.
- Lemlich, R. (2012) Adsorptive Bubble Separation Techniques. Elsevier.
- Leonard, R. A. and Blacyki, J. D. (1978) Multistage bubble fractionator. Industrial & Engineering Chemistry Process Design and Development, 17(3), 358-361.
- Li, Y. S., Yan, L., Xiang, C. B., and Hong, L. J. (2006) Treatment of oily wastewater by organic–inorganic composite tubular ultrafiltration (UF) membranes. Desalination, 196(1–3), 76-83.
- Li, X., Shaw, R., Evans, G. M., and Stevenson, P. (2010) A simple numerical solution to the Ward–Tordai equation for the adsorption of non-ionic surfactants. Computers & Chemical Engineering, 34(2), 146-153.
- Liggieri, L., Ravera, F., and Passerone, A. (1996) A diffusion-based approach to mixed adsorption kinetics. Colloids and Surfaces A: Physicochemical and Engineering Aspects, 114, 351-359.
- Liu, J. and Messow, U. (2000) Diffusion-controlled adsorption kinetics at the air/solution interface. Colloid and Polymer Science, 278(2), 124-129.
- Liu, J., Wang, C., and Messow, U. (2004) Adsorption kinetics at air/solution interface studied by maximum bubble pressure method. Colloid and Polymer Science, 283(2), 139-144.
- Liu, J. and Zhang, Y. (2006) Diffusion-controlled adsorption kinetics of aqueous submicellar and micellar solution at air/solution interface in the limit of short time. Korean Journal of Chemical Engineering, 23(5), 699-703.
- Liu, X., Zhao, Y., Li, Q., Jiao, T., and Niu, J. (2016) Surface and interfacial tension of nonylphenol polyethylene oxides sulfonate. Journal of Molecular Liquids 216, 185-191.
- Malysa, K. and Lunkenheimer, K. (2008) Foams under dynamic conditions. Current Opinion in Colloid & Interface Science, 13(3), 150-162.
- Marinova, K. G., Basheva, E. S., Nenova, B., Temelska, M., Mirarefi, A. Y., Campbell, B., and Ivanov, I. B. (2009) Physico-chemical factors controlling the foamability and foam stability of milk proteins: Sodium caseinate and whey protein concentrates. Food Hydrocolloids, 23(7), 1864-1876.

- Masuelli, M., Marchese, J., and Ochoa, N. A. (2009) SPC/PVDF membranes for emulsified oily wastewater treatment. Journal of Membrane Science, 326(2), 688-693.
- Morgan, G. and Wiesmann, U. (2001) Single and multistage foam fractionation of rinse water with alkyl ethoxylate surfactants. Separation Science and Technology, 36(10), 2247-2263.
- Narsimhan, G. and Wang, Z. (2006) Rupture of equilibrium foam films due to random thermal and mechanical perturbations. Colloids and Surfaces A: Physicochemical and Engineering Aspects, 282, 24-36.
- Perez, M., Rodriguez-Cano, R., Romero, L. I., and Sales, D. (2007) Performance of anaerobic thermophilic fluidized bed in the treatment of cutting-oil wastewater. Bioresource Technology, 98(18), 3456-3463.
- Phan, C. M., Le, T. N., and Yusa, S.-i. (2012) A new and consistent model for dynamic adsorption of CTAB at air/water interface. Colloids and Surfaces A: Physicochemical and Engineering Aspects, 406, 24-30.
- Pondstabodee, S., Scamehorn, J. F., Chavedej, S., and Harwell, J. H. (1998) Cleanup of oily wastewater by froth flotation: Effect of microemulsion formation. Separation Science and Technology, 33(4), 591-609.
- Pugh, R. J. (2005) Experimental techniques for studying the structure of foams and froths. Advances in Colloid and Interface Science, 114–115(0), 239-251.
- Pugh, R. J. (2016) Bubble and Foam Chemistry. Switzerland, Europe: Cambridge University Press.
- Rojas, Y. V., Phan, C. M., and Lou, X. (2010) Dynamic surface tension studies on poly(N-vinylcaprolactam/N-vinylpyrrolidone/N,N-dimethylaminoethyl methacrylate) at the air–liquid interface. Colloids and Surfaces A: Physicochemical and Engineering Aspects, 355(1), 99-103.
- Rosen, M. and Solash, J. (1969) Factors affecting initial foam height in the Ross-Miles foam test. Journal of the American Oil Chemists' Society, 46(8), 399-402.
- Rosen, M. J. (2004) Surfactants and Interfacial Phenomena. Hoboken, New Jersey: Wiley-Interscience.

- Rosen, M. J. and Kunjappu, J. T. (2012) Surfactants and Interfacial Phenomena. Hoboken: Wiley.
- Rujirawanich, V., Chavadej, S., O'Haver, J. H., and Rujiravanit, R. (2010) Removal of trace  $\text{Cd}^{2+}$  using continuous multistage ion foam fractionation: Part I—The effect of feed SDS/Cd molar ratio. Journal of Hazardous Materials, 182(1–3), 812-819.
- Rujirawanich, V., Chavadej, S., O'Haver, J. H., and Rujiravanit, R. (2011) Removal of trace  $\text{Cd}^{2+}$  using continuous multistage ion foam fractionation: Part II—The effects of operational parameters. Separation Science and Technology, 46(10), 1673-1683.
- Rujirawanich, V., Chuyingsakultrip, N., Triroj, M., Malakul, P., and Chavadej, S. (2012) Recovery of surfactant from an aqueous solution using continuous multistage foam fractionation: Influence of design parameters. Chemical Engineering and Processing: Process Intensification, 52(0), 41-46.
- Scamehorn, J. F. and Harwell, J. H. (1988) Surfactant-based treatment of aqueous process streams. Surfactants in Chemical/Process Engineering, 28, 78-98.
- Scamehorn, J. F. and Harwell, J. H. (2000) Current trends and future developments in surfactant-based separations. American Chemical Society, 740, 1-14.
- Schramm, L. L., Stasiuk, E. N., and Marangoni, D. G. (2003) 2 Surfactants and their applications. Annual Reports Section "C"(Physical Chemistry), 99(0), 3-48.
- Li, S.-Q., Zhou, P.-J., Ding, L., and Feng, K. (2011) Treatment of oily wastewater using composite flocculant of polysilicate ferro-aluminum sulfate-rectorite. Journal of Water Resource and Protection, 3, 253-261.
- Stevenson, P. (2012) Foam Engineering: Fundamentals and Applications. Chichester, West Sussex, UK: Wiley.
- Stevenson, P. and Lambert, N. W. A. (2012) Froth phase phenomena in flotation. Foam engineering (pp. 227-249). Chichester:Wiley-Blackwell.
- Stevenson, P. and Li, X. (2014) Foam Fractionation: Principles and Process Design. Boca Raton : Taylor & Francis.
- Stubenrauch, C. and Khristov, K. (2005) Foams and foam films stabilized by  $\text{C}_n\text{TAB}$ : Influence of the chain length and of impurities. Journal of Colloid and Interface Science, 286(2), 710-718.

- Szymański, A. (2008) Determination of sulfonamide residues in food by micellar liquid chromatography. Toxicology Mechanisms and Methods 18(6), 473-481.
- Tadros, T. F. (2005) Adsorption of surfactants at the air/liquid and liquid/liquid interfaces. Applied surfactants (pp. 73-84). Weinheim, Germany: Wiley-VCH Verlag GmbH & Co. KGaA.
- Tadros, T. F. (2005) Introduction. Applied surfactants (pp. 1-17). Weinheim, Germany: Wiley-VCH Verlag GmbH & Co. KGaA.
- Tadros, T. F. (2005) Surfactants in foams. Applied Surfactants (pp. 259-284). Weinheim, Germany: Wiley-VCH Verlag GmbH & Co. KGaA.
- Tamura, T., Takeuchi, Y., and Kaneko, Y. (1998) Influence of surfactant structure on the drainage of nonionic surfactant foam films. Journal of Colloid and Interface Science, 206(1), 112-121.
- Tan, S. N., Fornasiero, D., Sedev, R., and Ralston, J. (2004) The interfacial conformation of polypropylene glycols and foam behaviour. Colloids and Surfaces A: Physicochemical and Engineering Aspects, 250(1-3), 307-315.
- Tan, S. N., Fornasiero, D., Sedev, R., and Ralston, J. (2005) The role of surfactant structure on foam behaviour. Colloids and Surfaces A: Physicochemical and Engineering Aspects, 263(1-3), 233-238.
- van der Net, A., Blondel, L., Saugey, A., and Drenckhan, W. (2007) Simulating and interpreting images of foams with computational ray-tracing techniques. Colloids and Surfaces A: Physicochemical and Engineering Aspects, 309(1), 159-176.
- Wang, J., Nguyen, A. V., and Farrokhpay, S. (2015) A critical review of the growth, drainage and collapse of foams. Advances in Colloid and Interface Science, 228, 55-70.
- Wang, J., Nguyen, A. V., and Farrokhpay, S. (2016) Foamability of sodium dodecyl sulfate solutions: Anomalous effect of dodecanol unexplained by conventional theories. Colloids and Surfaces A: Physicochemical and Engineering Aspects, 495, 110-117.

- Wang, L.K. (2006) Adsorptive bubble separation and dispersed air flotation. In L.K. Wang, Y.-T. Hung, and N.K. Shamma (Eds.), Advanced physicochemical treatment processes (pp. 81-122). Totowa, New Jersey: Humana Press.
- Wang, Z. and Narsimhan, G. (2007) Rupture of draining foam films due to random pressure fluctuations. Langmuir, 23(5), 2437-2443.
- Ward, A. and Tordai, L. (1946) Time-dependence of boundary tensions of solutions I. The role of diffusion in time-effects. The Journal of Chemical Physics, 14(7), 453-461.
- Wasan, D. T., Ginn, M. E., and Shah, D. O. (1988) Surfactants in Chemical/Process Engineering. New York: Dekker.
- Watcharasing, S., Angkathunyakul, P., and Chavadej, S. (2008) Diesel oil removal from water by froth flotation under low interfacial tension and colloidal gas aphyron conditions. Separation and Purification Technology, 62(1), 118-127.
- Watcharasing, S., Chavadej, S., and Scamehorn, J. F. (2008) Diesel oil removal by froth flotation under low interfacial tension conditions II: Continuous mode of operation. Separation Science and Technology, 43(8), 2048-2071.
- Watcharasing, S., Kongkowitz, W., and Chavadej, S. (2009) Motor oil removal from water by continuous froth flotation using extended surfactant: Effects of air bubble parameters and surfactant concentration. Separation and Purification Technology, 70(2), 179-189.
- Wills, B. A. and Finch, J. A. (2016) Chapter 12-Froth flotation. Wills' Mineral Processing Technology (Eighth Edition) (pp.265-380). Boston, Butterworth-Heinemann.
- Wong, C., Hossain, M., and Davies, C. (2001) Performance of a continuous foam separation column as a function of process variables. Bioprocess and Biosystems Engineering, 24(2), 73-81.
- Wood, R. and Tran, T. (1966) Surface adsorption and the effect of column diameter in the continuous foam separation process. The Canadian Journal of Chemical Engineering, 44(6), 322-326.
- Yan, L., Hong, S., Li, M. L., and Li, Y. S. (2009) Application of the Al<sub>2</sub>O<sub>3</sub>-PVDF nanocomposite tubular ultrafiltration (UF) membrane for oily wastewater

treatment and its antifouling research. Separation and Purification Technology, 66(2), 347-352.

Yanatatsaneejit, U., Chavadej, S., Rangsunvigit, P., and Scamehorn, J. F. (2005) Ethylbenzene removal by froth flotation under conditions of middle-phase microemulsion formation II: Effects of air flow rate, oil-to-water ratio, and equilibration time. Separation Science and Technology, 40(8), 1609-1620.

Yanatatsaneejit, U., Chavadej, S., and Scamehorn, J. F. (2008) Diesel oil removal by froth flotation under low interfacial tension conditions I: Foam characteristics, and equilibration time. Separation Science and Technology, 43(6), 1520-1534.

Yanatatsaneejit, U., Witthayapanyanon, A., Rangsunvigit, P., Acosta, E. J., Sabatini, D. A., Scamehorn, J. F., and Chavadej, S. (2005) Ethylbenzene removal by froth flotation under conditions of middle-phase microemulsion formation I: Interfacial tension, foamability, and foam stability. Separation Science and Technology, 40(7), 1537-1553.

Zeng, Y., Yang, C., Zhang, J., and Pu, W. (2007) Feasibility investigation of oily wastewater treatment by combination of zinc and PAM in coagulation/flocculation. Journal of Hazardous Materials, 147(3), 991-996.

## APPENDIX

### Surface Tension of Surfactant Solution at 25 °C

**Table A1** Surface tension of surfactant Alfoterra<sup>®</sup> C145–8PO with and without 1.5% (w/v) NaCl addition at 25°C.

Initial surfactant concentration (% w/v)	Surface tension (mN/m)	
	With NaCl	Without NaCl
0.10	71.00	69.63
0.20	70.77	69.23
0.30	69.23	68.50
0.40	68.43	66.63
0.50	67.40	64.07
0.60	65.87	61.70
0.80	61.70	57.87
1.00	57.77	54.80
2.00	49.27	45.10
3.00	43.83	39.27
4.00	41.67	34.93
5.00	39.57	31.47
6.00	38.53	28.50
8.00	37.37	26.97
10.0	35.77	26.87
20.0	35.60	26.93
30.0	35.43	26.93
40.0	35.57	26.87
50.0	35.63	-



**Table A2** Surface tension of all studied anionic surfactant solutions at 25 °C

Surfactant concentration	Surface tension (mN/m)			
	MES <sub>14</sub>	MES <sub>16</sub>	MES <sub>18</sub>	SDS
2.0			72.4	72.0
3.0			72.3	71.8
4.0			72.2	71.2
6.0			71.4	71.0
8.0			69.2	70.5
10.0		71.5	66.9	69.5
15.0		71.2	63.7	64.6
20.0		70.6	60.1	60.3
30.0	71.2	67.9	55.3	58.6
40.0	71.0	64.7	50.2	57.2
60.0	68.5	60.9	45.4	55.3
80.0	66.2	56.6	40.5	54.1
100.0	63.5	51.8	38.6	52.9
200.0	58.7	46.4	38.6	51.9
300.0	54.6	40.8	38.7	50.6
400.0	51.9	39.7	38.6	47.9
500.0	48.7	38.8	38.6	44.6
600.0	47.6	38.8		41.1
700.0	46.5	38.7		39.2
800.0	45.6			37.7
900.0	44.1			36.5
1000.0	42.6			35.6
1500.0	40.3			35.6
2000.0	37.4			35.4
3000.0	36.5			72.0
4000.0	36.4			71.8
5000.0				71.2
6000.0				71.0
7000.0				70.5
8000.0				69.5
9000.0				64.6

**Table A3** Surface tension of all studied non-ionic surfactant solutions at 25 °C

Surfactant concentration	Surface tension (mN/m)			
	C <sub>12</sub> EO <sub>3</sub>	C <sub>12</sub> EO <sub>5</sub>	C <sub>12</sub> EO <sub>7</sub>	C <sub>12</sub> EO <sub>9</sub>
0.10	72.2	73.1	72.4	72.1
0.20	72.2	72.7	72.2	72.3
0.40	72.1	72.4	72.2	72.2
0.60	72.0	72.3	72.0	71.1
0.80	72.0	72.3	71.7	70.0
1.00	72.0	72.1	71.1	68.7
2.00	71.6	72.0	69.3	63.1
4.00	71.5	69.7	63.9	58.1
6.00	71.0	64.8	60.1	54.7
8.00	68.5	62.4	57.2	53.1
10.0	65.0	59.4	55.3	51.3
15.0	60.4	55.7	52.1	49.5
20.0	55.0	51.9	48.6	47.2
30.0	51.5	48.0	46.0	45.3
40.0	47.2	43.5	42.5	41.9
60.0	40.7	39.5	39.2	38.5
80.0	33.0	35.6	36.6	37.3
100.0	32.6	33.5	35.0	36.5
200.0	32.8	33.1	34.6	36.1
300.0	32.6	33.2	34.5	36.2
400.0	32.6	33.4	34.4	36.4
500.0	32.8	33.5	34.6	36.5

## CURRICULUM VITAE

**Name:** Ms. Paweena Kanokkarn

**Date of Birth:** December 1, 1986

**Nationality:** Thai

**University Education:**

2008-2009 Master Degree of Science, The Petroleum and Petrochemical College, Chulalongkorn University, Thailand

2004–2007 Bachelor Degree of Engineering (Second Class Honors), Department of Petrochemical and Polymeric Materials, Faculty of Engineering and Industrial Technology, Silpakorn University, Nakhon Pathom, Thailand

**Publications:**

1. Kanokkarn, P., Shiina, T., Suttikul, T. and Chavadej, S. (2016) Removal of motor oil by continuous multistage froth flotation: Effect of operational parameters. Separation Science and Technology, 51(11): 1847-1861.
2. Kanokkarn, P., Shiina, T., Santikunaporn, M. and Chavadej, S. (2017) Equilibrium and dynamic surface tension in relation to diffusivity and foaming properties: Effects of surfactant type and structure. Colloids and Surfaces A: Physicochemical and Engineering Aspects, 524: 135-142.

**Presentations:**

1. Kanokkarn, P. and Chavadej, S. (2012, January 11–13) Motor oil removal by multistage froth flotation. Poster presented at The Pure and Applied Chemistry International Conference 2012, Chiangmai, Thailand.
2. Kanokkarn, P. and Chavadej, S. (2012, Apr 29–May 2) Motor oil removal by multistage froth flotation: The effect of operational parameters. Poster presented at The 103<sup>rd</sup> AOCS Annual Meeting & Expo 2012, Long Beach, California, USA.
3. Kanokkarn, P. and Chavadej, S. (2013, June 9–12) Continuous multistage froth flotation for motor oil removal: The effect of operational parameters. Oral presented at The Asian Conference on the Social Sciences 2013, Osaka, Japan.

4. Kanokkarn, P. and Chavadej, S. (2015, June 11–13) Continuous multistage froth flotation for motor oil removal. Oral presented at RGJ-Ph.D. Congress XVI “ASEAN: Emerging Research Opportunities 2015, Chonburi, Thailand.